Tests of gravity with radio pulsars

Paulo C. C. Freire

Max-Planck-Institut für Radioastronomie
Bonn, Germany

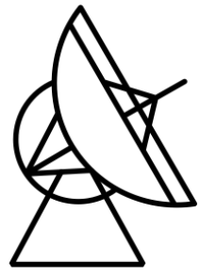

The WE-Heraeus and NARIT Cosmology School 2025 - Galaxies and Beyond, Chiang Mai, Thailand, 2025 October 13-17

In this talk…

1. Why it is important to test GR

2. Why tests of gravity theories with radio pulsars?

3. The double pulsar

4. Tests of the nature of gravitational waves and of alternative theories of gravity

    4.1. Searching for dipolar gravitational waves

    4.2. Searching for spontaneous scalarisation

    4.3. Searching for a violation of the UFF

5. Consequences for our understanding of gravity and alternative gravity theories

Not included: Pulsar Timing Arrays!

1. Why it is important to test GR

Why Gravity?

Nature's most fundamental and mysterious force

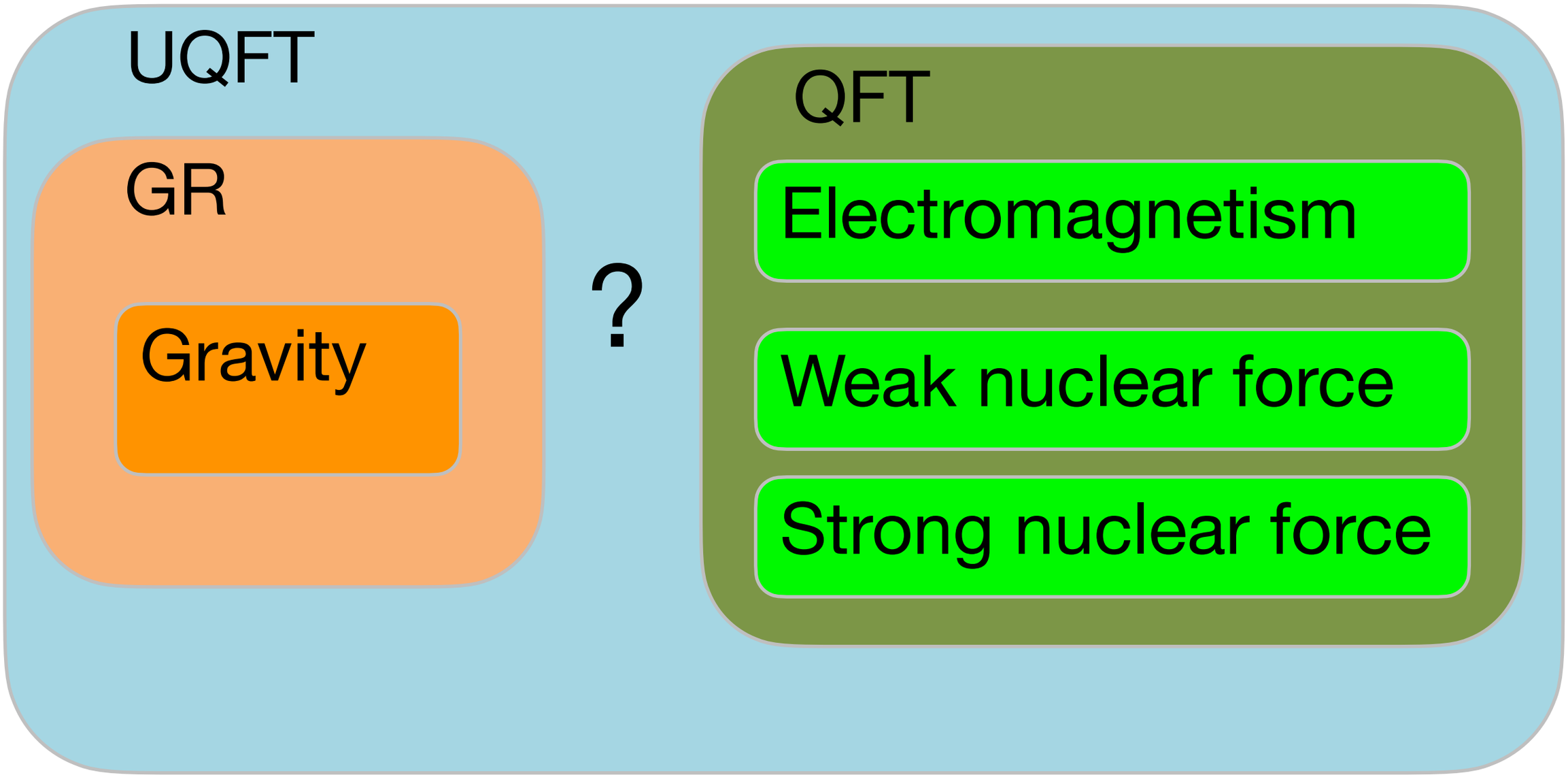

Why Gravity?

Nature's most fundamental and mysterious force

To achieve a full, coherent picture of the Universe, we must understand gravity!

Do we understand it? GR cannot be the ultimate gravity theory because of:

- singularities,
- incompatibility with quantum mechanics

It must fail at the Planck scale!

Are there any deviations at measurable scales?

Measurable deviations?

We don‘t know many things:

What caused cosmic inflation?

What is Dark Matter?

What is Dark Energy?

Cosmic "makeup". Credit: ESA/Planck

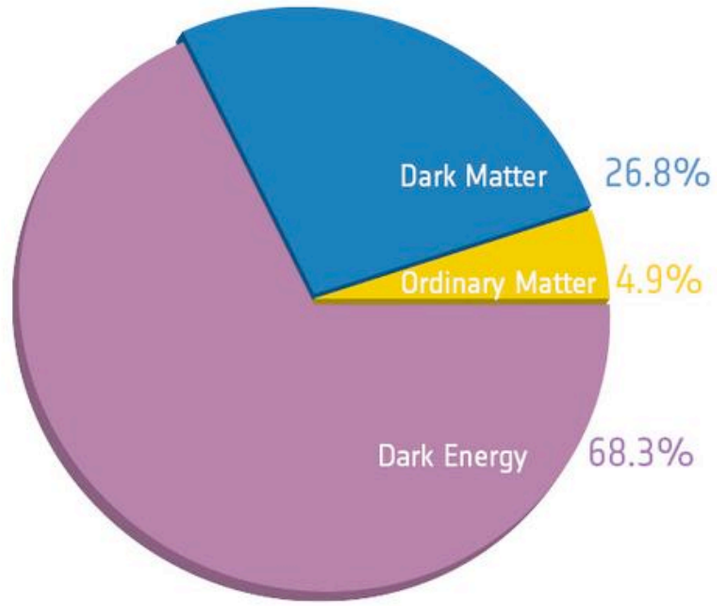

Instead of this many new fields, could our understanding of gravity be at fault?

MANY alternative theories of gravity have been proposed to explain these phenomena, with significant deviations from GR below the Planck scale *that can be observed in binary pulsar experiments*!

Thus, falsifying or confirming such theories has implications beyond the study of gravity – also for the study of the origin, evolution and contents of our Universe.

2. Why tests of gravity theories with radio pulsars?

General relativity

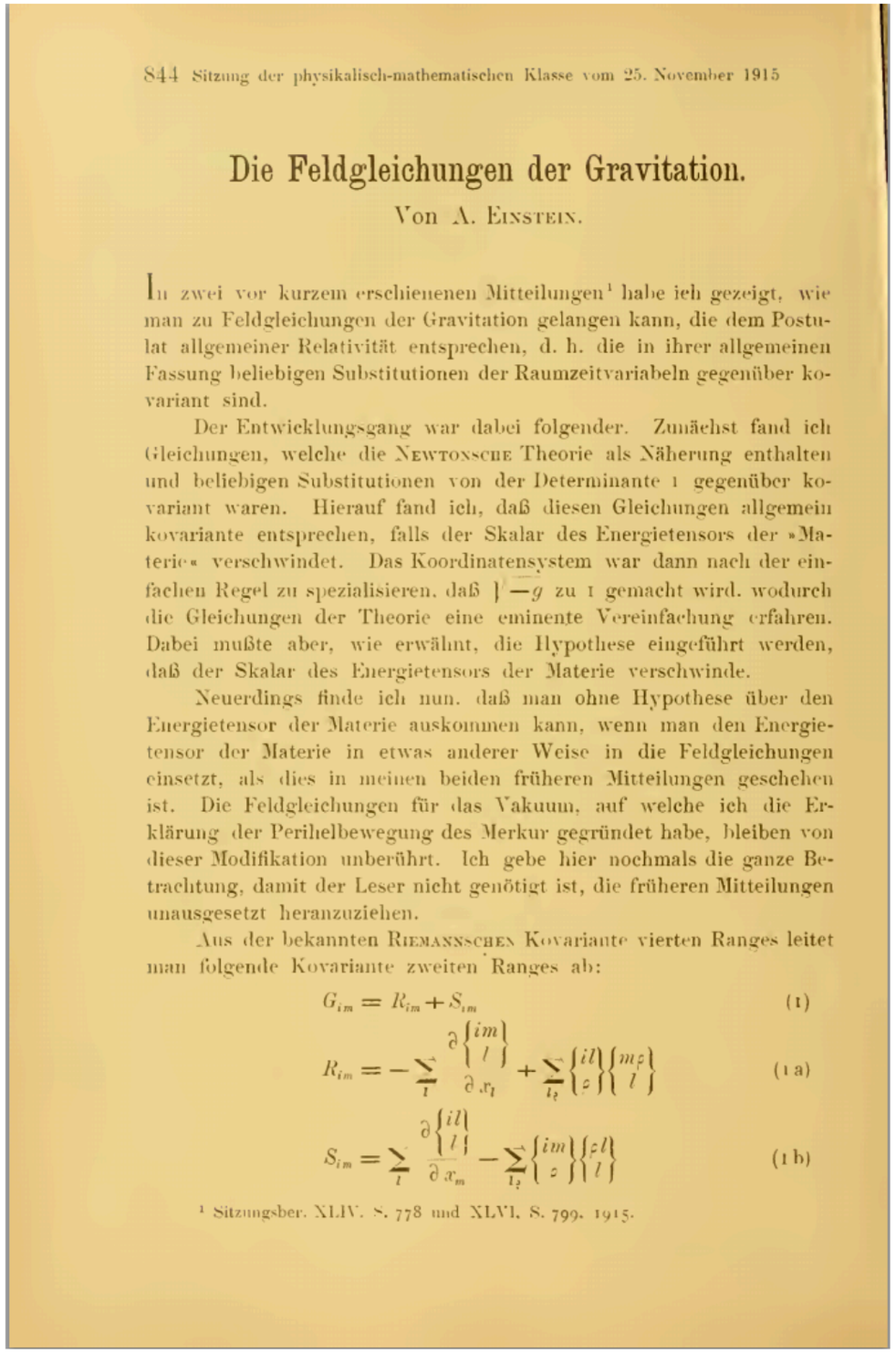

844 Sitzung der physikalisch-mathematischen Klasse vom 25. November 1915

Die Feldgleichungen der Gravitation.

Von A. Einstein.

In zwei vor kurzem erschienenen Mitteilungen[1] habe ich gezeigt, wie man zu Feldgleichungen der Gravitation gelangen kann, die dem Postulat allgemeiner Relativität entsprechen, d. h. die in ihrer allgemeinen Fassung beliebigen Substitutionen der Raumzeitvariabeln gegenüber kovariant sind.

Der Entwicklungsgang war dabei folgender. Zunächst fand ich Gleichungen, welche die Newtonsche Theorie als Näherung enthalten und beliebigen Substitutionen von der Determinante 1 gegenüber kovariant waren. Hierauf fand ich, daß diesen Gleichungen allgemein kovariante entsprechen, falls der Skalar des Energietensors der »Materie« verschwindet. Das Koordinatensystem war dann nach der einfachen Regel zu spezialisieren, daß $\sqrt{-g}$ zu 1 gemacht wird, wodurch die Gleichungen der Theorie eine eminente Vereinfachung erfahren. Dabei mußte aber, wie erwähnt, die Hypothese eingeführt werden, daß der Skalar des Energietensors der Materie verschwinde.

Neuerdings finde ich nun, daß man ohne Hypothese über den Energietensor der Materie auskommen kann, wenn man den Energietensor der Materie in etwas anderer Weise in die Feldgleichungen einsetzt, als dies in meinen beiden früheren Mitteilungen geschehen ist. Die Feldgleichungen für das Vakuum, auf welche ich die Erklärung der Perihelbewegung des Merkur gegründet habe, bleiben von dieser Modifikation unberührt. Ich gebe hier nochmals die ganze Betrachtung, damit der Leser nicht genötigt ist, die früheren Mitteilungen unausgesetzt heranzuziehen.

Aus der bekannten Riemannschen Kovariante vierten Ranges leitet man folgende Kovariante zweiten Ranges ab:

$$G_{im} = R_{im} + S_{im} \qquad (1)$$

$$R_{im} = -\sum_{l} \frac{\partial \left\{ \begin{matrix} im \\ l \end{matrix} \right\}}{\partial x_l} + \sum_{l_2} \left\{ \begin{matrix} il \\ \varrho \end{matrix} \right\} \left\{ \begin{matrix} m\varrho \\ l \end{matrix} \right\} \qquad (1a)$$

$$S_{im} = \sum_{l} \frac{\partial \left\{ \begin{matrix} il \\ l \end{matrix} \right\}}{\partial x_m} - \sum_{l_2} \left\{ \begin{matrix} im \\ \varrho \end{matrix} \right\} \left\{ \begin{matrix} \varrho l \\ l \end{matrix} \right\} \qquad (1b)$$

[1] Sitzungsber. XLIV. S. 778 und XLVI. S. 799. 1915.

Einstein published the field equations of general relativity in November 1915.

General relativity has since passed *all* experimental tests!

Until 1974, all tests of this theory were made in the Solar System (very weak fields, very low velocities).

But what if the fields are much stronger? What if we have objects moving much faster, and with much stronger gravitational fields? – After all, this is what made Newtonian gravity fail…

The discovery of pulsars

- In August 1967, Jocelyn Bell, then a graduate student at Cambridge, finds a radio signal in the constellation Sagitta (the Little Arrow) pulsating with a period of 1.33 seconds. She found this to appear 4 minutes earlier every day, indicating a sidereal source!

- For this discovery, her supervisor, Anthony Hewish earns the Nobel Prize in Physics 1974.

The discovery of pulsars

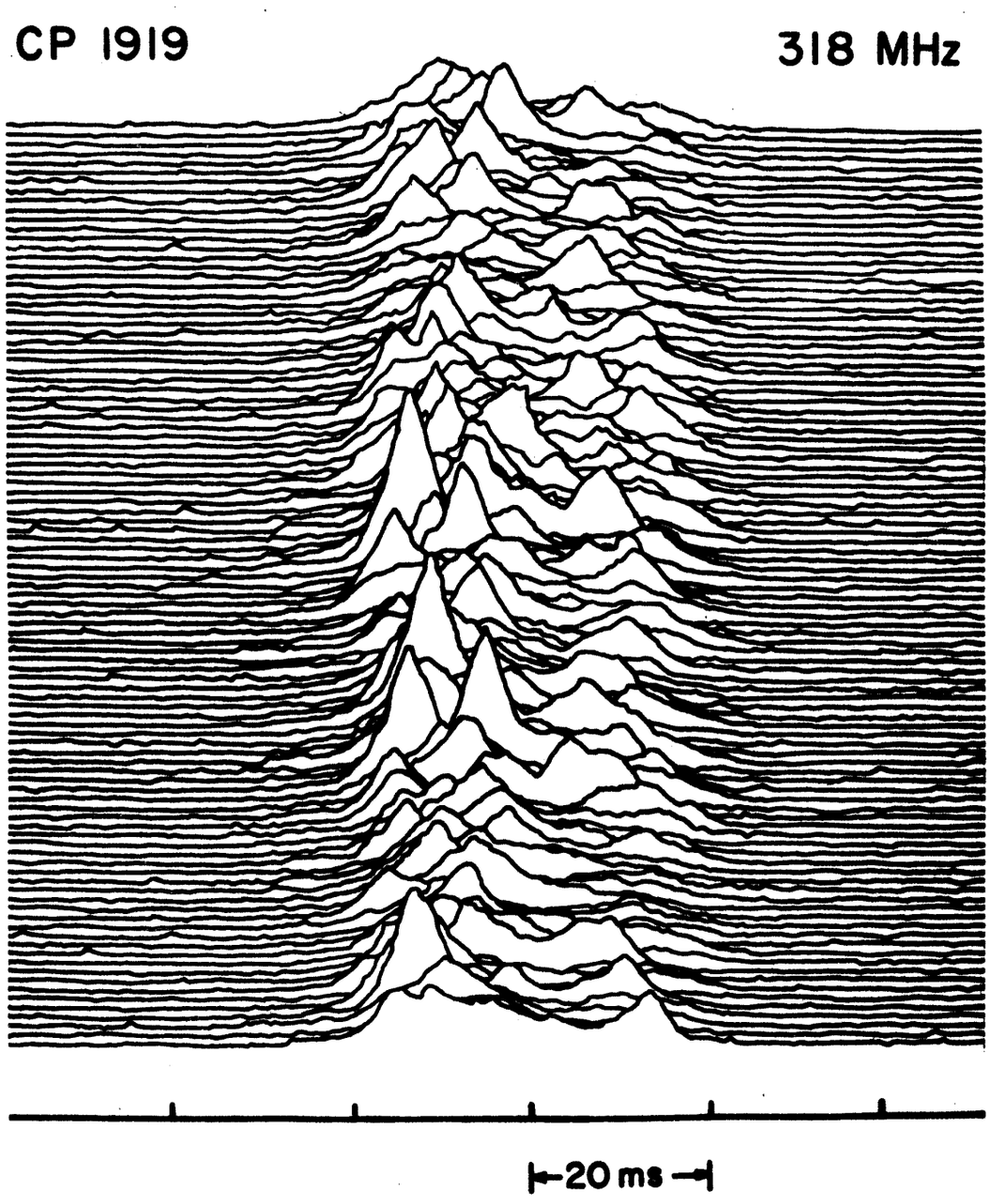

Sound of PSR B1919+21, as observed at Arecibo on the 13th of June 2006:

Figure on the left: Single pulses from PSR B1919+21 observed at Arecibo. From: Craft HD (1970), ``Radio Observations of the Pulse Profiles and Dispersion Measures of Twelve Pulsars." PhD thesis, Cornell University, New York

What are pulsars?

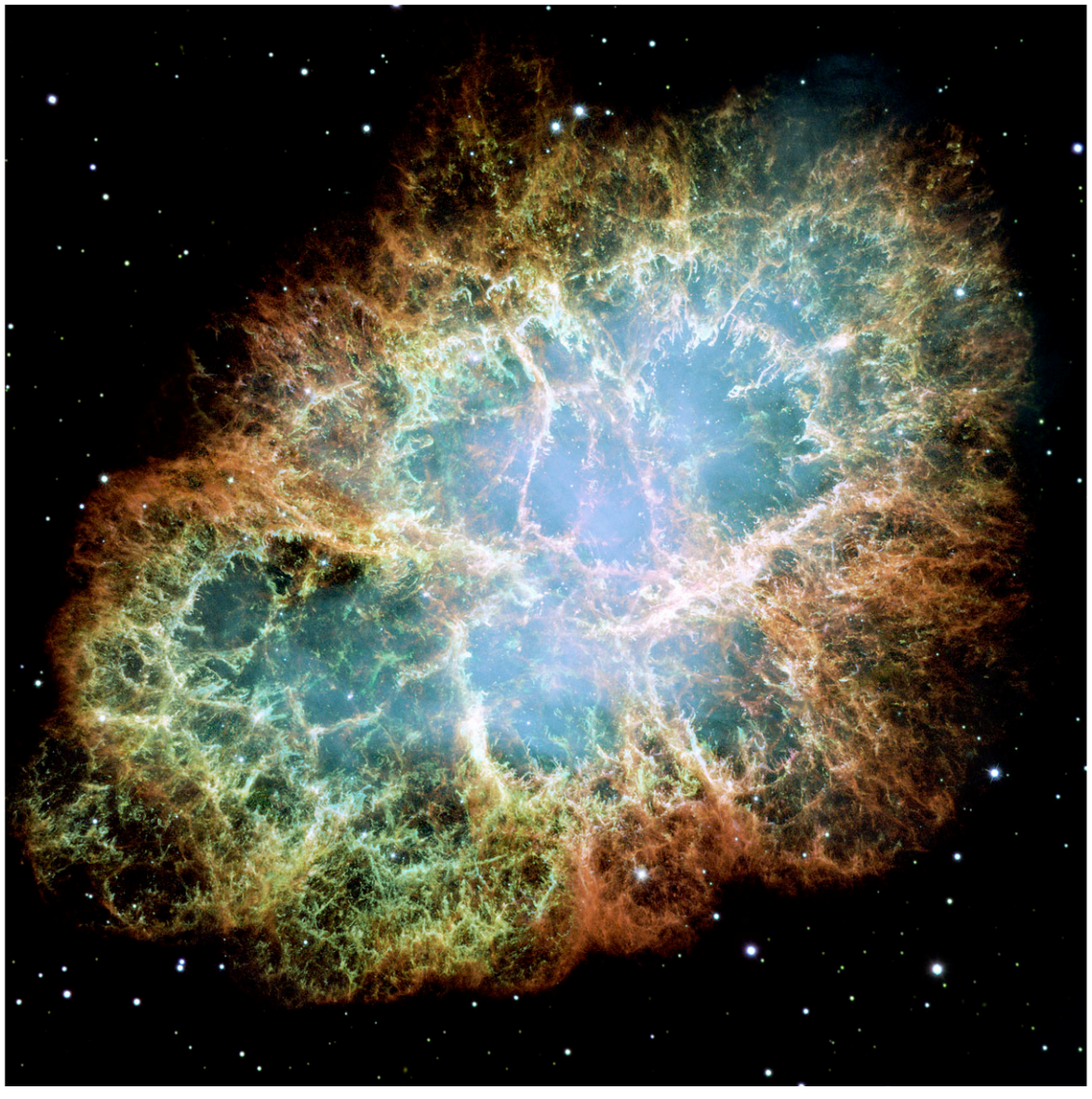

Neutron stars are the remnants of extremely massive stars. Towards the end of their lives they explode as Supernovae:

- The result is a sphere of neutrons with R ~ 11-13 km, and M ~ 460000 times the Earth's mass
- Gravitational binding energy: about –40 000 Earth masses!
- Density in the core is several hundred million tons per cubic cm – significantly higher than at the atomic nucleus!

Some neutron stars emit radio waves anisotropically. Their rotation then makes them appear to pulse, like a lighthouse – a pulsar!

Why are pulsars interesting for gravity?

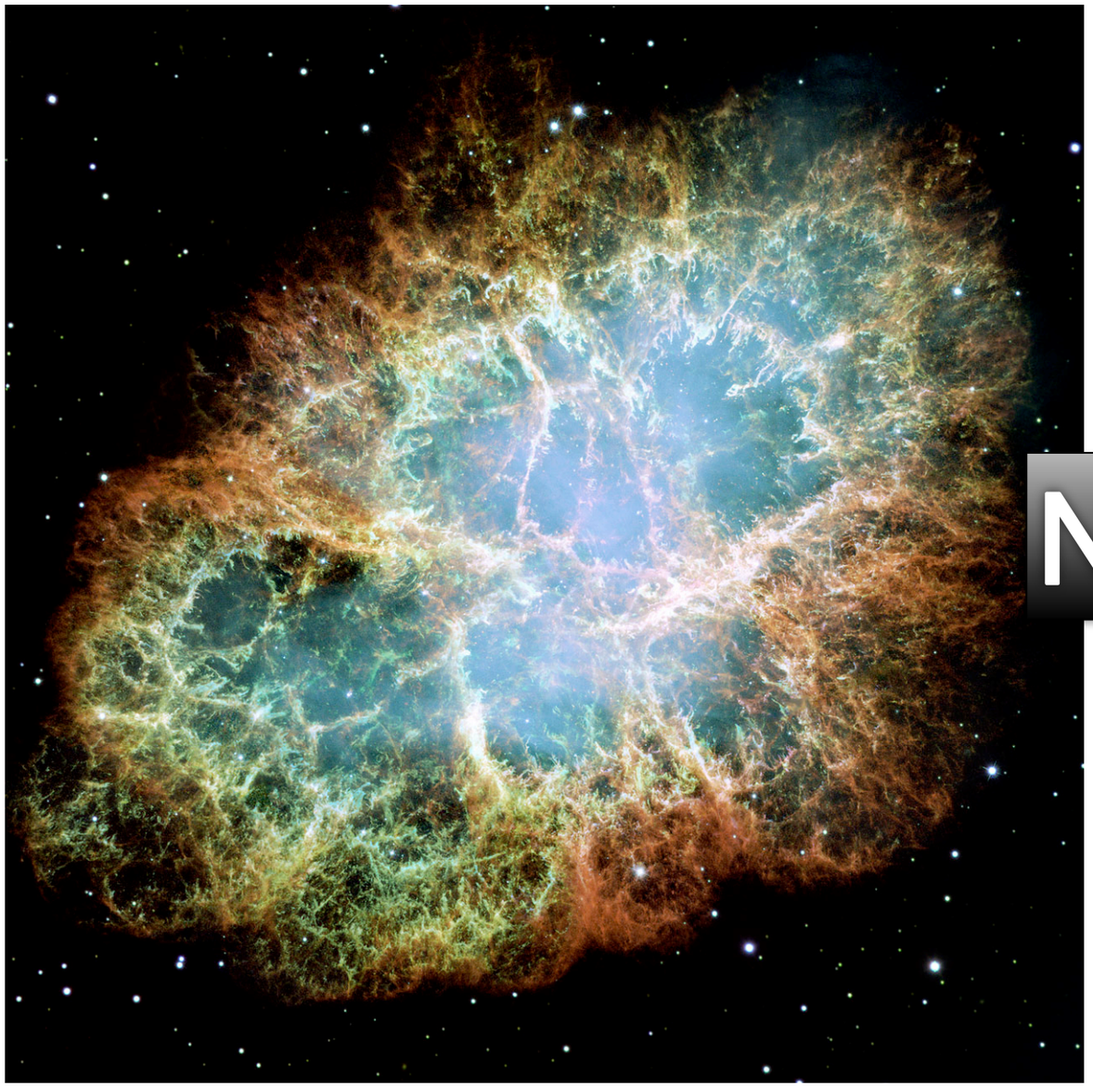

Neutron stars are the remnants of extremely massive stars. Towards the end of their lives they explode as Supernovae:

POINT MASSES

Non-trivial grav. Prop.

This stuff is so dense we don't know what it is.

We can time them precisely!

The timing technique

Since these discoveries, we have been actively observing these pulsars in order to derive their timing solutions.

Pulsar timing measures pulsar arrival time at the telescope (TOA):

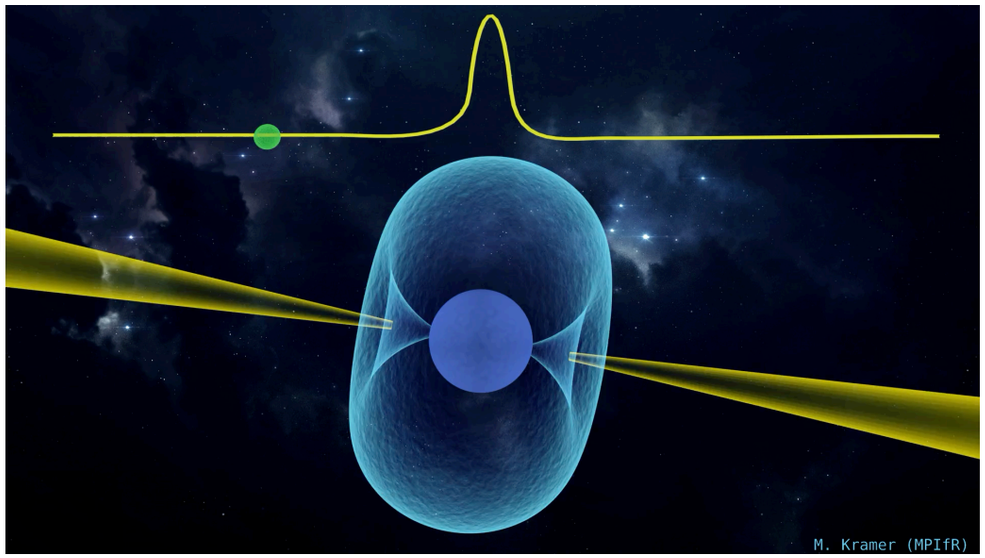

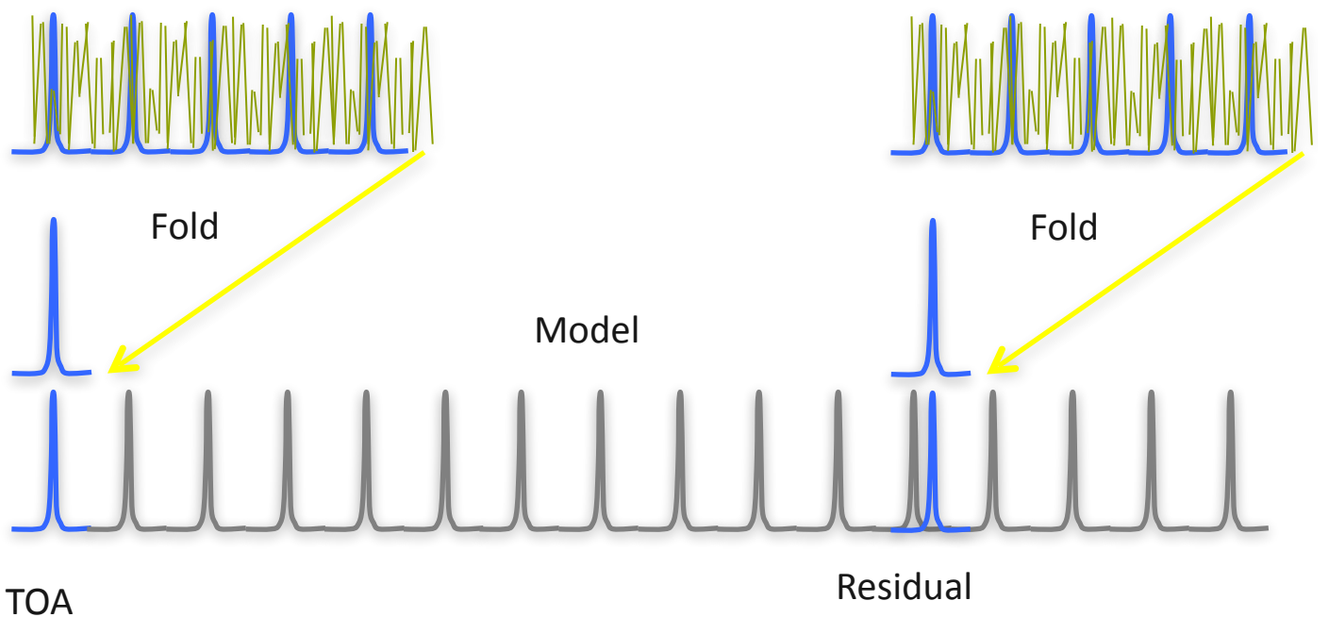

Credit:
Rotating pulsar: M. Kramer
Timing plots: David Champion

The first binary pulsar - 1974

"Here was a system that featured, in addition to significant post-Newtonian gravitational effects, ***highly relativistic gravitational fields*** *associated with the pulsar (and possibly its companion) and the possibility of the* ***emission of gravitational radiation*** *by the binary system." (Clifford Will, TEGP 2018)*

PSR B1913+16

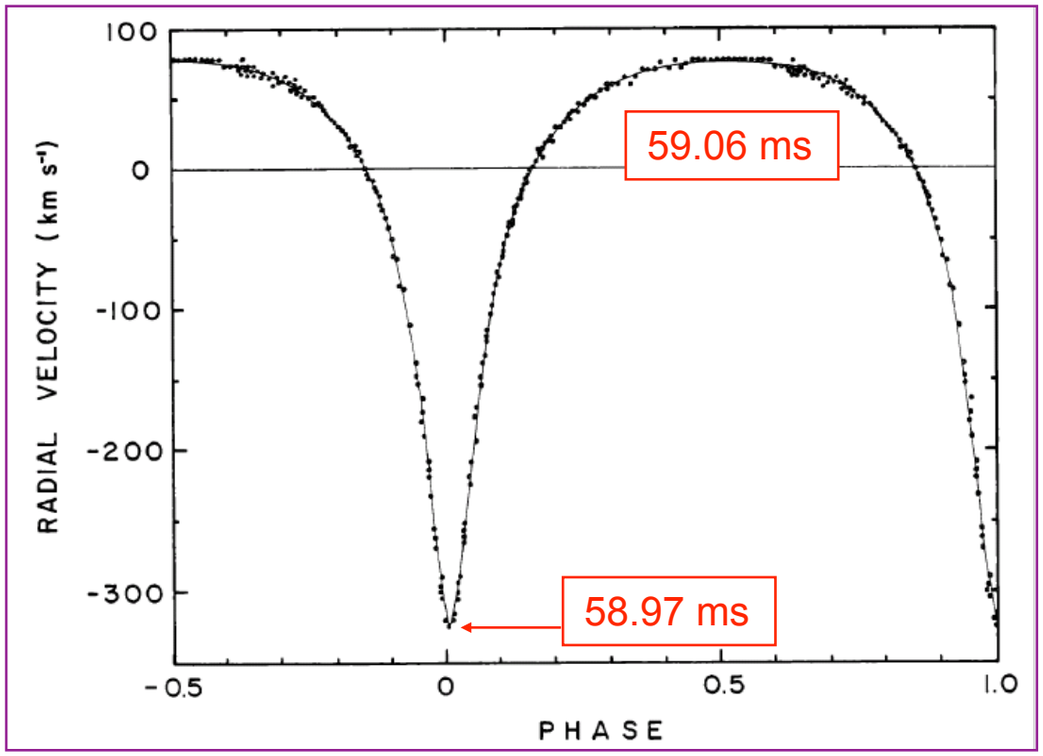

Pulse period P:	59.0 ms
Orbital period P_b:	7.75 h
Eccentricity e:	0.617
Pulsar mass m_p:	1.44 $M_\odot$
Companion mass m_c:	1.39 $M_\odot$ (neutron star)

From: Hulse & Taylor, 1975, ApJ, 195, 51

PSR B1913+16

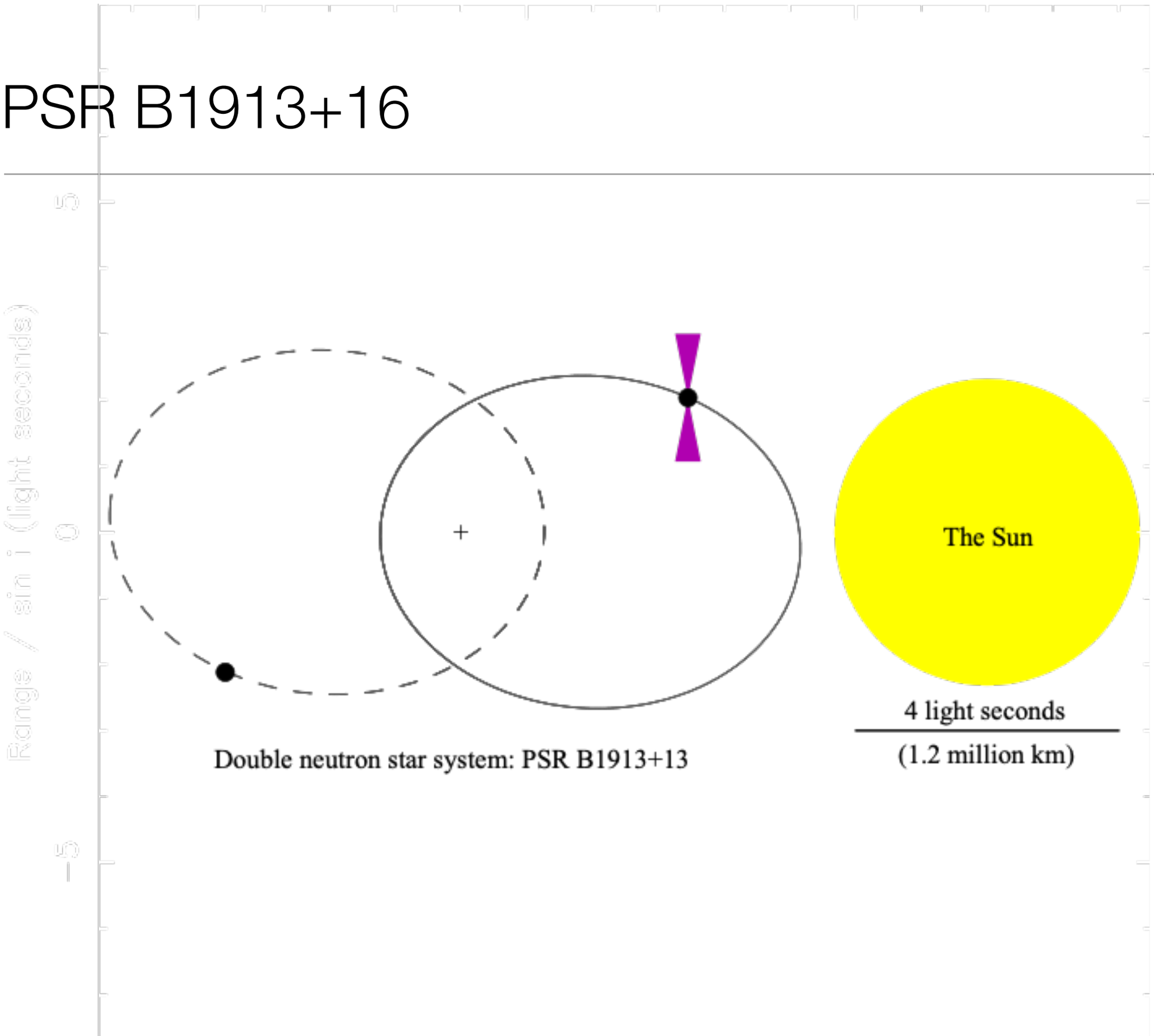

Double neutron star system: PSR B1913+13

Where do binary pulsars come from?

Figure from: Lorimer, D., *Living Rev. Relativity* 11 (2008), 8

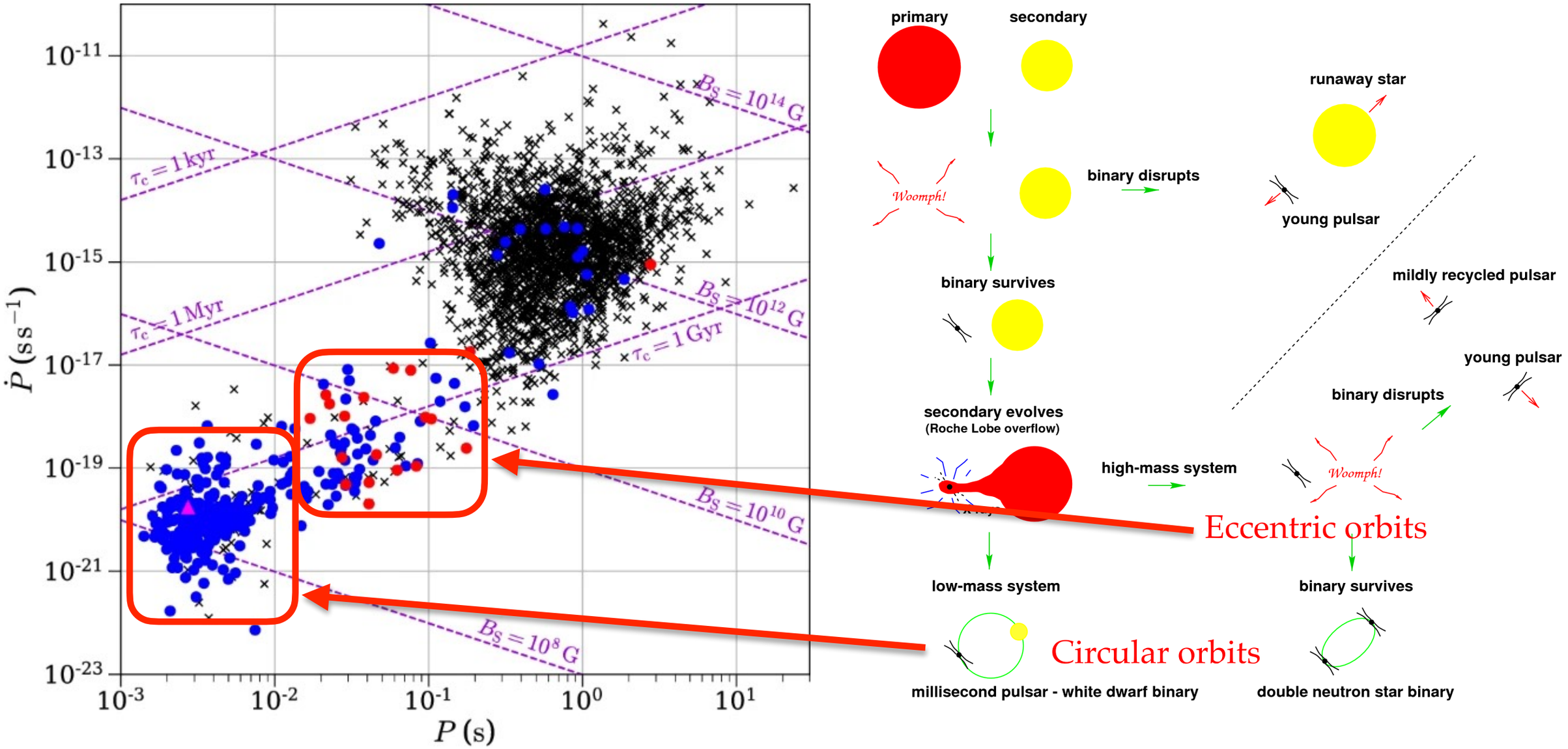

Figure from: Freire & Wex., *Living Rev. Relativity, 27* (2024), 5

Why a pulsar in a binary system is a big deal

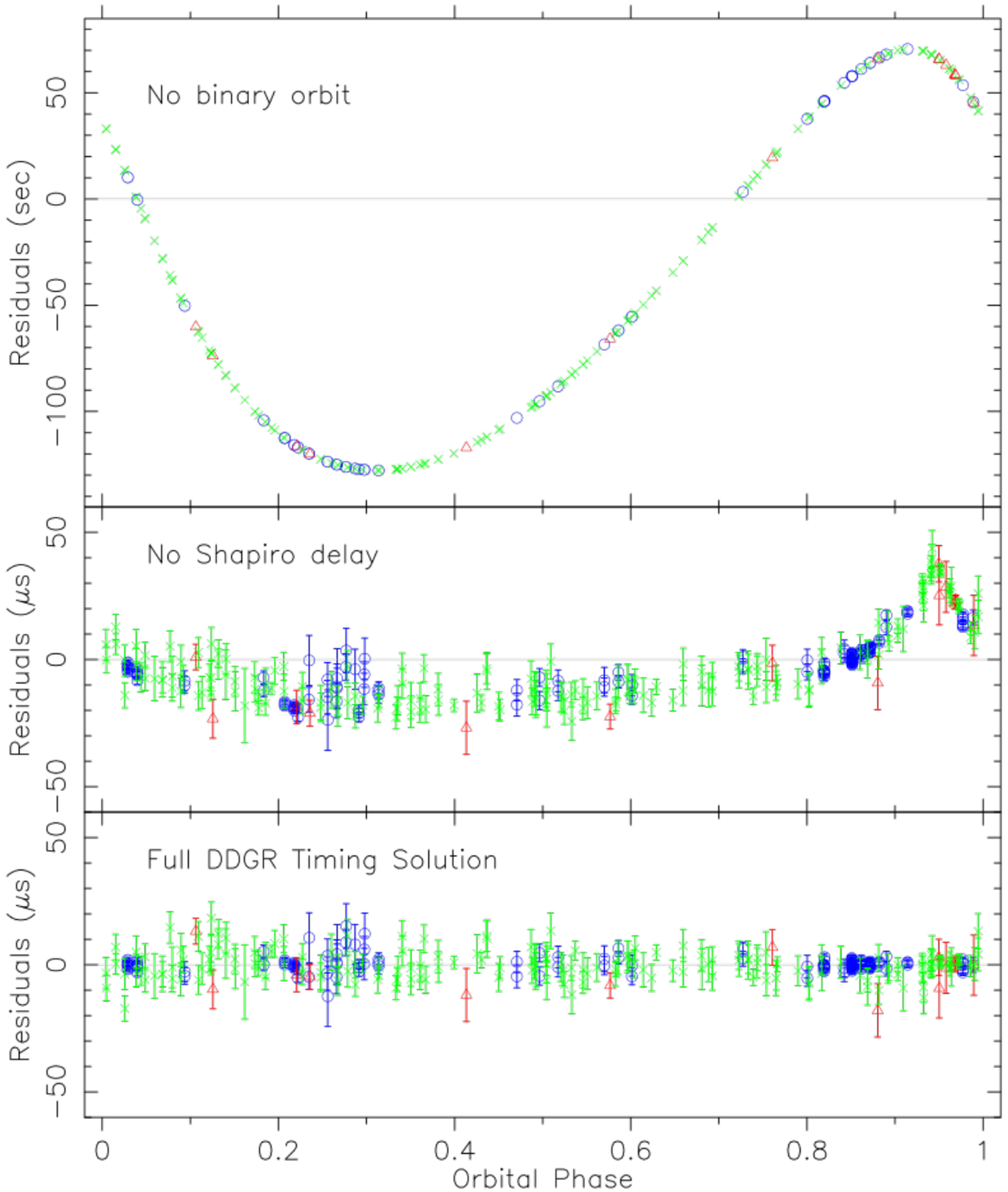

- In a binary pulsar, having a clock in the system allows us to measure the *range* relative to the center of mass of the binary.
- The 5 Keplerian orbital parameters derived from pulsar timing are *thousands of times* more precise than derived from Doppler measurements – *with the same observational data*!
- This feature is unique to pulsars, and is the fundamental reason why they are superior astrophysical tools.
- This precision allows the measurement of post-Keplerian parameters!

Figure: Scott Ransom

Mass function

For most binary pulsars, all we have are the Keplerian parameters and all we can derive is the mass function:

$$f(M_\mathrm{p}, M_\mathrm{c}, i) \equiv \frac{(M_\mathrm{c} \sin i)^3}{(M_\mathrm{p} + M_\mathrm{c})^3} = \frac{4\pi^2}{T_\odot} \frac{x^3}{P_\mathrm{b}^2}$$

$$T_\odot \equiv \frac{(\mathscr{G}\mathscr{M})_\odot^\mathrm{N}}{c^3} = 4.925490947641266978\ldots\,\mu\mathrm{s}$$

One equation, three (known) unknowns!
☹

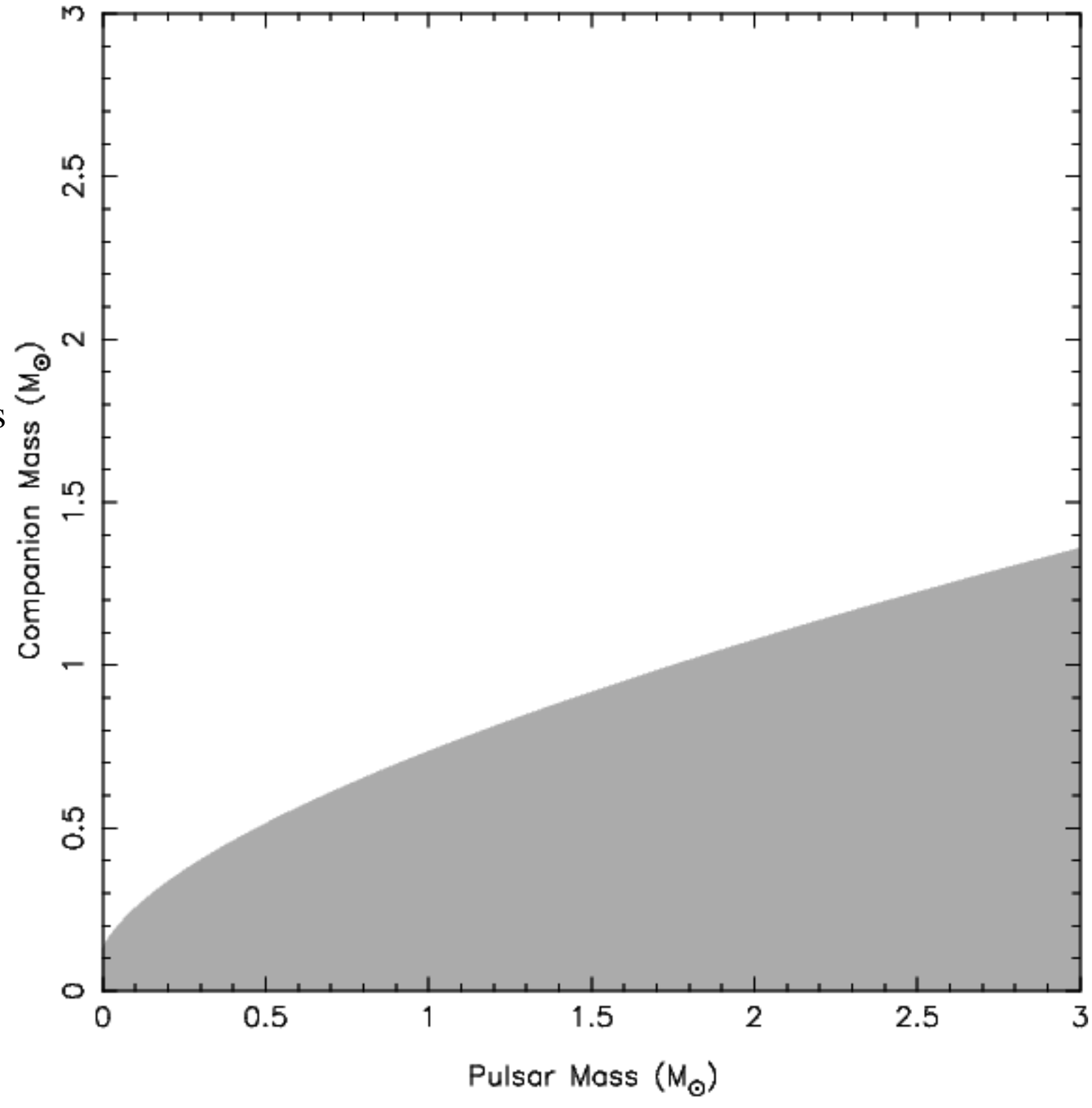

Relativistic effects

IF a binary pulsar is compact and eccentric – which B1913+16 certainly is – the timing precision allows the measurement of several relativistic effects:

- The advance of periastron
- The Einstein delay

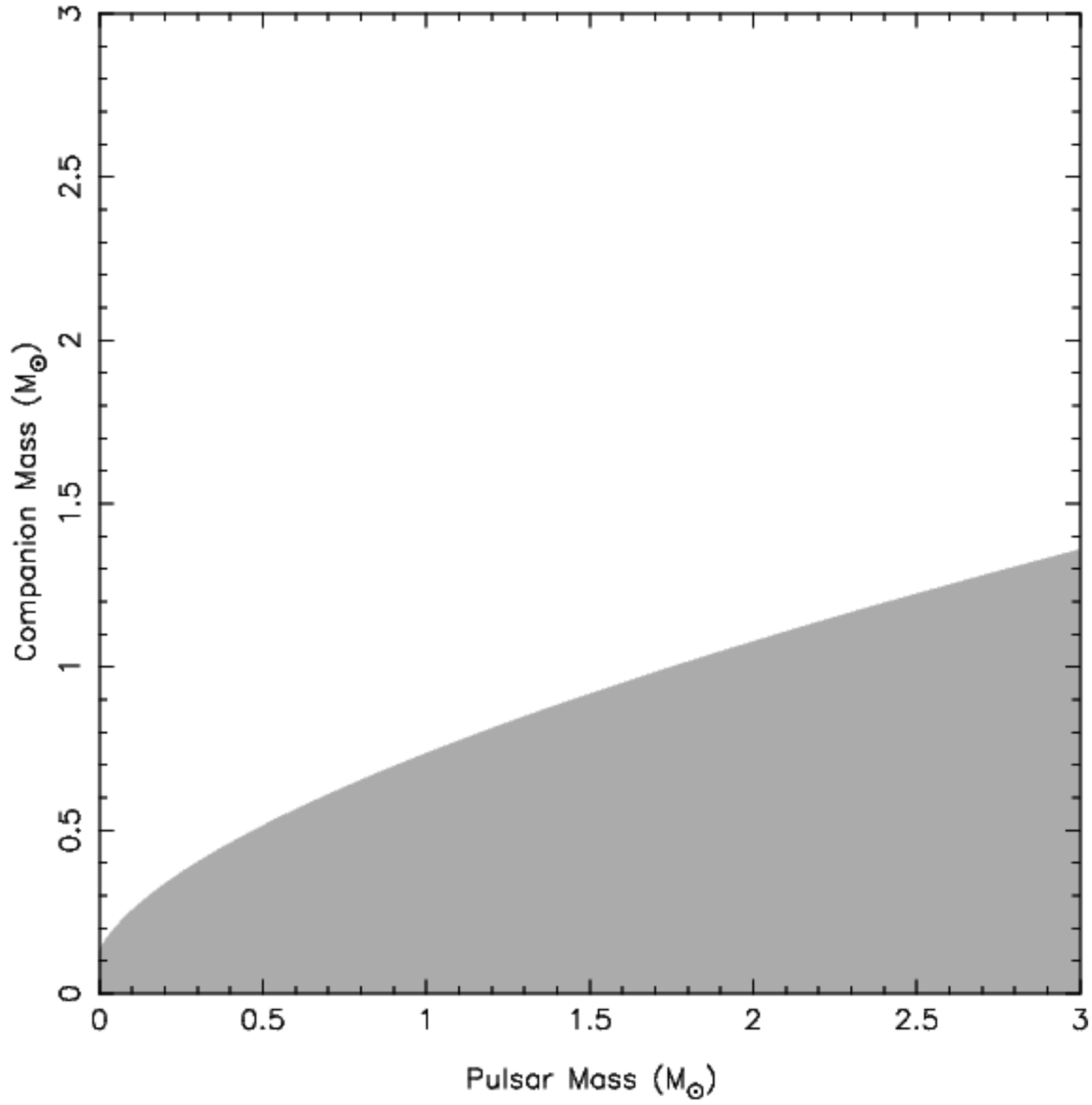

Precession of Orbit of B1913+16 and its Companion

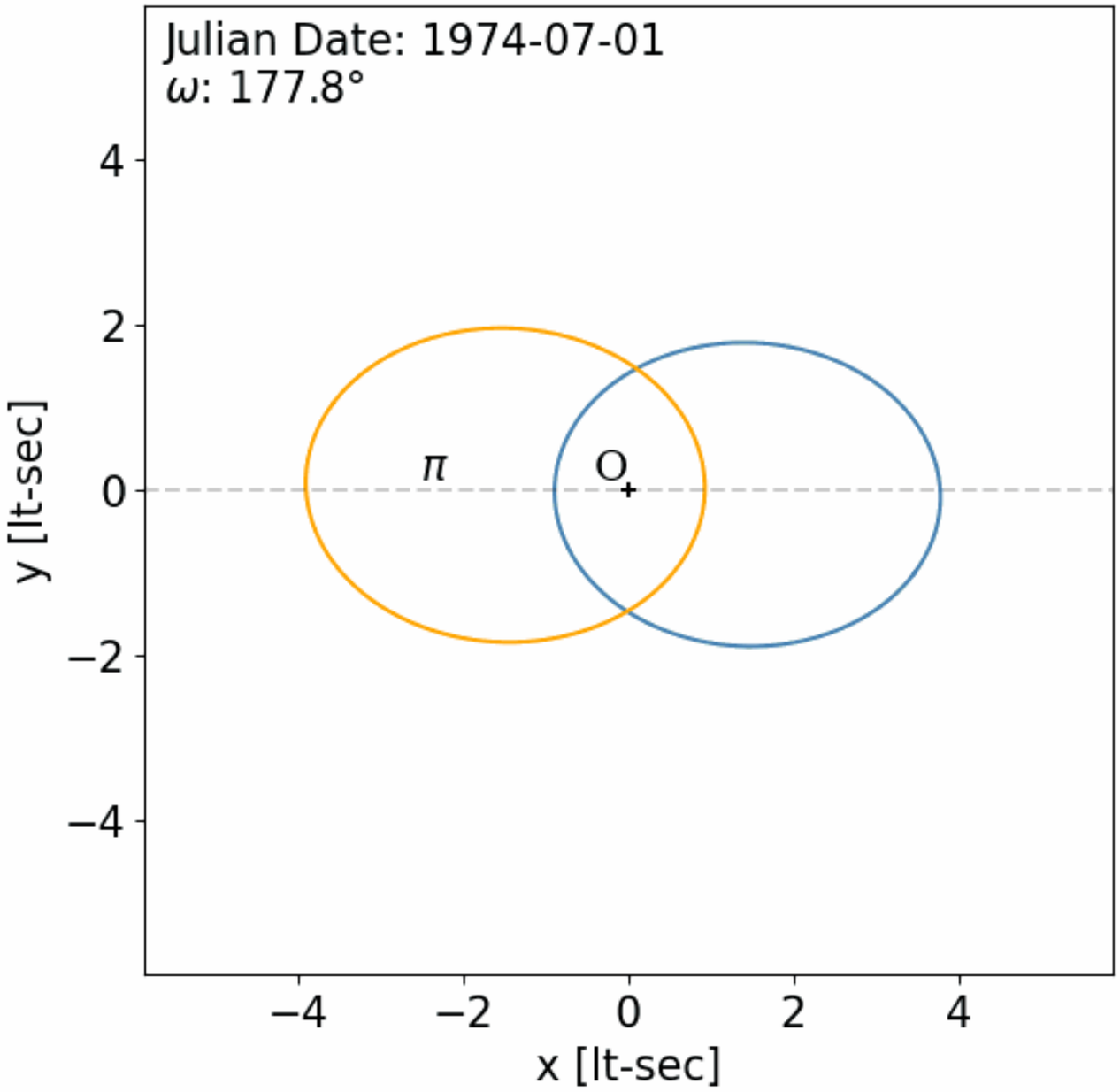

Epoch of the first Orbit:
1974-07-01 (MJD 42229.0)

Orbit of B1913+16
Orbit of Companion

$\omega_0 = 292.54°$

$\dot{\omega} = 4.23°$ / year

Orbital Period: $P_b = 0.32$ days

π - Plane of the sky

O - One of the foci (COM of the system)

Orbits are plotted for next 50 years with an interval of 1 years

Animation: Sanket Bangar

Periastron advance

Assuming GR, to 1 PN:

$$M = M_{\rm p} + M_{\rm c}$$

$$n_{\rm b} = \frac{2\pi}{P_{\rm b}}$$

$$\dot{\omega} = \frac{3 n_{\rm b}^{5/3}}{1-e^2} (M T_\odot)^{2/3}$$

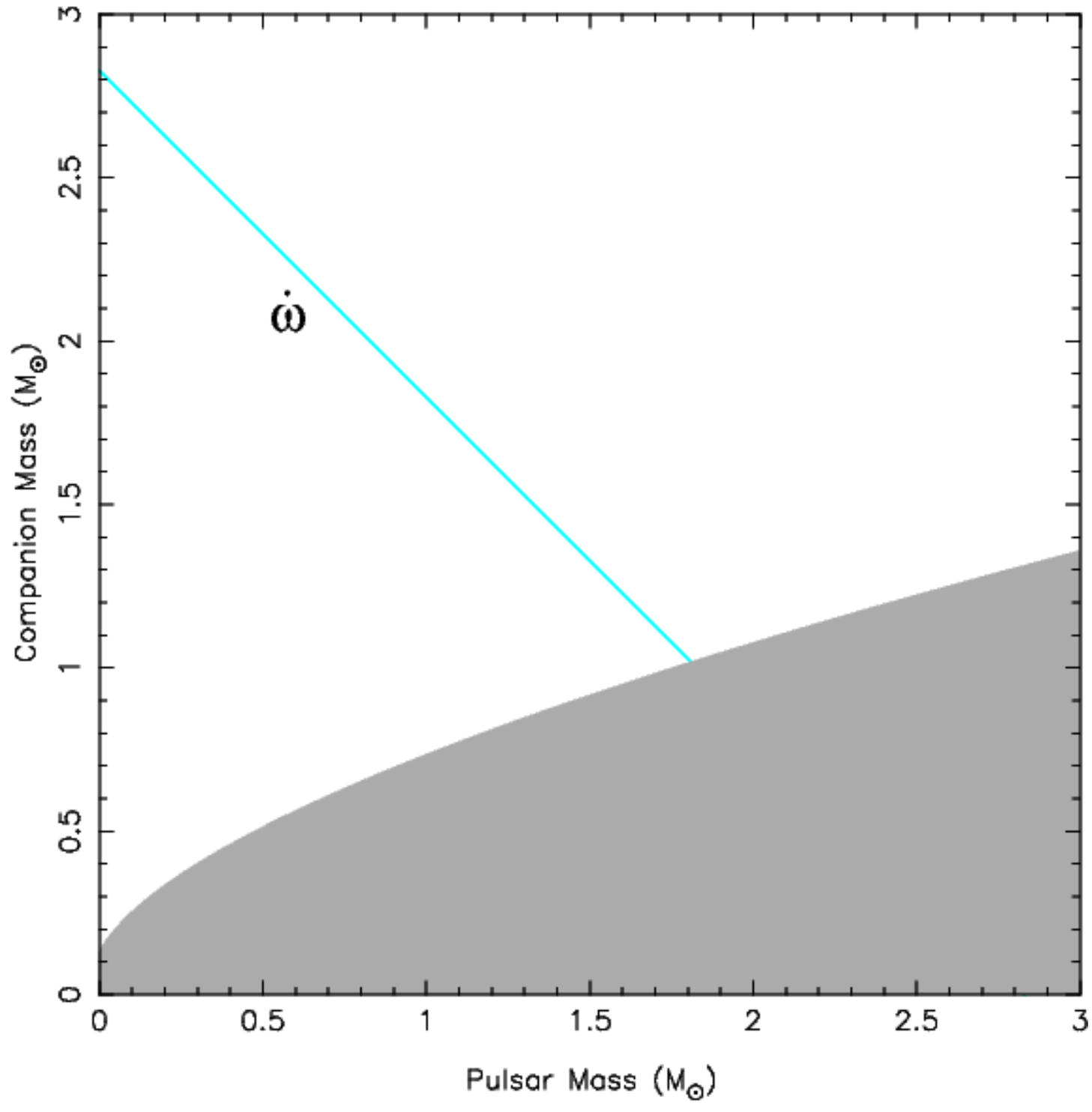

Einstein delay

Assuming GR, to 1 PN:

$$M = M_{\rm p} + M_{\rm c}$$

$$n_{\rm b} = \frac{2\pi}{P_{\rm b}}$$

$$\dot{\omega} = \frac{3 n_{\rm b}^{5/3}}{1-e^2} (M T_\odot)^{2/3}$$

$$\gamma = \frac{e T_\odot^{2/3}}{n_{\rm b}^{1/3}} \frac{M_{\rm c}(2M_{\rm c} + M_{\rm p})}{M^{4/3}}$$

- 3 equations for 3 unknowns! Precise masses can be derived!
- This was at the time the most precise measurement of any mass outside the solar system.

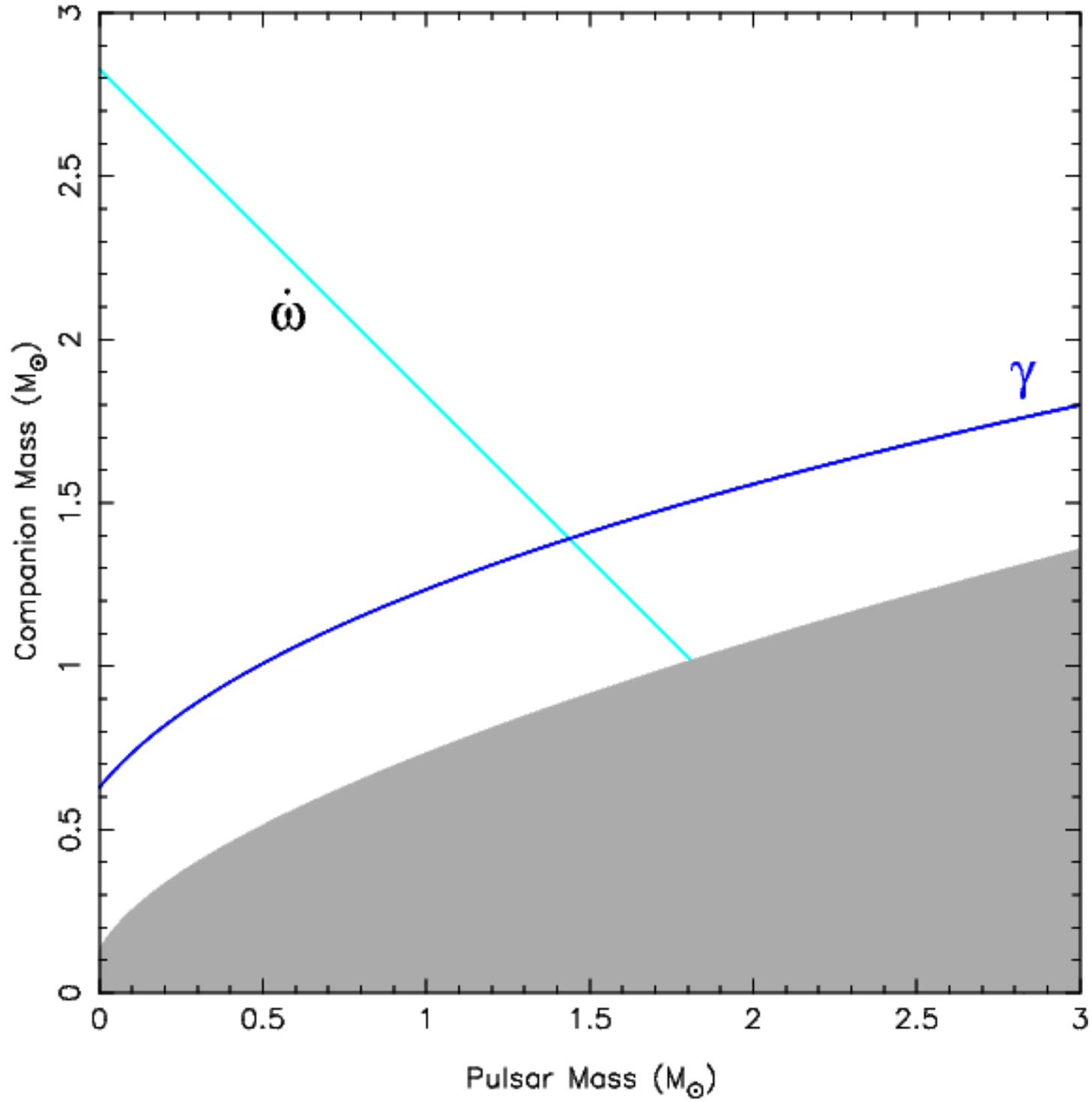

Orbital decay

- *A third relativistic effect soon became measurable – the orbital decay due to GW emission!*

- *Assuming* GR, LO PN [$(v/c)^5$]:

$$\dot{P}_{\rm b} = -\frac{192}{5}(n_{\rm b}T_{\odot})^{5/3} f_e \frac{M_{\rm p}M_{\rm c}}{M^{1/3}}$$

$$f_e = \frac{1}{(1-e^2)^{7/2}}\left(1 + \frac{73}{24}e^2 + \frac{37}{96}e^4\right)$$

- Prediction: the orbital period should decrease at a rate of –2.40247 × 10^{-12} s/s (or 75 μs per year!)

- *Effect not detectable in Solar System*!

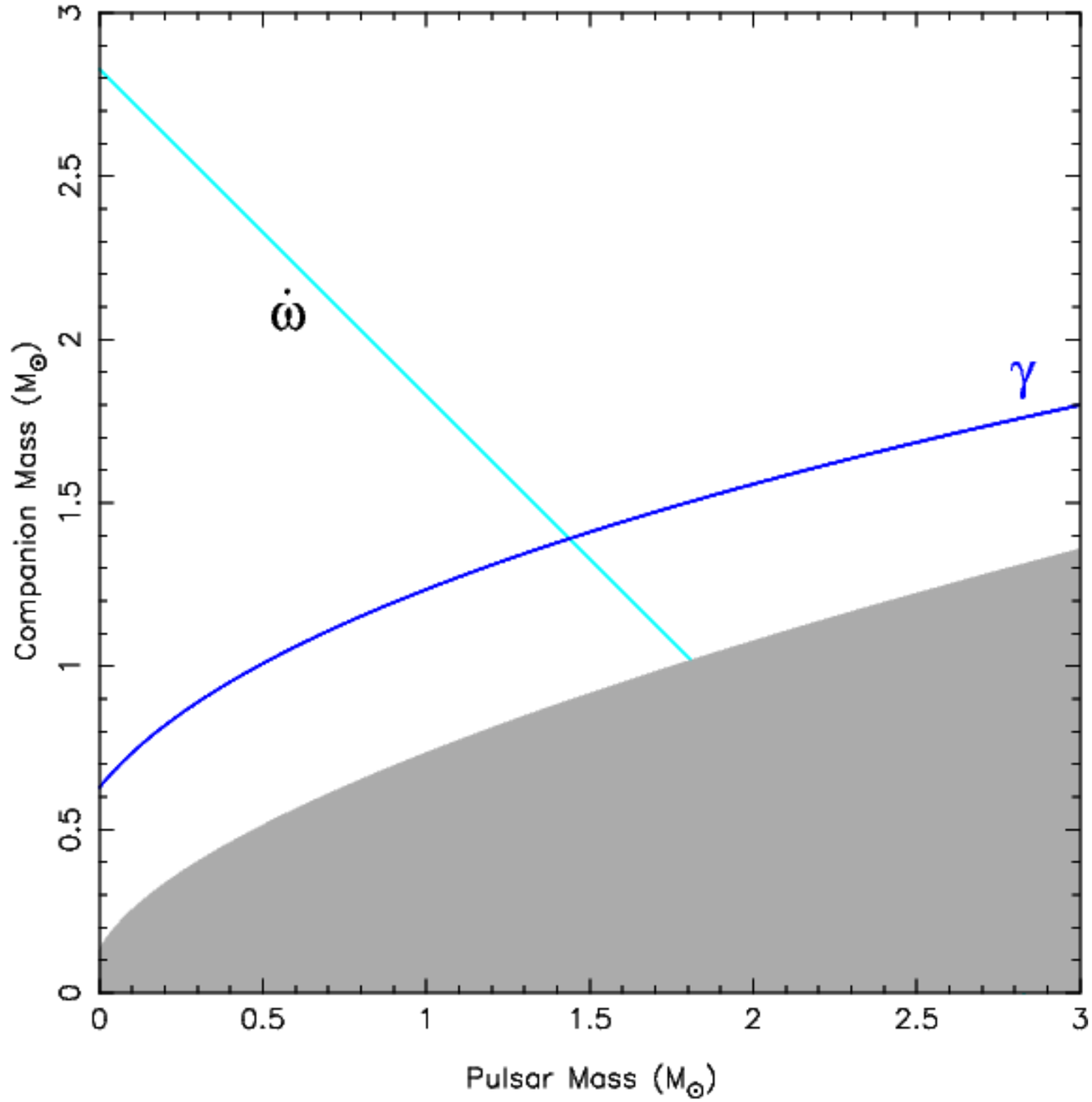

Test of general relativity

- Rate is –2.4085(52) x 10^{-12} s/s. Agreement with GR is perfect!

- GR gives a self-consistent estimate of the component masses!

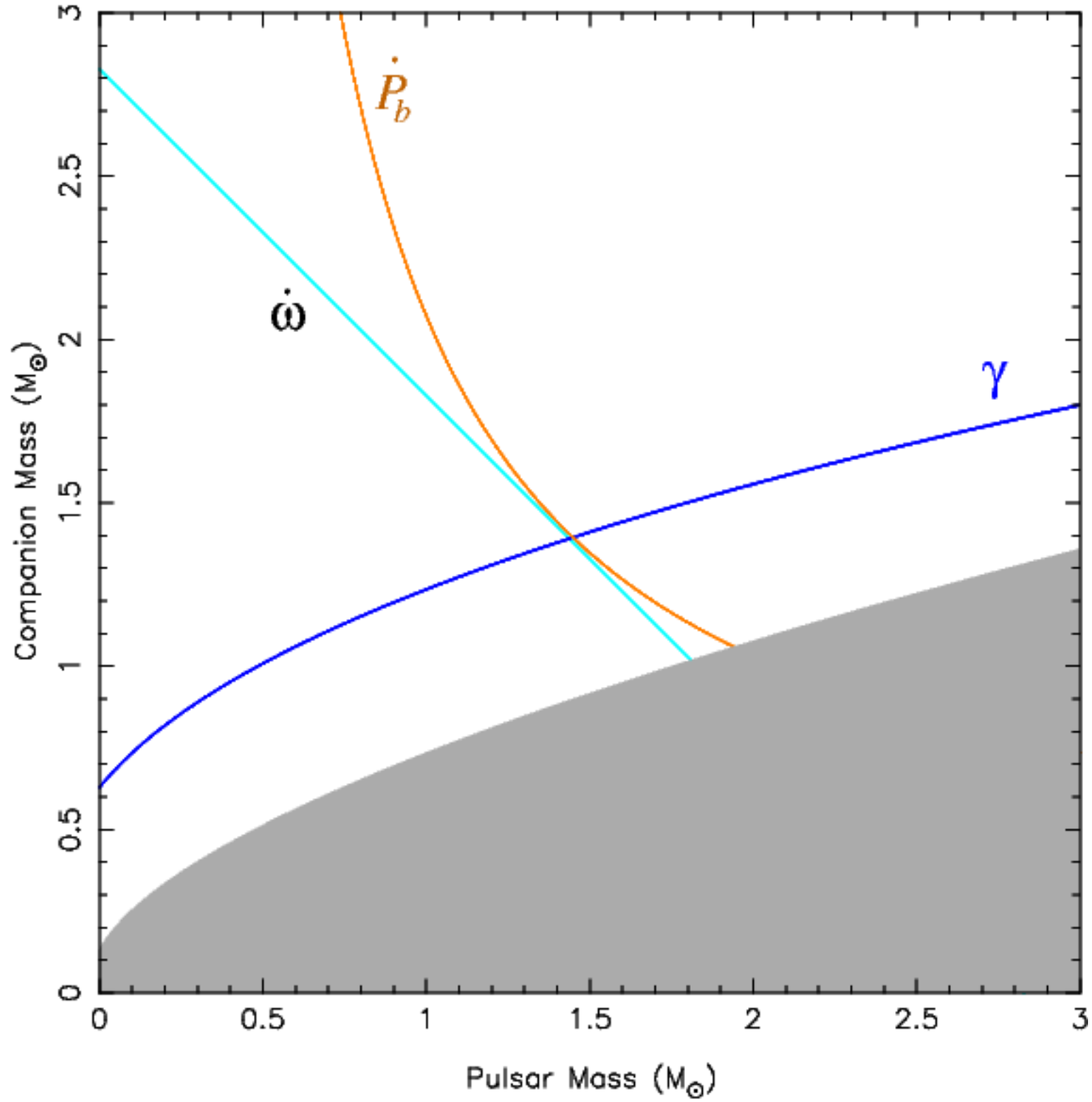

PSR B1913+16

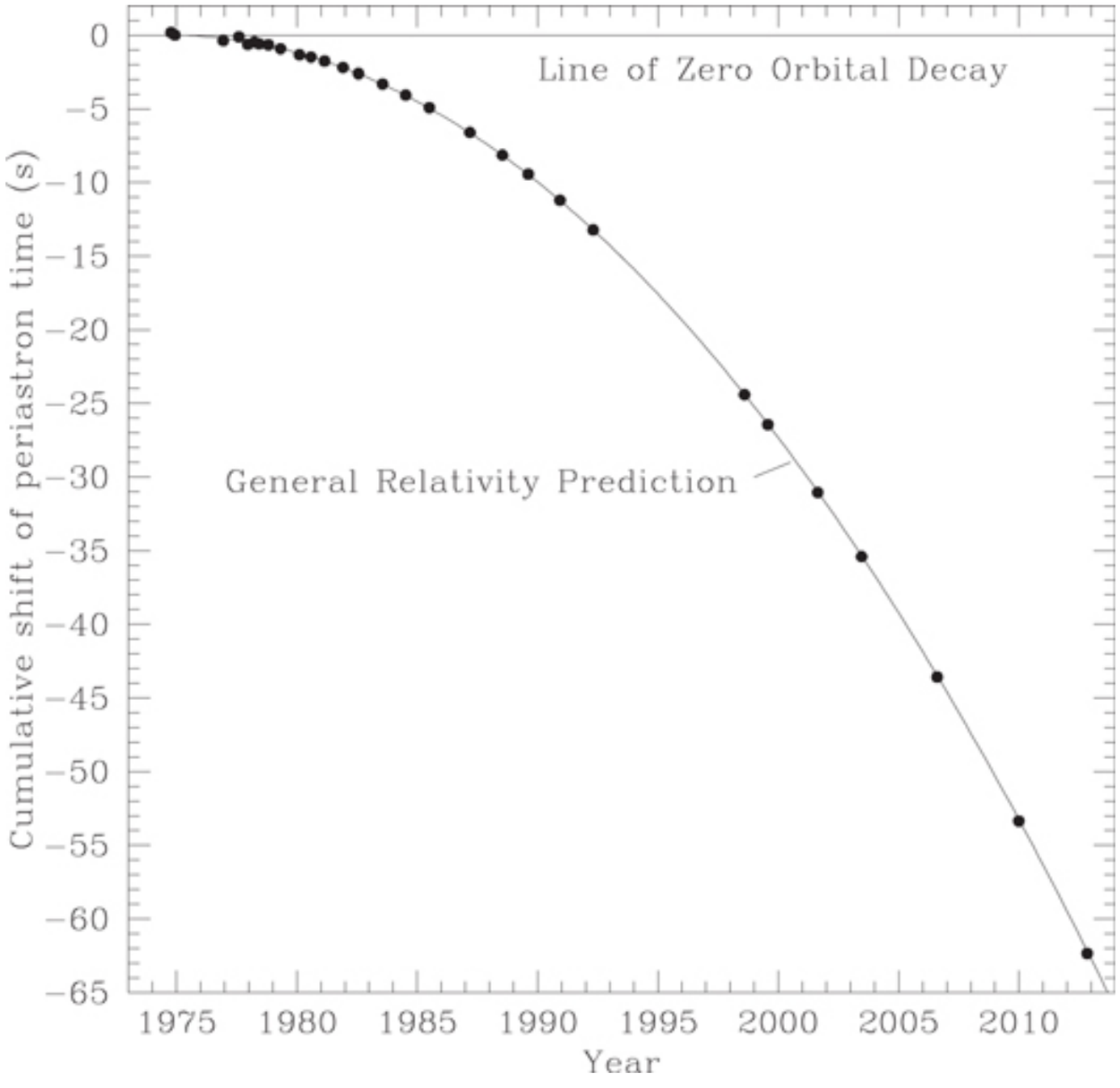

Gravitational waves exist!

Weisberg, J.M., and Huang, Y., 2016, ApJ. 829, 55

Variation of the orbital period

- Even for two point masses, the $\dot{P}_b$ is affected by kinematic effects, from the proper motion and from the… difference between the acceleration of the system and the acceleration of our Solar system projected along the line of sight from the Earth to the pulsar (a). Thus

$$\left(\frac{\dot{P}_b}{P_b}\right)_{\rm obs} = \left(\frac{\dot{P}_b}{P_b}\right)_{\rm int} + \frac{\mu^2 d}{c} + \frac{a}{c}$$

- This is one of the best-known corrections to the PK parameters. It limits the precision that can be achieved in orbital decay tests with the Hulse-Taylor pulsar, and will eventually limit it for the double pulsar. For a detailed account, see e.g., Damour & Taylor (1991, ApJ, 762, 94)

- *Because of the constant loss of orbital energy, the Hulse-Taylor binary will merge in 300 Myr*!

- *There must be many other such systems in the Universe*!

… and then came LIGO and Virgo…

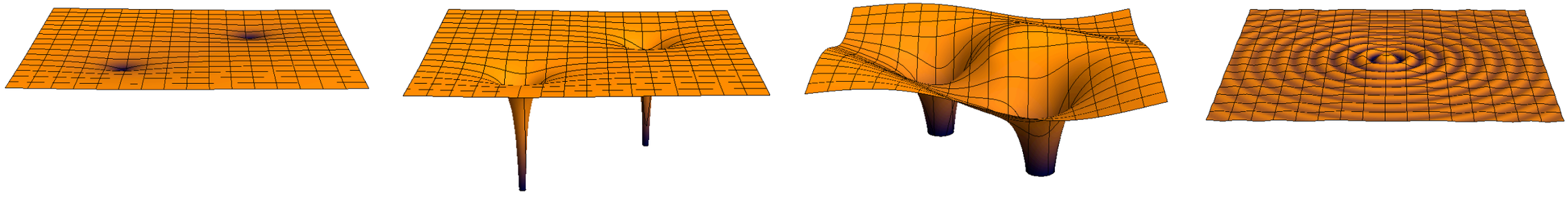

Figure 1: Illustration of the different gravity regimes used in this review.

From: Wex (2014)

3. The double pulsar

PSR J0737−3039

Discovered in the Galactic anti-center survey with Parkes (Burgay et al. 2003, Nature, 426, 531)

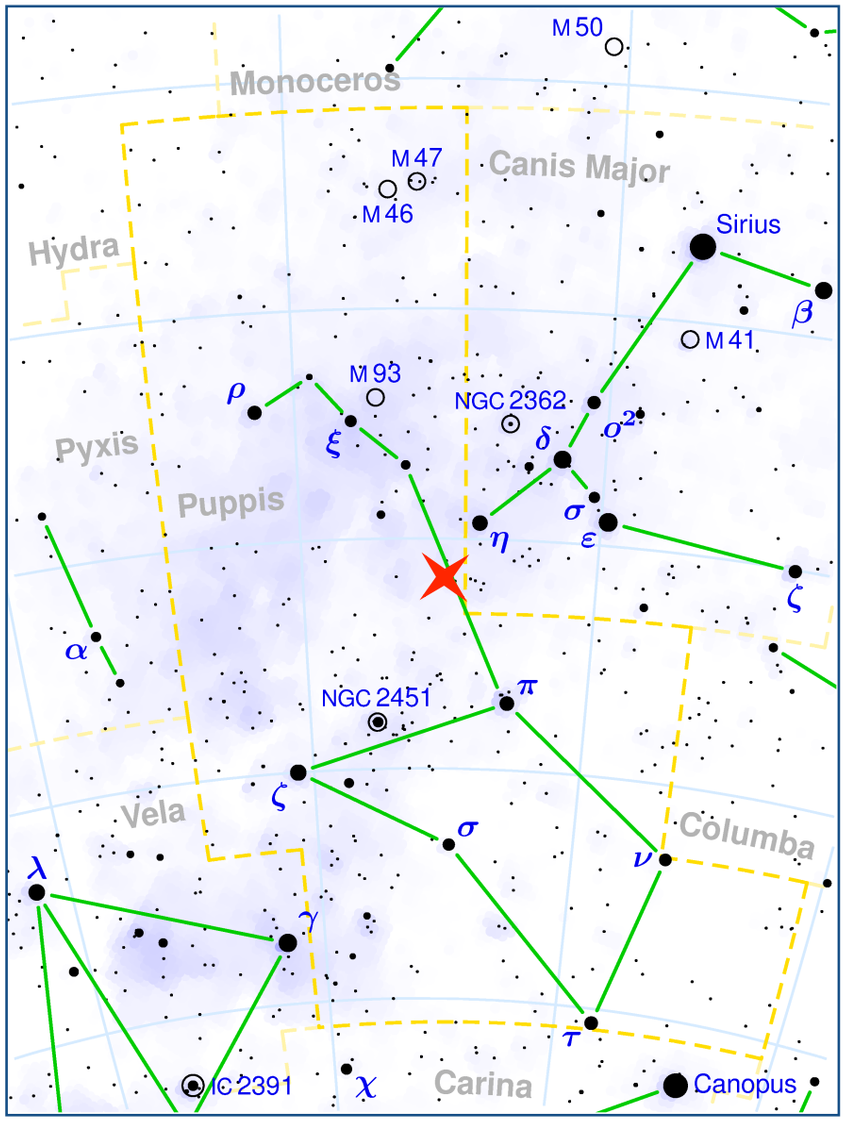

A compact pulsar - neutron star system

Nature sometimes is extremely generous! In this case, for many reasons...

#1: Orbital period of $2^h\ 27^m$, it was at the time *the most relativistic double neutron star system known*!

Advance of periastron and orbital decay are more prominent!

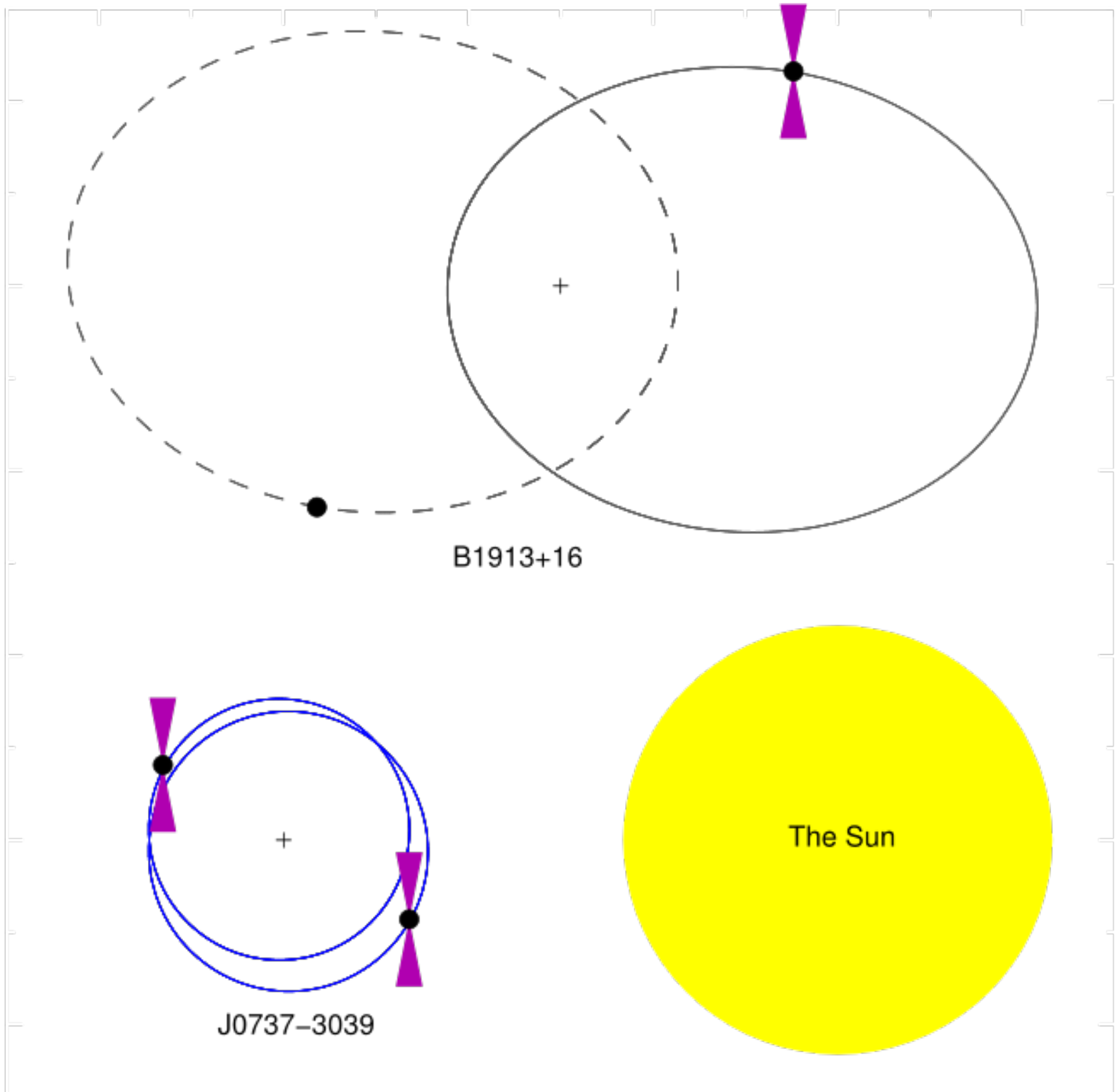

Detection of the Shapiro delay

#2: the system has *the highest orbital inclination for any binary pulsar*! The Shapiro delay is very precisely measured, providing two extra mass constraints!

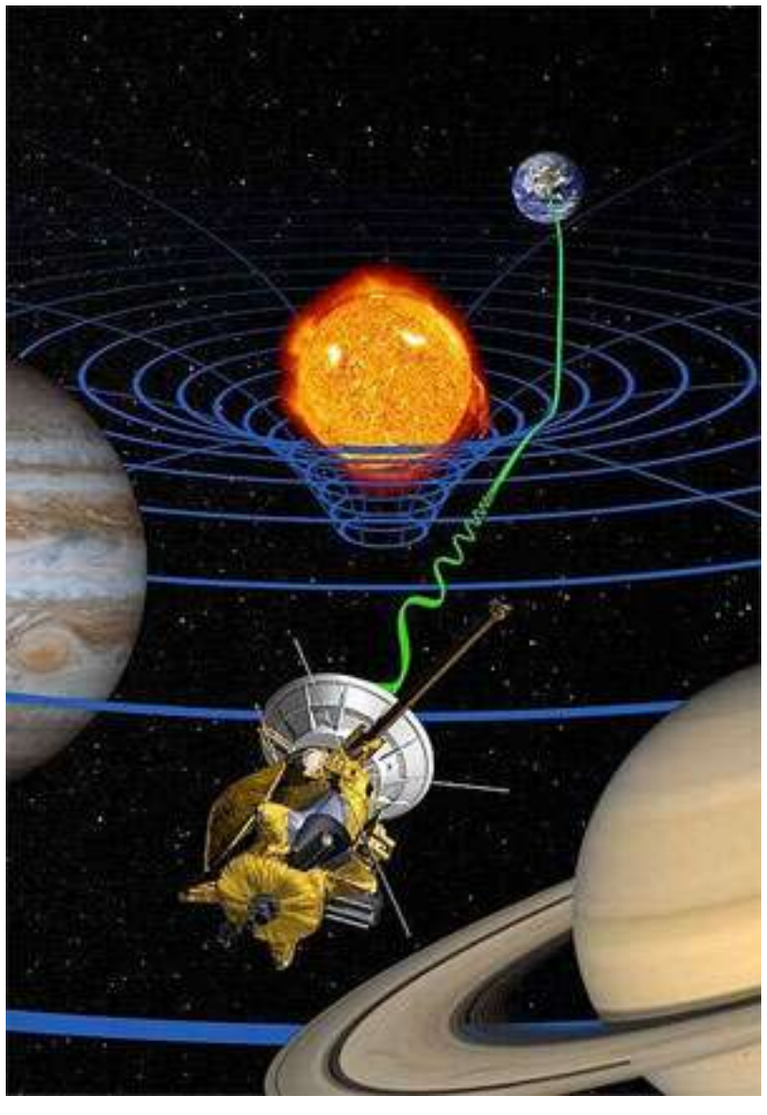

Credit: NASA

From: Kramer et al. (2006), Science, 314, 97

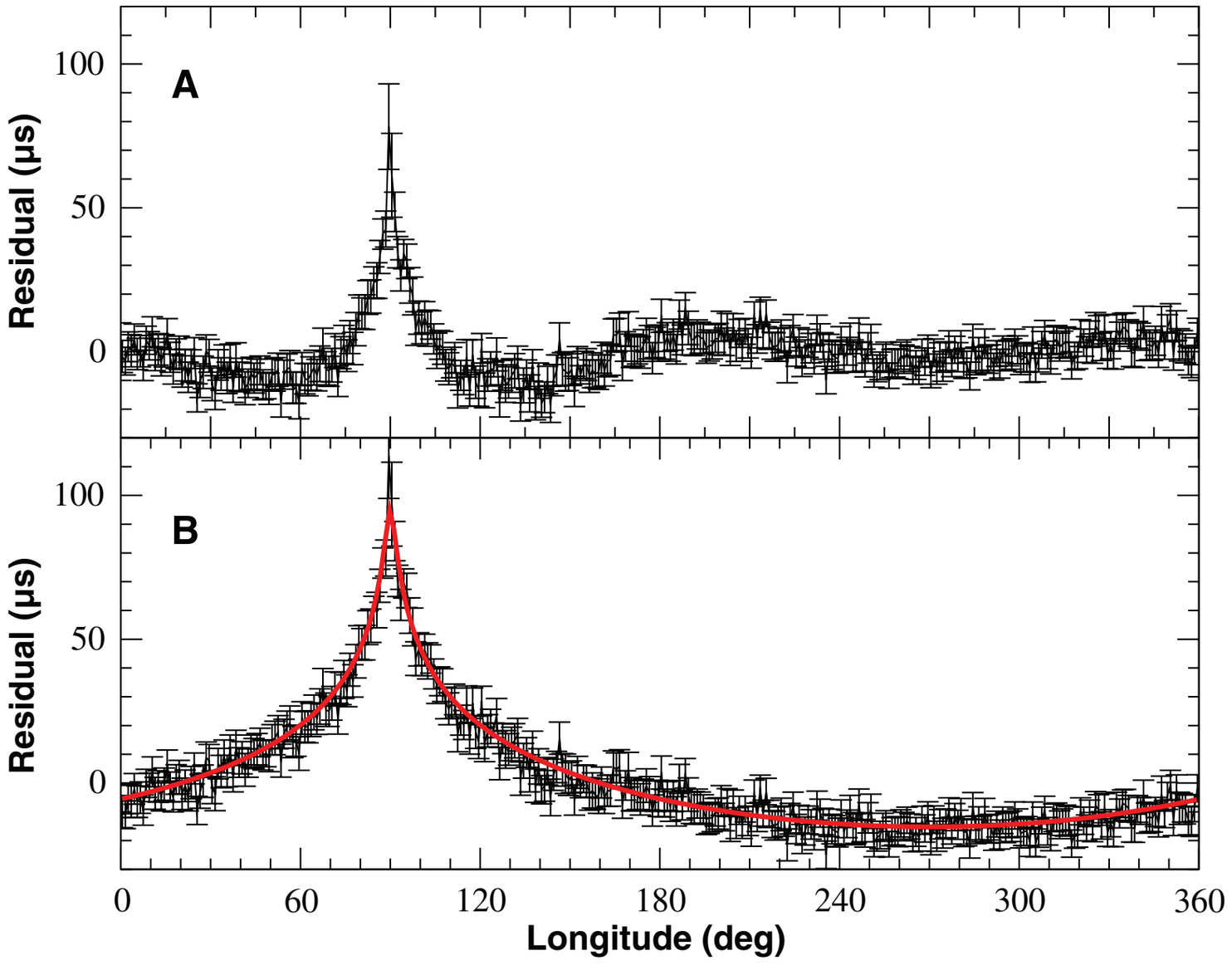

A double pulsar!

- **#3**: The second NS in the system (PSR J0737–3039B) *was detectable as a radio pulsar*!

- Finding such a system was one of the ``holy grails" of pulsar astronomy!

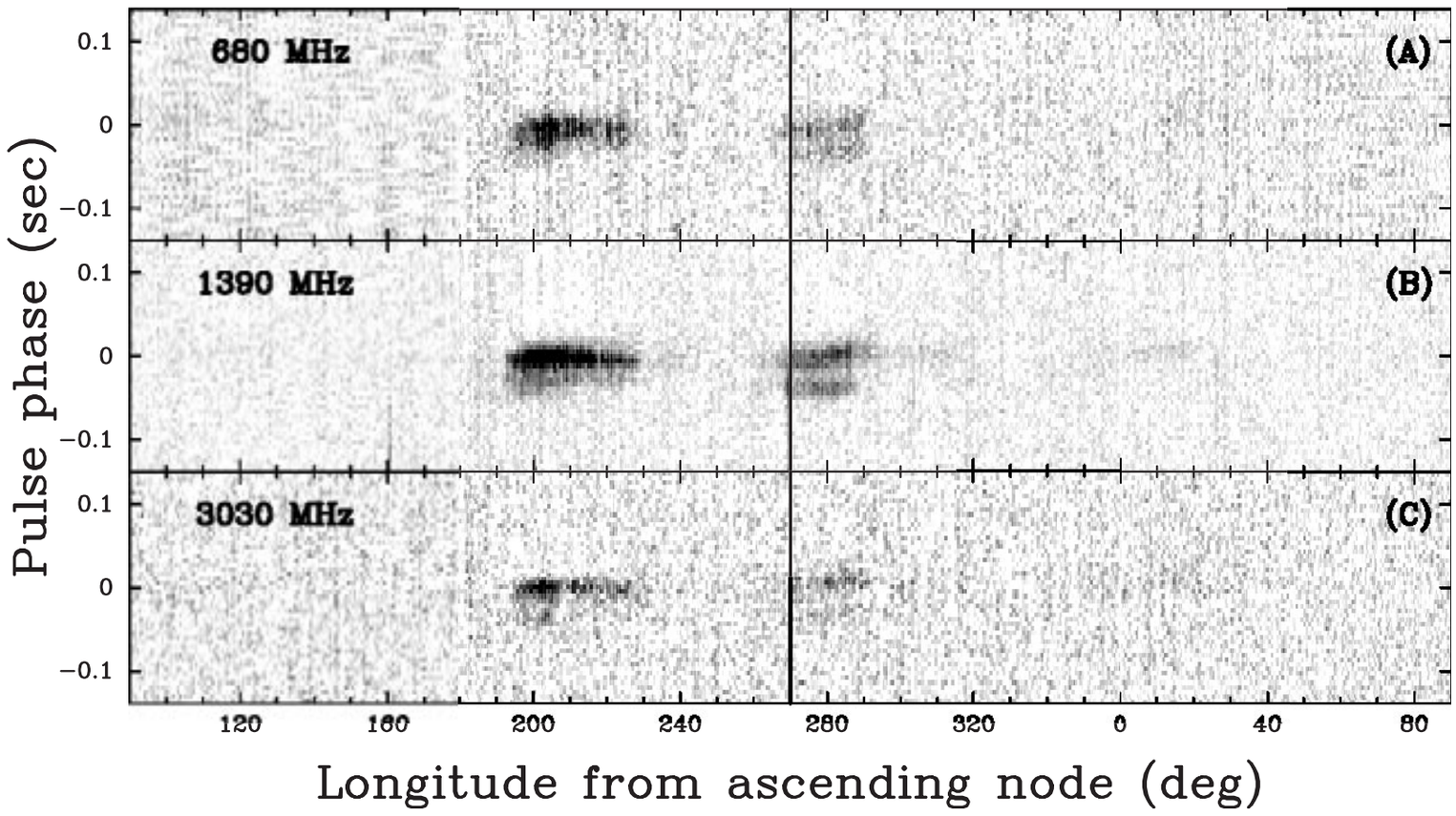

From: Lyne et al. (2004)

$$R = \frac{M_A}{M_B} = \frac{x_B}{x_A}$$

6 mass constraints for 2 unknowns! ***4 independent tests of GR****!*

DNS J0737−3039

- *GR passes all 4 tests!*
- There is a fifth test, from geodetic precession of PSR J0737−3039B (Breton et al. 2008, Science).

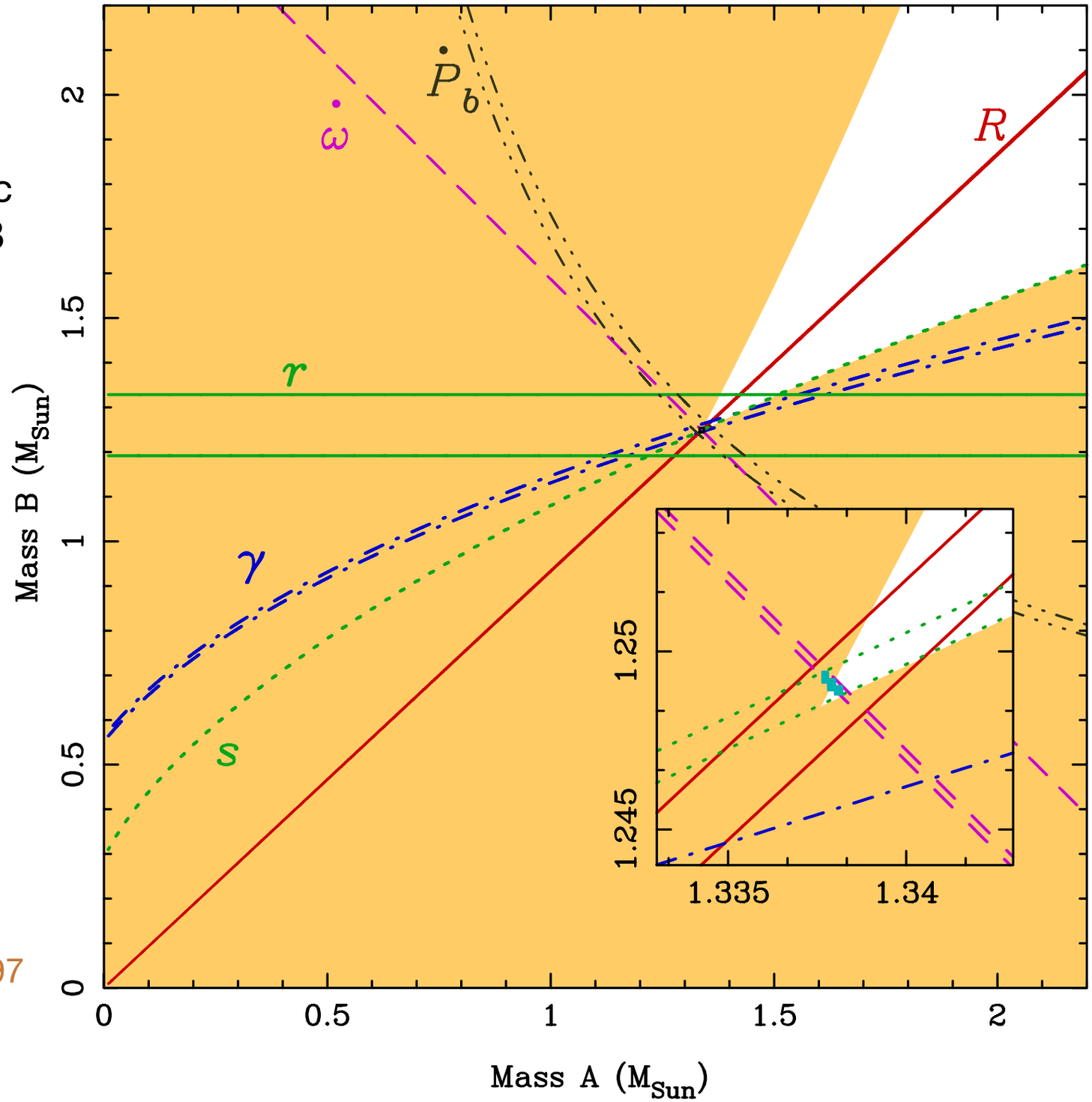

From: Kramer et al. (2006), Science, 314, 97

Measurement of the geodetic precession rate

Measurement of rate of geodetic precession was determined from shape of eclipses of this system:

$$\Omega_{\rm B} = 4.77 \pm 0.65\,{\rm deg/yr}$$

From: *Breton et al. 2008*

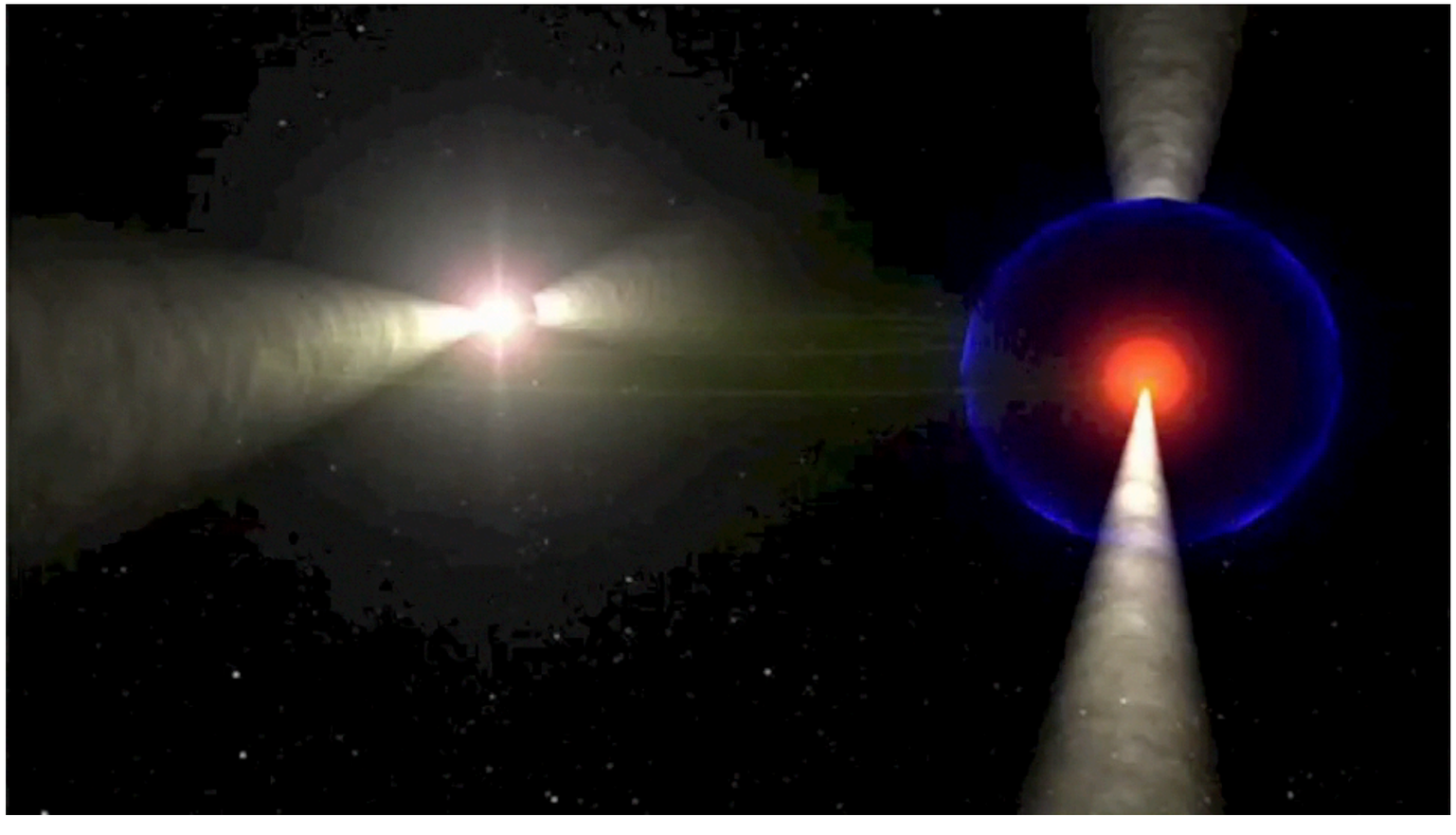

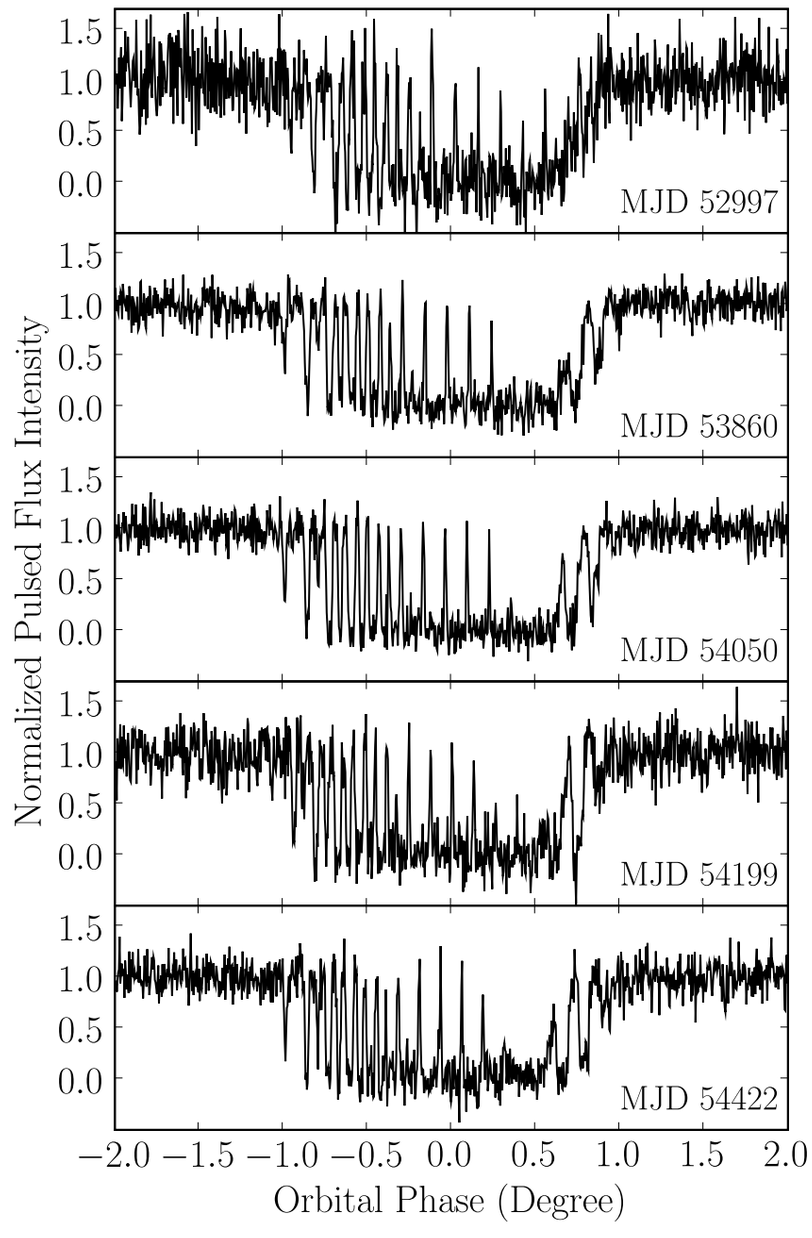

PHYSICAL REVIEW X **11,** 041050 (2021)

Featured in Physics

Strong-Field Gravity Tests with the Double Pulsar

M. Kramer,[1,2,*] I. H. Stairs,[3] R. N. Manchester,[4] N. Wex,[1] A. T. Deller,[5,6] W. A. Coles,[7] M. Ali,[1,8] M. Burgay,[9] F. Camilo,[10] I. Cognard,[11,12] T. Damour,[13] G. Desvignes,[14,1] R. D. Ferdman,[15] P. C. C. Freire,[1] S. Grondin,[3,16] L. Guillemot,[11,12] G. B. Hobbs,[4] G. Janssen,[17,18] R. Karuppusamy,[1] D. R. Lorimer,[19] A. G. Lyne,[2] J. W. McKee,[1,20] M. McLaughlin,[19] L. E. Münch,[1] B. B. P. Perera,[21] N. Pol,[19,22] A. Possenti,[9,23] J. Sarkissian,[4] B. W. Stappers,[2] and G. Theureau[11,12,24]

[1]*Max-Planck-Institut für Radioastronomie, Auf dem Hügel 69, D-53121 Bonn, Germany*
[2]*Jodrell Bank Centre for Astrophysics, The University of Manchester, Oxford M13 9PL, United Kingdom*
[3]*Department of Physics and Astronomy, University of British Columbia, 6224 Agricultural Road, Vancouver, British Columbia V6T 1Z1, Canada*
[4]*Australia Telescope National Facility, CSIRO Space and Astronomy, P.O. Box 76, Epping, New South Wales 1710, Australia*
[5]*Centre for Astrophysics and Supercomputing, Swinburne University of Technology, P.O. Box 218, Hawthorn, Victoria 3122, Australia*
[6]*ARC Centre of Excellence for Gravitational Wave Discovery (OzGrav), P.O. Box 218, Hawthorn, Victoria 3122, Australia*
[7]*Electrical and Computer Engineering, University of California at San Diego, La Jolla, California 92093, USA*
[8]*Perimeter Institute for Theoretical Physics, 31 Caroline Street North, Waterloo, Ontario, Canada N2L 2Y5*
[9]*INAF-Osservatorio Astronomico di Cagliari, Via della Scienza 5, 09047 Selargius (CA), Italy*
[10]*South African Radio Astronomy Observatory, 2 Fir Street, Black River Park, Observatory 7925, South Africa*
[11]*Laboratoire de Physique et Chimie de l'Environnement et de l'Espace LPC2E CNRS-Université d'Orléans, F-45071 Orléans, France*
[12]*Station de Radioastronomie de Nançay, Observatoire de Paris, CNRS/INSU, F-18330 Nançay, France*
[13]*Institut des Hautes Études Scientifiques, 91440 Bures-sur-Yvette, France*
[14]*LESIA, Observatoire de Paris, Universit PSL, CNRS, Sorbonne Université, Universit de Paris,*

16 yr of observations with many radio telescopes!

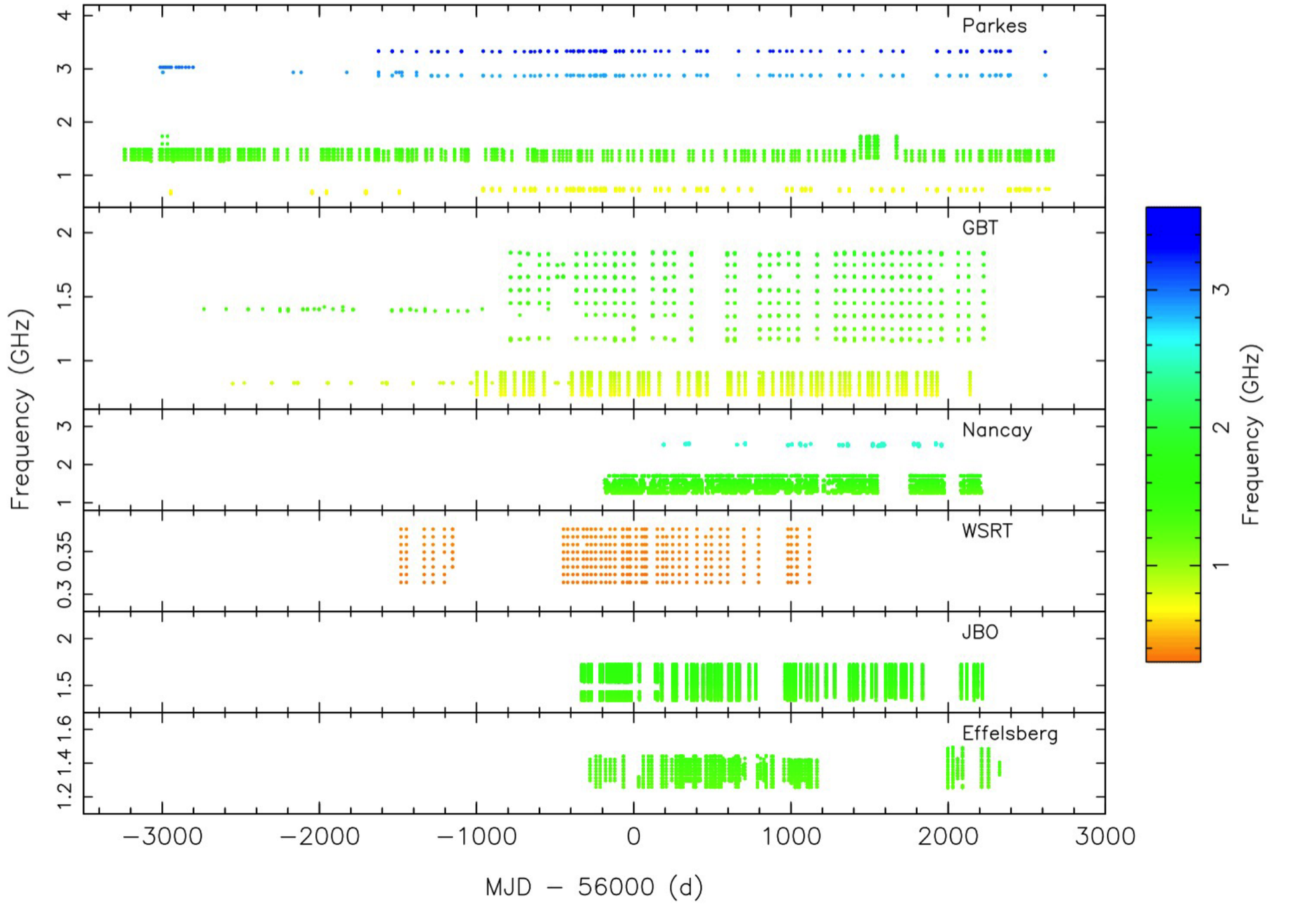

Kramer et al. (2021)

FIG. 1. Time and frequency coverage of the 4-min-sampled ToAs from the contributing observatories.

Unprecedented precision!

Right ascension (R.A.), α (J2000)	$07^{h}37^{m}51^{s}.248115(10)$[a]
Declination (Dec), δ (J2000)	$-30°39'40''.70485(17)$[a]
Proper motion R.A., μ_α ($\mathrm{mas\,yr^{-1}}$)	$-2.567(30)$[a]
Proper motion Dec., μ_δ ($\mathrm{mas\,yr^{-1}}$)	$2.082(38)$[a]
Parallax, π_c (mas)	$1.36(+0.12,-0.10)$[a]
Position epoch (MJD)	55045.0000
Rotational frequency (freq.), ν (Hz)	44.054 068 641 962 81(17)[b]
First freq. derivative, $\dot{\nu}$ ($\mathrm{Hz\,s^{-1}}$)	$-3.4158071(11)\times10^{-15}$[b]
Second freq. derivative, $\ddot{\nu}$ ($\mathrm{Hz\,s^{-2}}$)	$-2.286(29)\times10^{-27}$[b]
Third freq. derivative, $\dddot{\nu}$ ($\mathrm{Hz\,s^{-3}}$)	$1.28(26)\times10^{-36}$[b]
Fourth freq. derivative, $\ddddot{\nu}$ ($\mathrm{Hz\,s^{-4}}$)	$4.580(86)\times10^{-43}$[b]
Timing epoch, t_0 (MJD)	55700.0
Profile evolution, FD parameter c_1	0.0000180(75)
Profile evolution, FD parameter c_2	−0.0001034(10)
Profile evolution, FD parameter c_3	0.0000474(26)
Dispersion measure, DM ($\mathrm{pc\,cm^{-3}}$)	48.917 208
Orbital period, P_b (day)	0.102 251 559 297 3(10)
Projected semimajor axis, x (s)	1.415 028 603(92)
Eccentricity (Kepler equation), e_T	0.087 777 023(61)
Epoch of periastron, T_0 (MJD)	55 700.233 017 540(13)
Longitude of periastron, ω_0 (deg)	204.753 686(47)
Periastron advance, $\dot{\omega}$ ($\mathrm{deg\,yr^{-1}}$) [c]	16.899 323(13)
Change of orbital period, $\dot{P}_\mathrm{b}$	$-1.247920(78)\times10^{-12}$
Einstein delay amplitude, γ_E (ms)	0.384 045(94)
Logarithmic Shapiro shape, z_s	9.65(15)
Range of Shapiro delay, r (μs)	6.162(21)
NLO factor for signal prop., q_NLO	1.15(13)
Relativistic deformation of orbit, δ_θ	$13(13)\times10^{-6}$
Change of proj. semimajor axis, $\dot{x}$	$8(7)\times10^{-16}$
Change of eccentricity, $\dot{e}_T$ ($\mathrm{s^{-1}}$)	$3(6)\times10^{-16}$

Kramer et al. (2021)

Mass-mass diagram in 2021

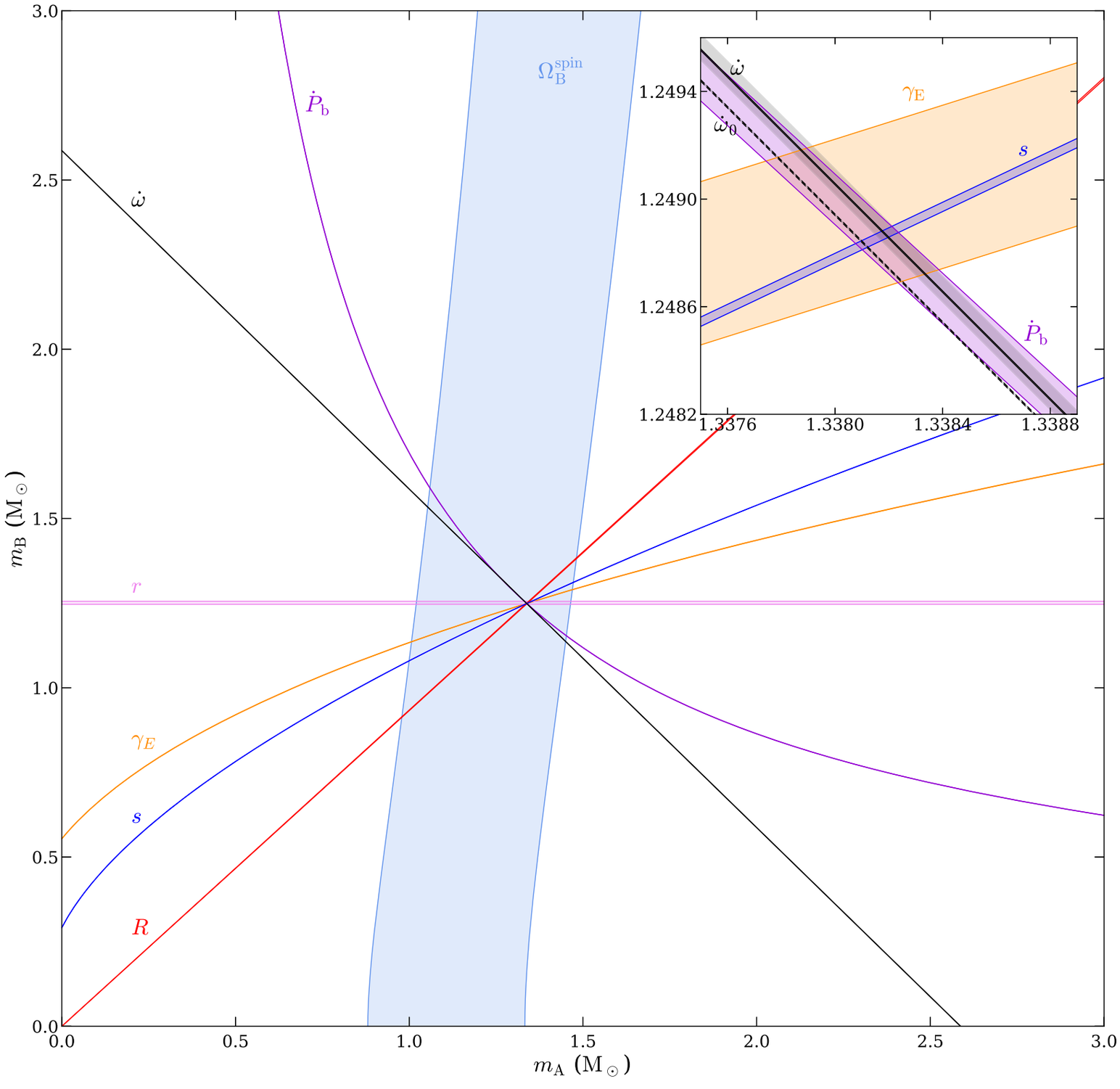

$$M_{\rm A} = 1.338185^{+0.000012}_{-0.000014}\,{\rm M}_\odot$$

$$M_{\rm B} = 1.248868^{+0.000013}_{-0.000011}\,{\rm M}_\odot$$

$$M = 2.587052^{+0.000009}_{-0.000007}\,{\rm M}_\odot$$

Kramer et al. (2021)

TABLE V. Summary of the relativistic effects measured in our analysis and list of the resulting independent strong-field tests of GR. For each test, the remaining PK parameters and the mass ratio are used to determine the masses of pulsars A and B as input for GR predictions. In addition, parameters that test the significance of specific higher-order contributions in the advance of periastron and the signal propagation are given.

Relativistic effect	Parameter	Obs./GR pred.
Shapiro delay shape	s	1.00009(18)
Shapiro delay range	r	1.0016(34)
Time dilation	$\gamma_{\rm E}$	1.00012(25)
Periastron advance	$\dot{\omega} \equiv n_{\rm b} k$	1.000015(26)
GW emission	$\dot{P}_{\rm b}$	0.999963(63)
Orbital deformation	δ_θ	1.3(13)
Spin precession	$\Omega_{\rm B}^{\rm spin}$	0.94(13)[a]
Tests of higher-order contributions		
Lense-Thirring contrib. to k	$\lambda_{\rm LT}$	0.7(9)
NLO signal propagation	$q_{\rm NLO}[\rm total]$	1.15(13)
… from signal deflection	$q_{\rm NLO}[\rm deflect]$	1.26(24)
… from signal retardation	$q_{\rm NLO}[\rm retard]$	1.32(24)

Kramer et al. (2021)

Advance of periastron

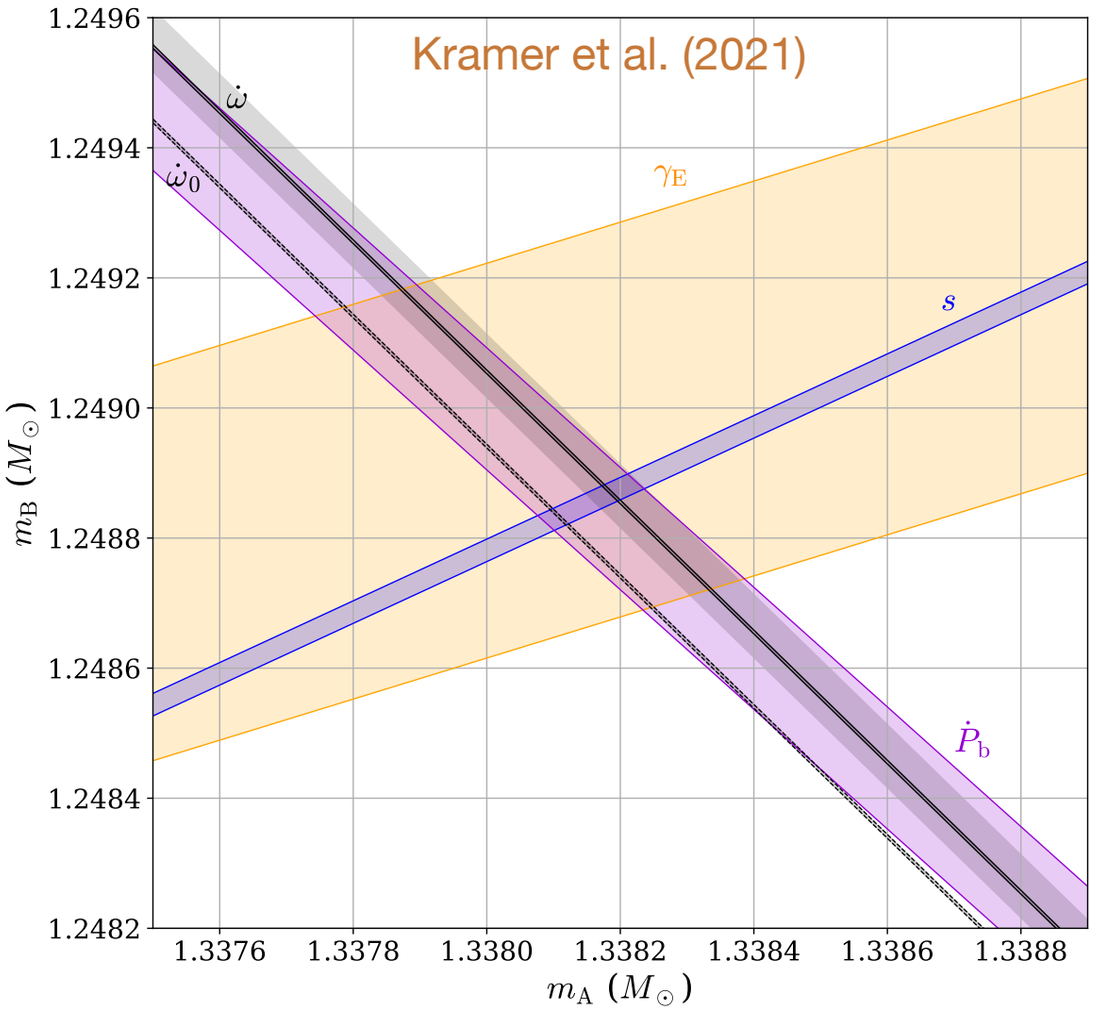

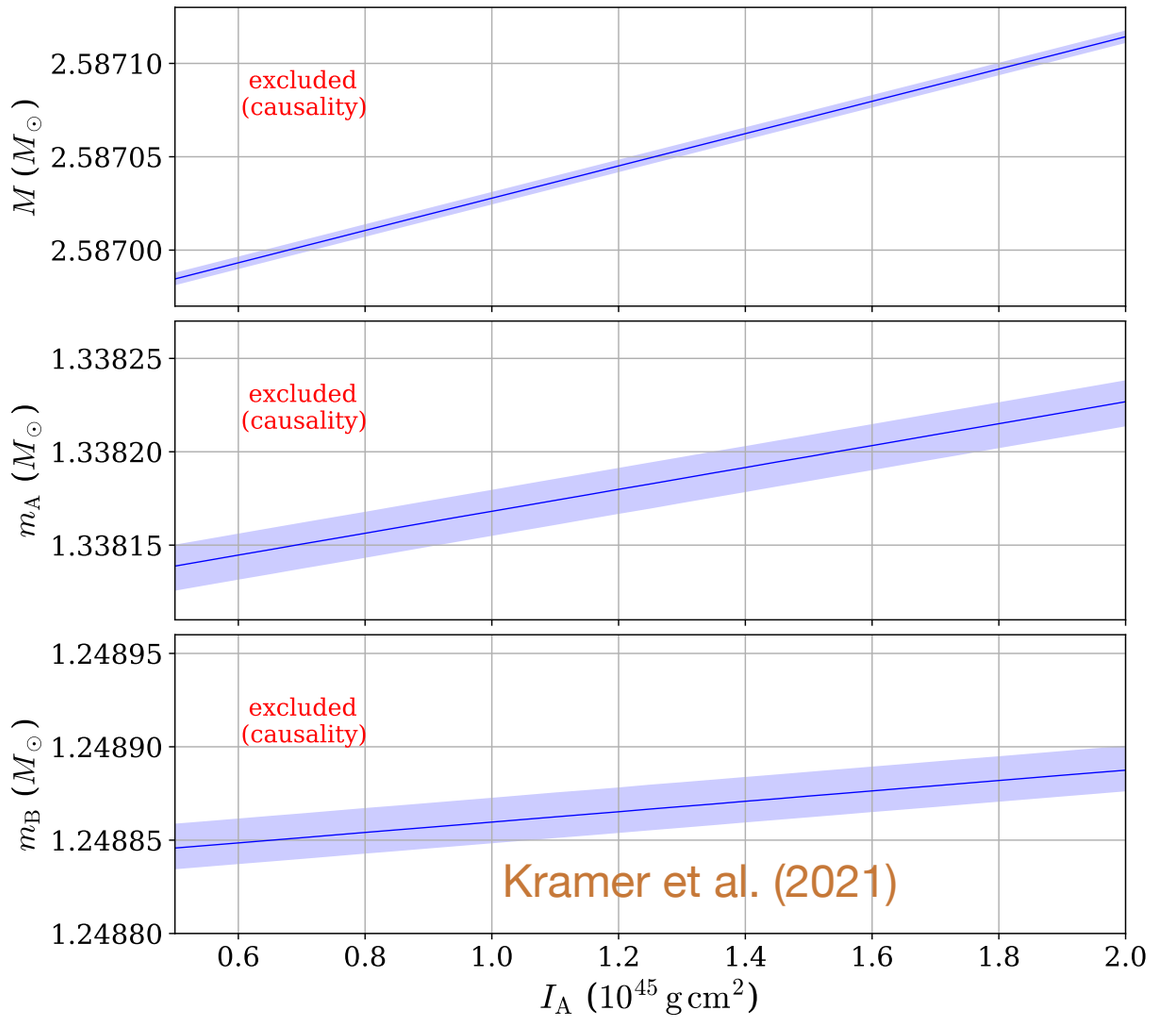

- To calculate masses correctly from the periastron advance, we need to take into account the relativistic spin-orbit coupling (Lense-Thirring effect) into account.
- This depends on the moment of inertia of the A pulsar!

Limits on the moment of inertia

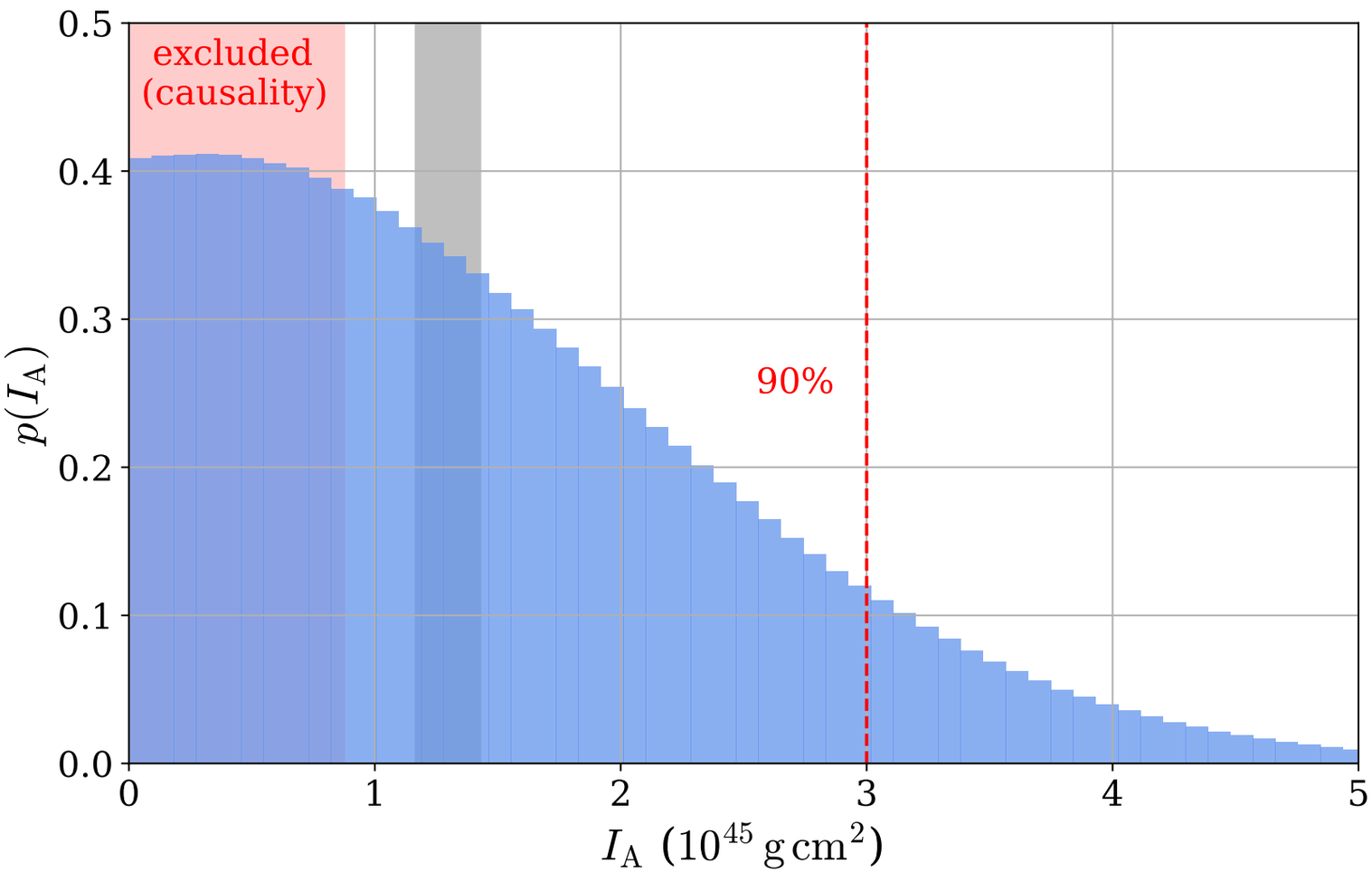

FIG. 6. Probability distribution for the MoI $I_{\rm A}$ of pulsar A derived from the $\dot{\omega} - s - \dot{P}_{\rm b}$ test. The vertical dashed red line indicates the upper bound with 90% confidence. $I_{\rm A} > 0$ has been assumed as a prior. The light grey band shows the 90% credible interval one obtains with the limits from [85] using the radius-MoI relation of [86]. The red area is excluded by the causality condition for the EoS [138].

- The agreement on the masses with the orbital decay (assuming GR) will provide a *measurement* of the moment of inertia.
- This is not too constraining yet, but the timing continues!
- Expect a measurement of the moment of inertia soon…
- This is an important test of the EOS of dense nuclear matter.

Kramer et al. (2021)

Orbital decay

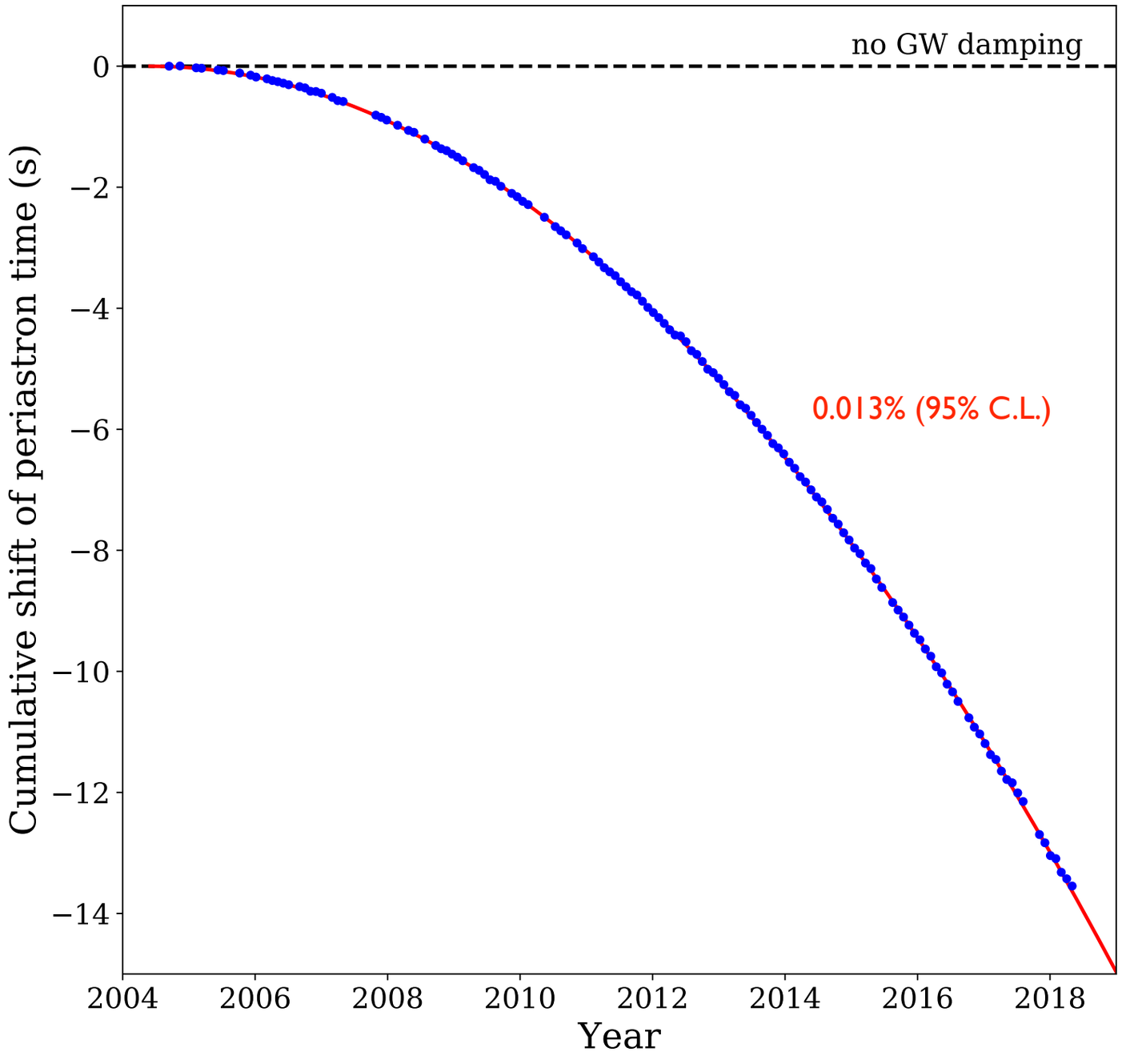

Figure: Norbert Wex

$$\dot{P}_{\rm b}^{\rm GW} = -\,1.247782(79) \times 10^{-12}$$

$$\dot{P}_{\rm b}^{\rm GW} = -\,39377.9 \pm 2.5\ {\rm ns\ yr}^{-1}$$

$$\frac{\dot{P}_{\rm b}^{\rm GW}}{\dot{P}_{\rm b}^{\rm GW,GR}} = 0.999963(63)$$

- Most precise test of the radiative properties of gravity
- Radiative test is now 25 times better that possible with the Hulse-Taylor binary!
- Next-to-leading order contributions to GW emission are becoming relevant!

Shapiro delay in the double pulsar

The Shapiro delay in the double pulsar is qualitatively different that what we see in the Solar system! This happens because:

- The high inclination of the system means that radiation is passing within 10000 km of the B pulsar, where curvature is 10^6 times large than for horizon of M87

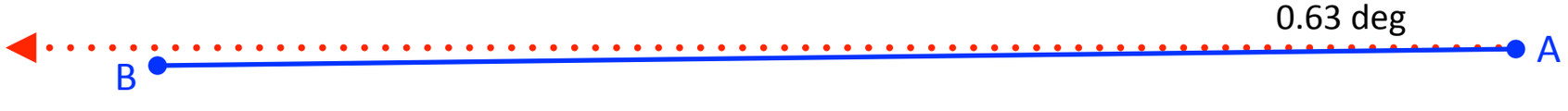

- In many alternative theories of gravity, the gravitational field of a NS is not qualitatively identical to that of the Sun!

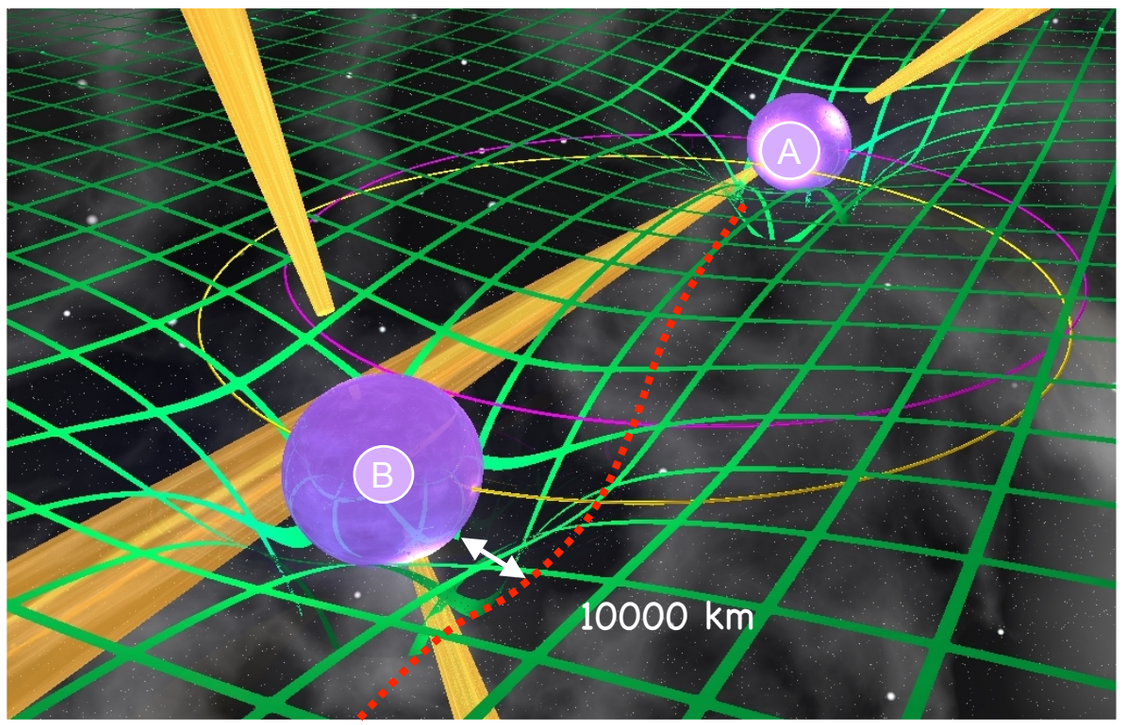

Figure: M. Kramer, N. Wex

Observed Shapiro delay in the double pulsar

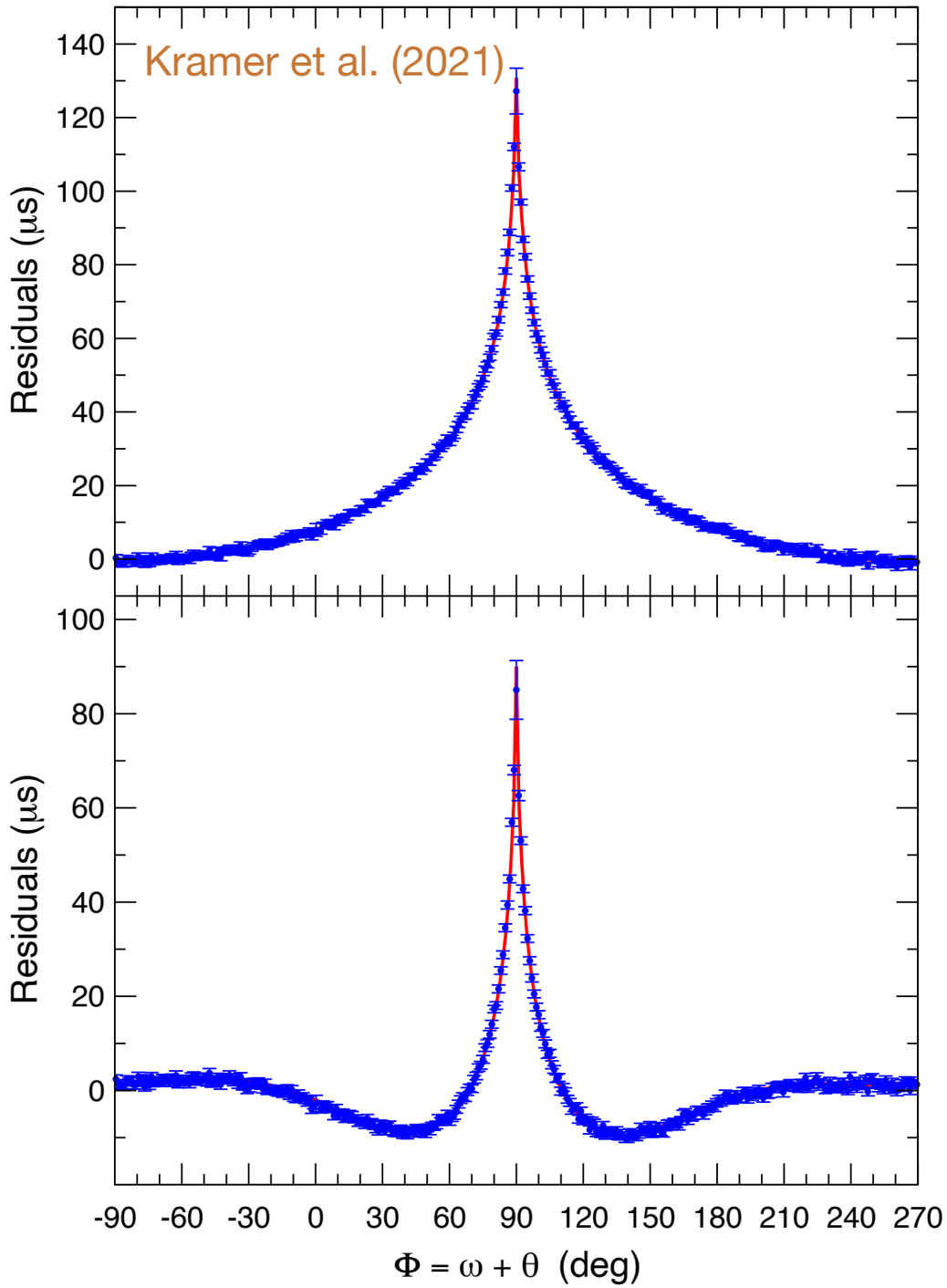

Despite this, the results agree with the GR predictions!

$$s^{\rm obs}/s^{\rm GR} = 1.00009(18)$$

$$r^{\rm obs}/r^{\rm GR} = 1.0016(34)$$

FIG. 11. Signature of the Shapiro delay in the timing residuals, plotted against A's angular orbital position $\psi = \omega + \theta$ with respect to the ascending node. The bottom shows the aggregated residuals as a function of orbital phase when not including the Shapiro delay parameters z_s (or, equivalently, $\sin i$) and r. The shape differs from the expected Shapiro delay curve shown in the top, as some signal power is absorbed in a fit for the orbital parameters, namely, the Rømer delay (see, e.g., Ref. [98]). The expected shape is recovered by computing the residuals when setting the Shapiro delay parameters to zero in the final timing solution. Note that the shown residuals are corrected for a slow variation in the curve due to the relativistic orbital precession. The red curves show the GR expectation using values of $\sin i$ and r derived from $\dot{\omega}$ and $\gamma_{\rm E}$. These are $(\sin i)^{\rm GR} = 0.99988(18)$ and $r^{\rm GR} = 6.1518(11)\ \mu$s, where the uncertainties are determined by those in $\dot{\omega}$ and γ_E. Note that the uncertainty in the prediction of $\sin i$ is correspondingly larger than that of the actually measured $\sin i$.

Higher-order terms of the Shapiro delay

Subtracting the 1 PN term, we can already see contributions from higher-order terms!

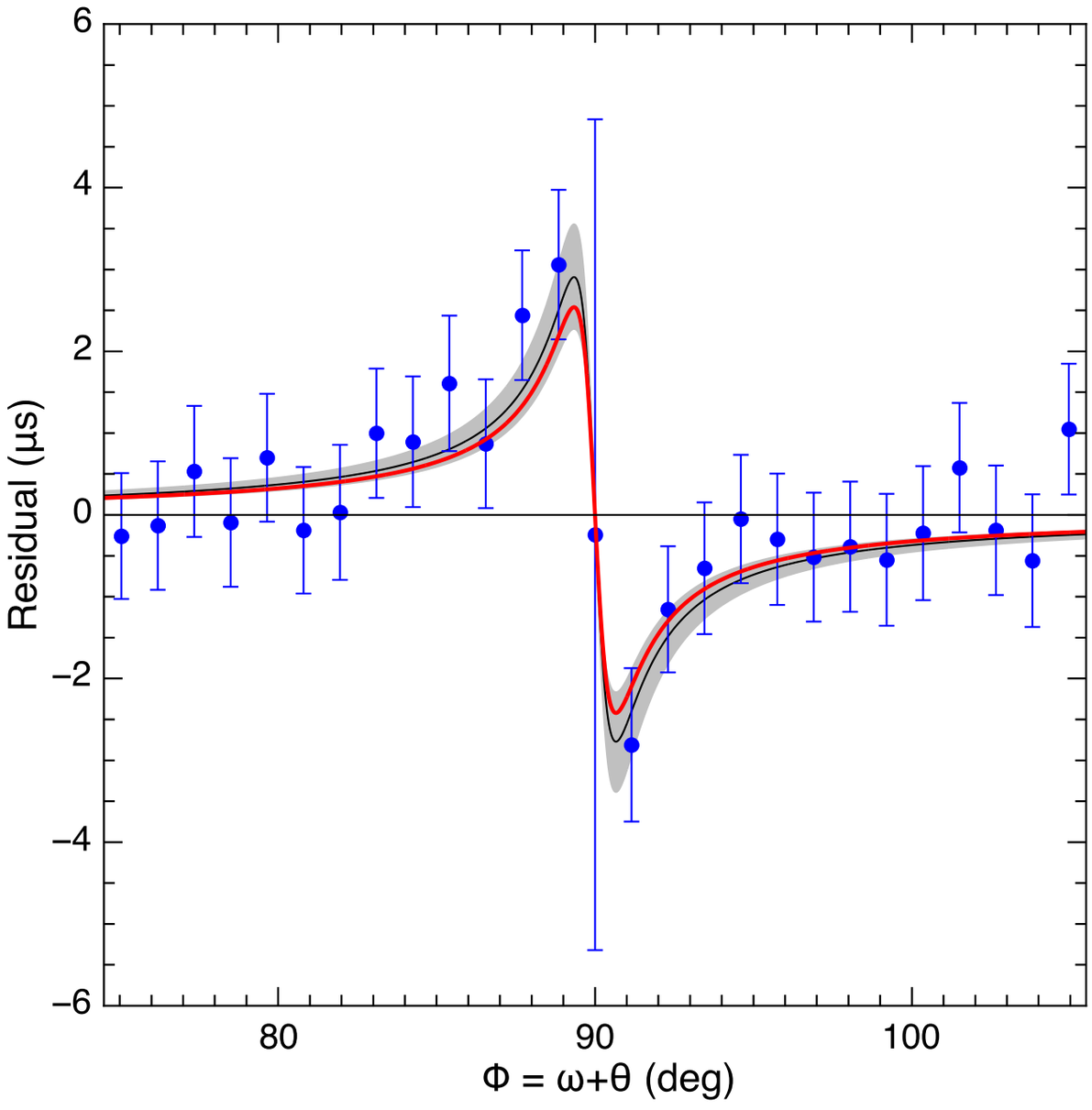

FIG. 12. Aggregated residuals (blue) due to NLO contributions in the Shapiro delay and the aberration, plotted against A's angular orbital position $\psi = \omega + \theta$ with respect to the ascending node. The red curve shows the theoretical prediction, and the black curve corresponds to the fitted $q_{\rm NLO}$ (see Table IV), with a 2σ range indicated by the light gray band. Residuals are rescaled by $(1 + e_T \cos\theta)^{-1}$ to account (to leading order) for a secular variation in the amplitude due to the precession of ω. A data point generally results from approximately 3000 aggregated residuals. The data point at $\psi = 90°$ (i.e., superior conjunction of A) has a much larger uncertainty, as this bin coincides with the 30-s-long eclipse of pulsar A, resulting in both many fewer TOAs available for aggregation and residuals of opposite sign being averaged.

Kramer et al. (2021)

Effect of the light bending in the Shapiro delay

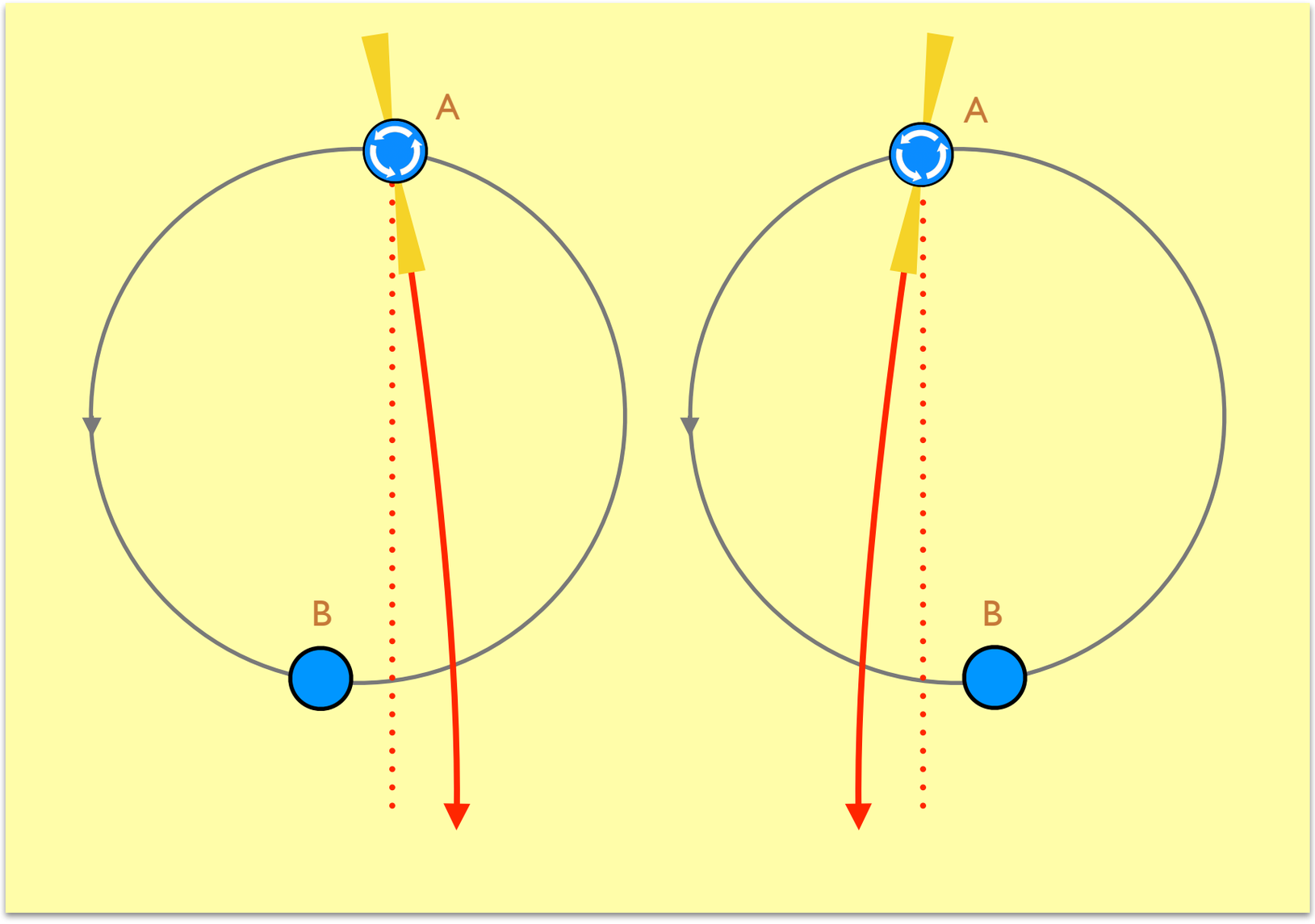

Figure: N. Wex

One of these is the bending delay, which depends on the spin period of the pulsar. The fact that we have observed this effect confirms that the pulsar really is a rotator, and that it rotates in the same sense as the orbital motion!

MeerKAT arrives…

Detections start pouring in…

The S/N of the detections of the double pulsar are three times better than the GBT detections.

This is true for pulsars located farther South.

Relative to Parkes, the improvement if a factor of 6 to 8! Big improvement for any objects deep in the Southern Hemisphere.

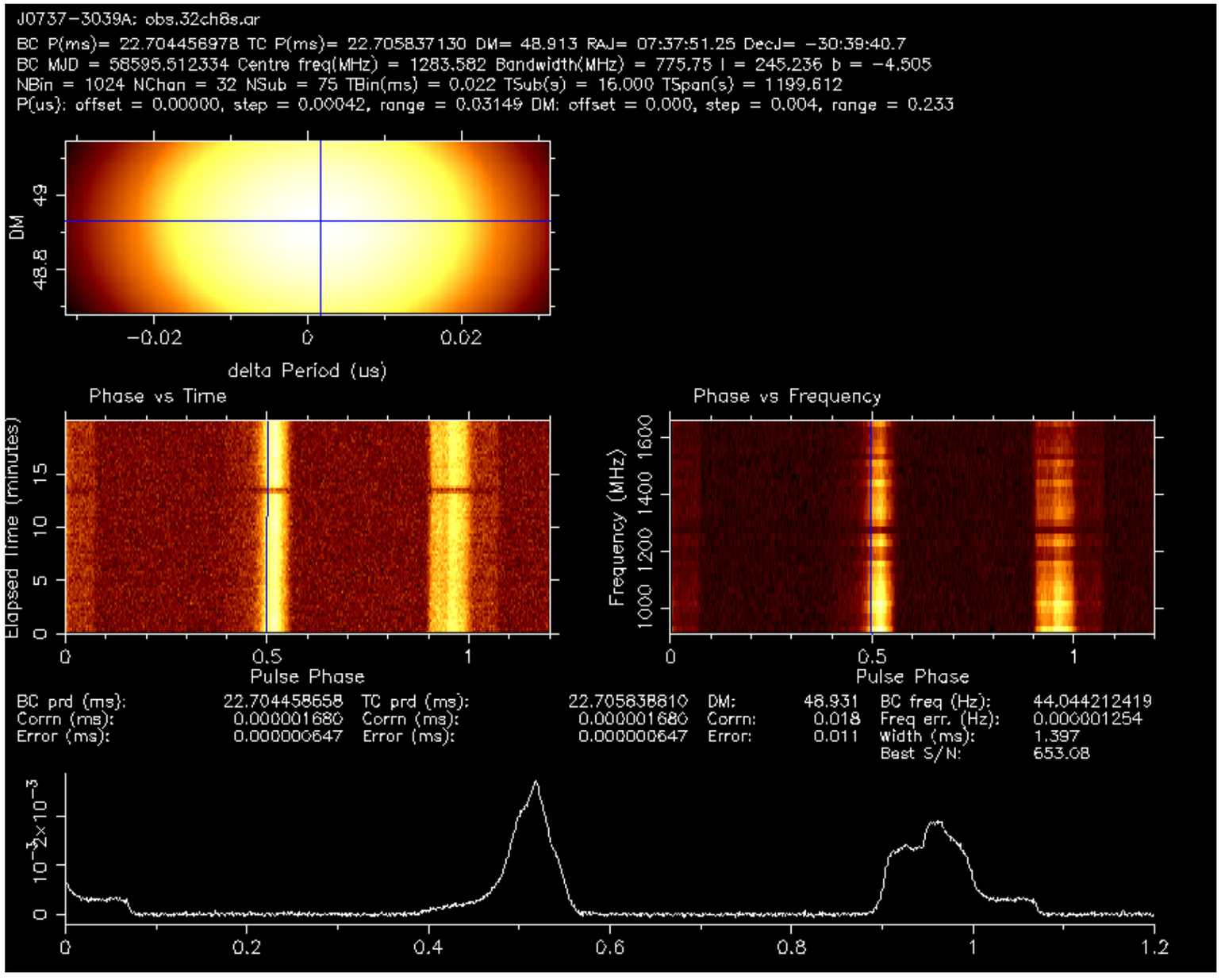

Credit: SARAO / MeerTIME consortium

Higher-order terms of the Shapiro delay

Much better now with MeerKAT!

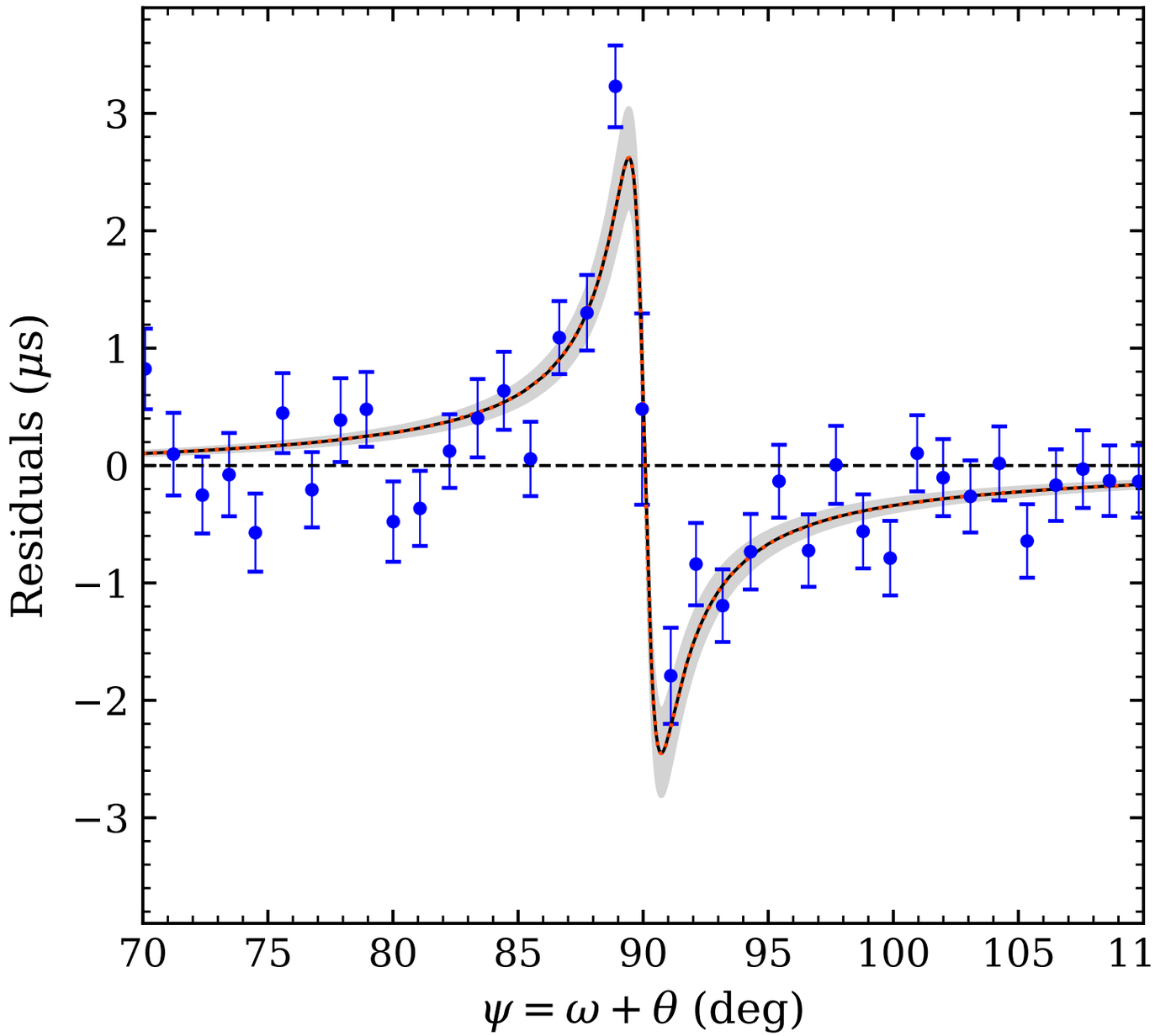

Fig. 5. Aggregated residuals (blue) due to NLO contributions in Shapiro and aberration delay, shown in the orbital phase ψ. Residuals are re-scaled by $(1 + e_{\rm T} \cos\theta)^{-1}$ to account for secular variations in amplitude due to the precession of periastron. The black curve indicates the fitted $q_{\rm NLO}$ (see Table 2) with the 2σ range shown by the grey shaded areas, which agrees very well with the theoretical prediction indicated by the red dotted line.

Hu et al. 2022, A&A, 667, A149

4.Tests of the nature of gravitational waves and of alternative theories of gravity

The Einstein equivalence principle

Figure: CNES

$$|\Delta| < 10^{-15}$$

Touboul et al. (2022),
Physical. Rev. Lett. 129, 121102

- Given the stringent constraints of the universality of free fall for test particles, and how well tested special relativity is, most alternative theories of gravity predict the Einstein equivalence principle.

- They do this by describing gravity as deformed space-time: They are ``Metric" theories.

The strong equivalence principle

- However, only GR fully embodies the *strong equivalence principle* (SEP). Generally, alternative theories of gravity violate it!

- The main consequence would be a **violation of the universality of free fall for self-gravitating objects.** This would have, for systems with two objects with different gravitational binding energies, two main consequences:

1. Orbital polarization (Nordtvedt effect) in an external gravitational field

$$\Delta \propto \alpha_0(\alpha_\mathrm{p} - \alpha_\mathrm{WD})$$

2. Dipolar gravitational wave (DGW) emission (tight orbits, 1.5 PN, or $1/c^3$)

$$\dot{P}_\mathrm{b}^D = -2\pi n_b \frac{G_* M_\mathrm{WD}}{c^3} \frac{q}{q+1} \frac{1+e^2/2}{(1-e^2)^{5/2}} (\alpha_\mathrm{p} - \alpha_\mathrm{WD})^2$$

- **Detecting these effects would falsify GR**! Not detecting them constrains alternatives!

- Because of the difference in binding energies, *pulsar – white dwarf systems might show these effects*!

3.1. Searching for dipolar GW emission

Limits on Dipolar GWs

- PSR J1738+0333 is a 5.85-ms pulsar in a 8.5-hour, low eccentricity orbit. It was discovered in 2001 in a Parkes Multi-beam high-Galactic latitude survey (Jacoby 2005, Ph.D. Thesis, Caltech).
- Companion WD detected at optical wavelenghts, and relatively bright!

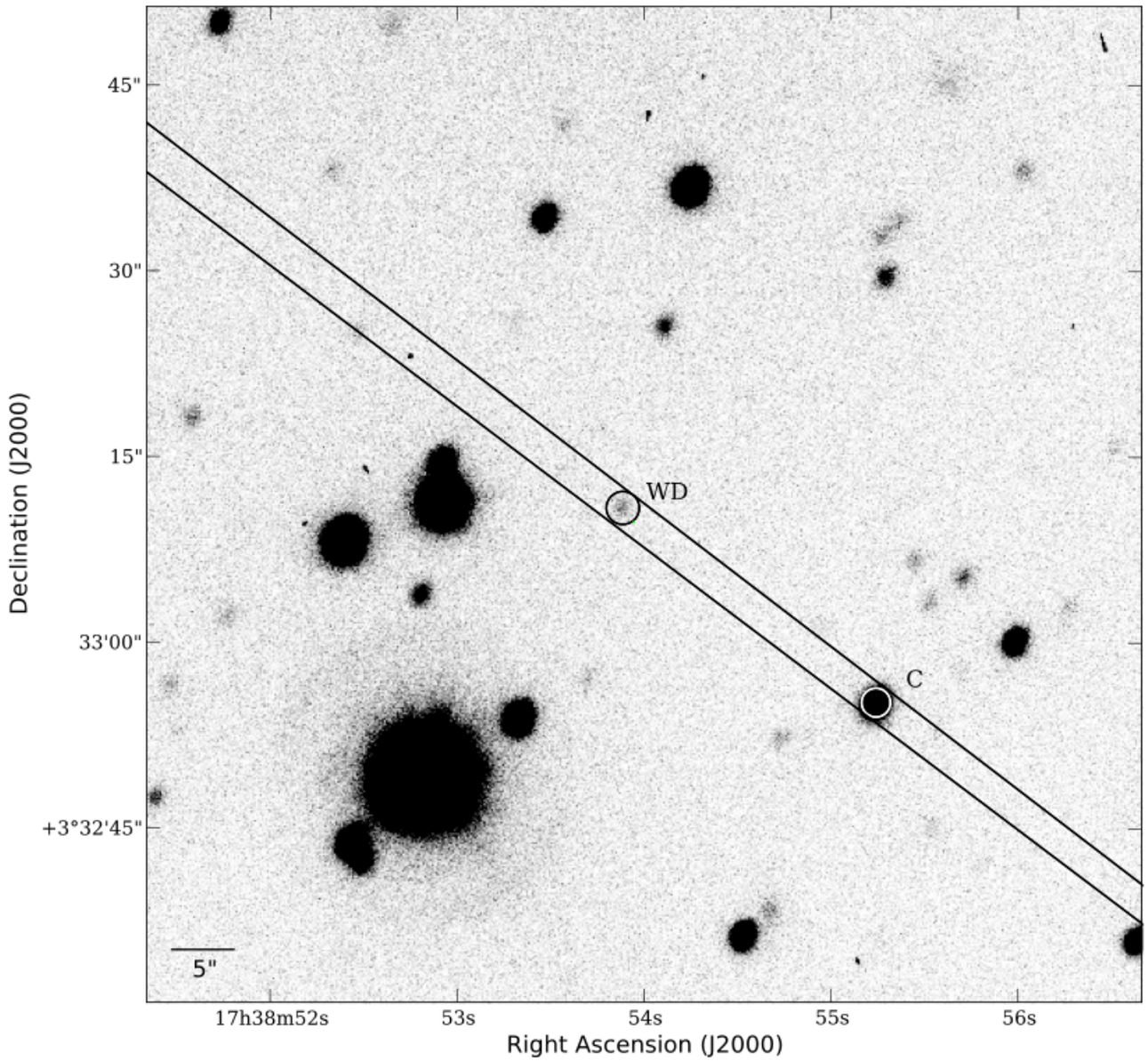

Antoniadis et al. (2012), MNRAS, 423, 3316

Optical observations of PSR J1738+0333

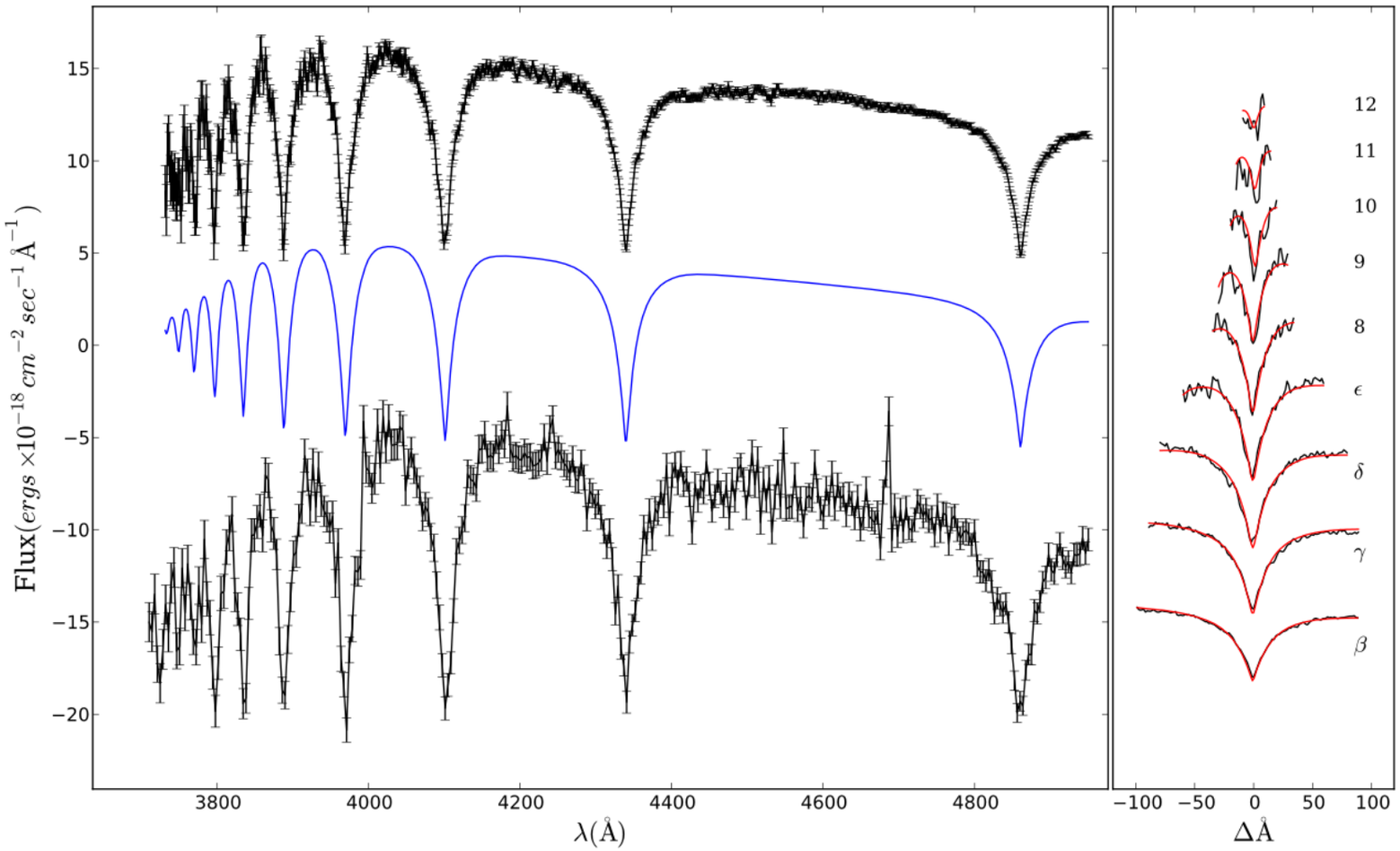

Antoniadis et al. (2012)

- The WD is bright enough for a study of the spectral lines!

- Together with WD models, these measurements allow an estimate of the WD mass: $0.181^{+0.007}_{-0.005}\,\mathrm{M}_{\odot}$.

Optical observations of PSR J1738+0333

- Shift in the spectral lines allows an estimate of the mass ratio: $q = 1.8 \pm 0.2.$

- This allows an estimate of the orbital inclination $(32.6 \pm 1.0^{\circ})$ and the pulsar mass: $1.46^{+0.07}_{-0.06}\,\mathrm{M}_{\odot}$

- Results in Antoniadis et al. 2012, MNRAS, 423, 3316.

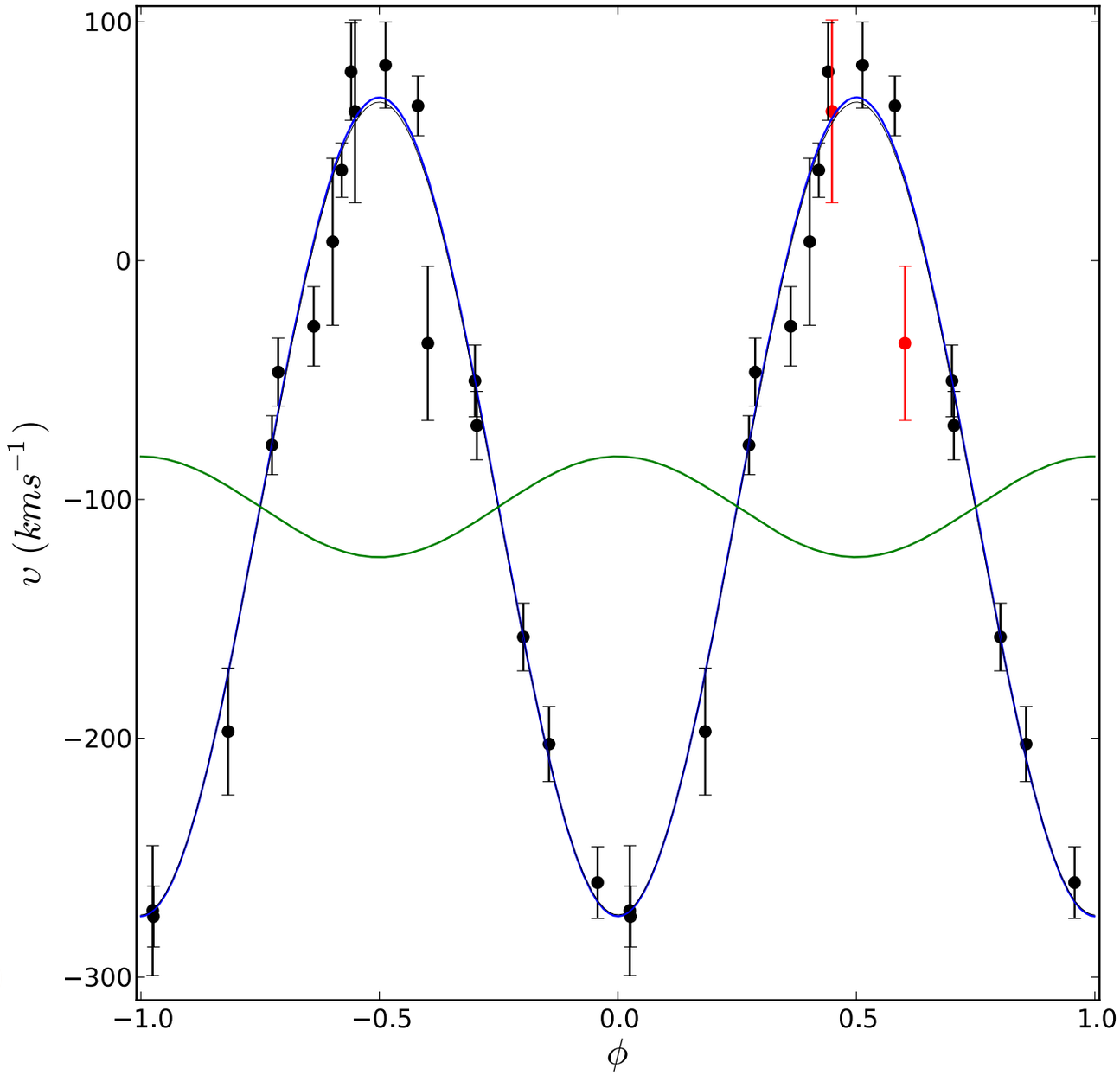

Antoniadis et al. (2012)

Prediction:

- Once the component masses are known, we can estimate the rate of orbital decay due to quadrupolar GW emission predicted by GR:

$$\dot{P}_{\rm B}^{\rm GR} = -\frac{192}{5}\left(n_{\rm B} T_{\odot} M_{\rm c}\right)^{5/3} \frac{q}{(q+1)^{1/3}} = -27.7^{+1.5}_{-1.9}\,{\rm fs\ s^{-1}}$$

… which is a change on the orbital period of $-0.86\,\mu{\rm s\ yr^{-1}}$!

- In the presence of ***dipolar GW*** emission this quantity must be larger (in absolute value) - If $\alpha_p \sim 1$, then

$$\dot{P}_{\rm b}^{D} = -2\pi n_b \frac{G_* M_{\rm WD}}{c^3} \frac{q}{q+1} \frac{1+e^2/2}{(1-e^2)^{5/2}} (\alpha_{\rm p} - \alpha_{\rm WD})^2 = -110{,}000\,\mu{\rm s\ yr^{-1}}\ (!!)$$

- *Which is it*?

Timing of PSR J1738+0333

10 years of timing with Parkes and Arecibo were necessary to measure this number precisely!

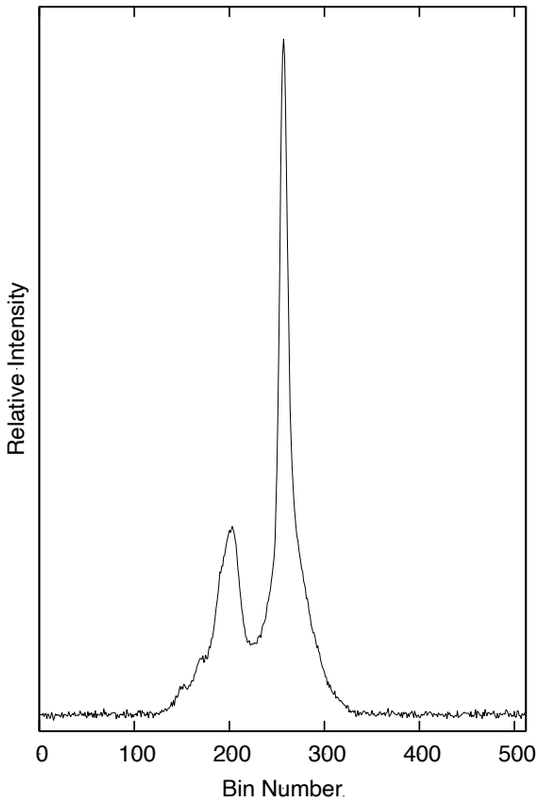

The (awesome) power of timing

- Number of rotations between MJD 52872.01692 and 55813.95899 (SSB): **43 449 485 656 ± 0.**
- Spin period (on 14th of May 2008 at 0h UTC): **0.005850095859775683 ± 0.00000000000000005 s**
- Orbital period: **8^h 30^m 53.9199264 ± 0.0000003** s
- Projected semi-major axis of the pulsar's orbit: **102957453 ± 6 m.**
- Eccentricity: **(3 ± 1) × 10^{-7}.** This means that the orbit deviates from a circle by (5 ± 3) μm!
- Proper motion: **7.037 ± 0.005 mas yr^{-1}, 5.073 ± 0.012 mas yr^{-1}**, parallax: **0.68 ± 0.05 mas.**
- **Orbital decay: –(25.9 ± 3.2) × 10^{-15} ss^{-1} (or 0.8 ± 0.1 μs yr^{-1}!). GR Does it again!!!!**

$$\dot{P}_{\rm b}^{\rm int} = \dot{P}_{\rm b}^{\rm obs} - \dot{P}_{\rm b}^{\rm Acc} - \dot{P}_{\rm b}^{\rm Shk}$$

Looking for dipolar GW: *not there*!

- Observed decay represents a 12% test of GR - not a very good test!
- However, the *difference* between the measured value and the GR prediction is tiny compared with the prediction for dipolar GW emission!
- Best constraint on the emission of dipolar GWs, and of their nature!
- Most constraining test for many alternative gravity theories.

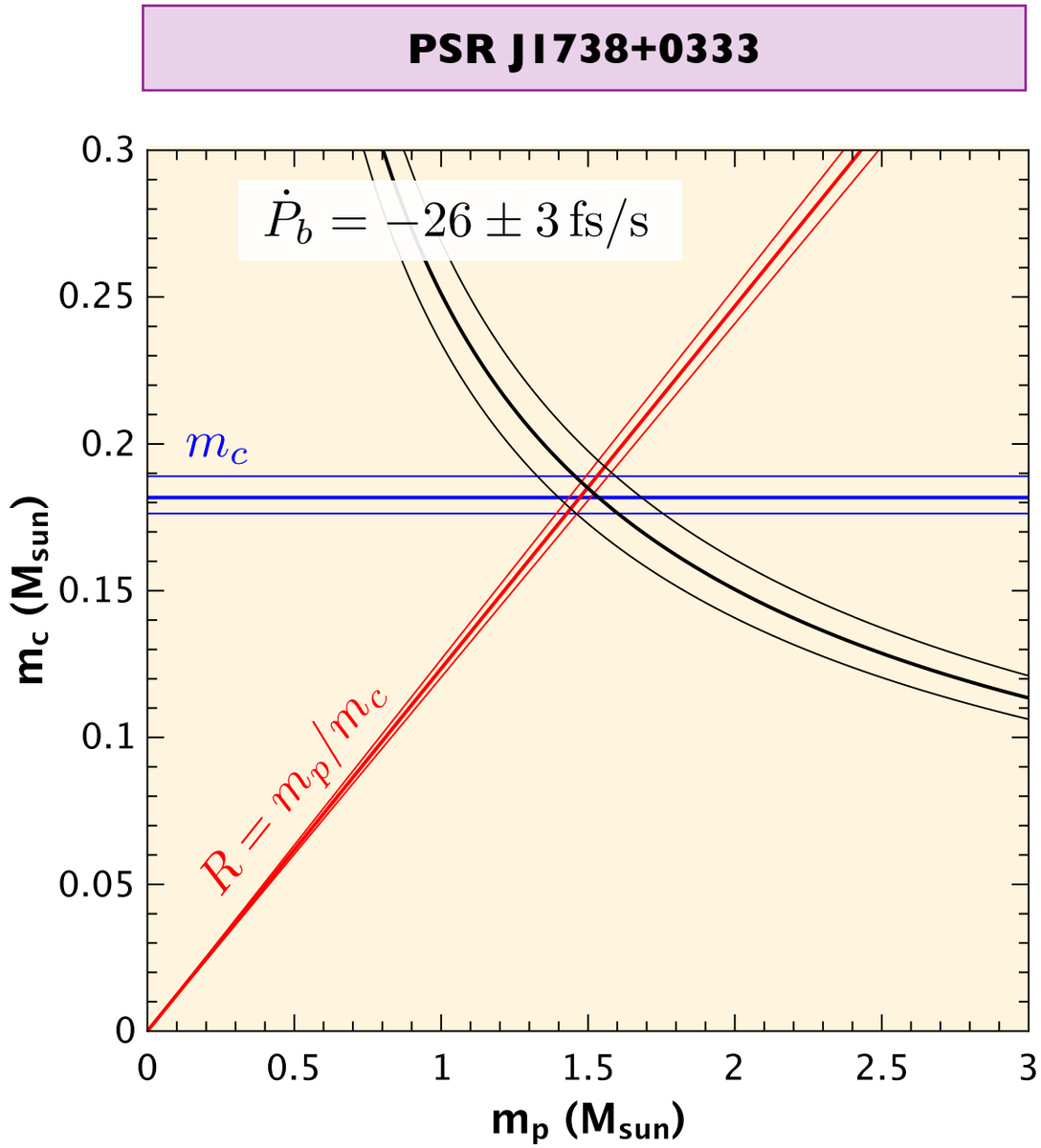

Figure: Norbert Wex

3.2. Searching for spontaneous scalarisation

VOLUME 70, NUMBER 15 PHYSICAL REVIEW LETTERS 12 APRIL 1993

Nonperturbative Strong-Field Effects in Tensor-Scalar Theories of Gravitation

Thibault Damour
Institut des Hautes Etudes Scientifiques, 91440 Bures sur Yvette, France
and Département d'Astrophysique Relativiste et de Cosmologie, Observatoire de Paris,
Centre National de la Recherche Scientifique, 92195 Meudon, France

Gilles Esposito-Farèse
Centre de Physique Théorique, Centre National de la Recherche Scientifique, Luminy, Case 907,
13288 Marseille CEDEX 9, France
(Received 15 January 1993)

It is shown that a wide class of tensor-scalar theories can pass the present weak-field gravitational tests and exhibit nonperturbative strong-field deviations away from general relativity in systems involving neutron stars. This is achieved without requiring either large dimensionless parameters, fine tuning, or the presence of negative-energy modes. This gives greater significance to tests of the strong gravitational field regime, notably binary pulsar experiments.

PACS numbers: 04.50.+h, 97.60.Jd

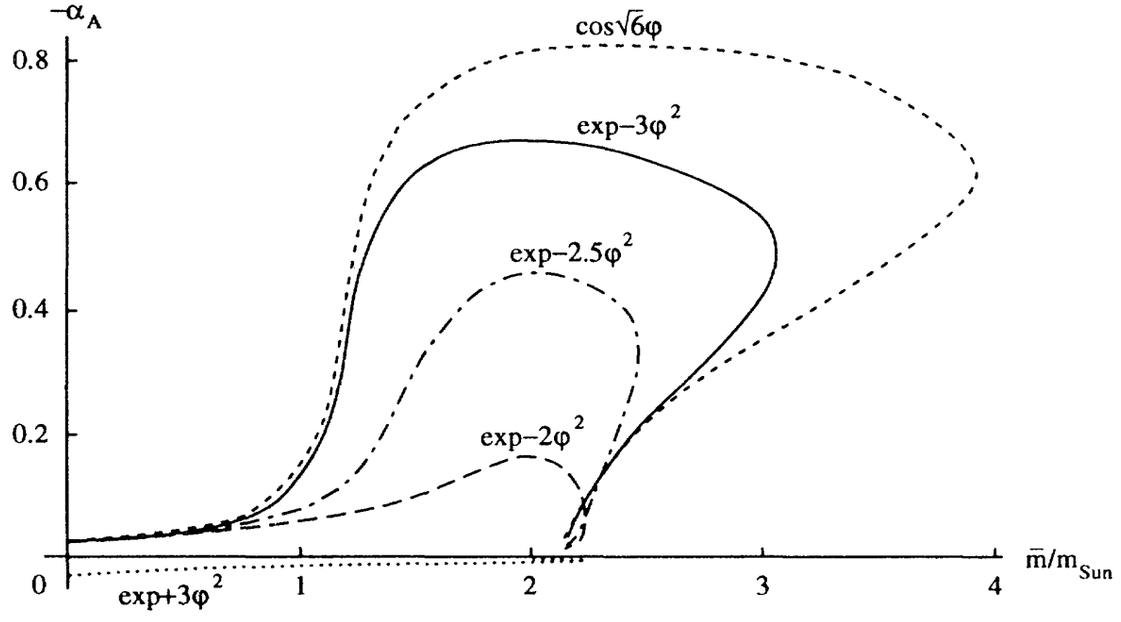

FIG. 2. Effective scalar coupling constant vs baryonic mass for the neutron star model of Fig. 1 computed within five different tensor-scalar theories. The labels indicate the corresponding coupling functions $A(\varphi)$. In each case, we chose the maximum value of φ_0 consistent with the two limits in Eq. (1).

Some important points about PSR J2222-0137

- P = 32.8 ms, P_b = 2.44 d, e = 0.00038
- Recycled pulsar with very massive WD companion.
- Kinematic effects can also be corrected very precisely (from the exquisite distance measurement)
- Mass measurement is precise, and measured with multiple PK parameters (periastron advance and very significant Shapiro delay)
- Most massive double degenerate system known, and largest NS birth mass!
- PB-dot is improving very fast.
- All this and the unusual mass yields a useful test of ST theories of gravity!

The Astrophysical Journal, 770:145 (9pp), 2013 June 20 doi:10.1088/0004-637X/770/2/145

VLBI ASTROMETRY OF PSR J2222–0137: A PULSAR DISTANCE MEASURED TO 0.4% ACCURACY

A. T. Deller[1], J. Boyles[2], D. R. Lorimer[2], V. M. Kaspi[3], M. A. McLaughlin[2], S. Ransom[4], I. H. Stairs[5], and K. Stovall[6,7]
[1] ASTRON, The Netherlands Institute for Radio Astronomy, Postbus 2, 7990 AA Dwingeloo, The Netherlands
[2] Department of Physics, West Virginia University, Morgantown, WV 26506, USA
[3] Department of Physics, McGill University, 3600 University Street, Montreal, QC H3A 2T8, Canada
[4] National Radio Astronomy Observatory, Charlottesville, VA 22903, USA
[5] Department of Physics and Astronomy, University of British Columbia, 6224 Agricultural Road, Vancouver, BC V6T 1Z1, Canada
[6] Center for Advanced Radio Astronomy and Department of Physics and Astronomy, University of Texas at Brownsville, Brownsville, TX 78520, USA
[7] Department of Physics and Astronomy, University of Texas at San Antonio, San Antonio, TX 78249, USA
Received 2012 October 31; accepted 2013 May 2; published 2013 June 5

ABSTRACT

The binary pulsar J2222−0137 is an enigmatic system containing a partially recycled millisecond pulsar and a companion of unknown nature. While the low eccentricity of the system favors a white dwarf companion, an unusual double neutron star system is also a possibility, and optical observations will be able to distinguish between these possibilities. In order to allow the absolute luminosity (or upper limit) of the companion object to be properly calibrated, we undertook astrometric observations with the Very Long Baseline Array to constrain the system distance via a measurement of annual geometric parallax. With these observations, we measure the parallax of the PSR J2222–0137 system to be $3.742^{+0.013}_{-0.016}$ mas, yielding a distance of $267.3^{+1.2}_{-0.9}$ pc, and measure the transverse velocity to be $57.1^{+0.3}_{-0.2}$ km s^{-1}. Fixing these parameters in the pulsar timing model made it possible to obtain a measurement of Shapiro delay and hence the system inclination, which shows that the system is nearly edge-on ($\sin i = 0.9985 \pm 0.0005$). Furthermore, we were able to detect the orbital motion of PSR J2222–0137 in our very long baseline interferometry (VLBI) observations and measure the longitude of ascending node Ω. The VLBI astrometry yields the most accurate distance obtained for a radio pulsar to date, and is furthermore the most accurate parallax for any radio source obtained at "low" radio frequencies (below ∼5 GHz, where the ionosphere dominates the error budget). Using the astrometric results, we show that the companion to PSR J2222–0137 will be easily detectable in deep optical observations if it is a white dwarf. Finally, we discuss the implications of this measurement for future ultra-high-precision astrometry, in particular in support of pulsar timing arrays.

Key words: astrometry – pulsars: general – pulsars: individual (J2222−0137) – techniques: interferometric

1. INTRODUCTION

PSR J2222−0137 was discovered in the Green Bank Telescope 350 MHz drift-scan pulsar survey carried out in 2007 (Boyles et al. 2013; Lynch et al. 2013). It has an observed spin period P of 32.82 ms and a spin period derivative $\dot{P}$ of

Characterizing the PSR J2222–0137 system and distinguishing between the possible evolutionary pathways will require multiwavelength data which can be reliably interpreted. This demands an accurate distance to the system, in order to convert observed flux densities to absolute luminosities. Very long baseline interferometry (VLBI) can provide astrometric accu-

Shapiro delay for PSR J2222-0137

Guo et al. (2021), A&A, 654, A16

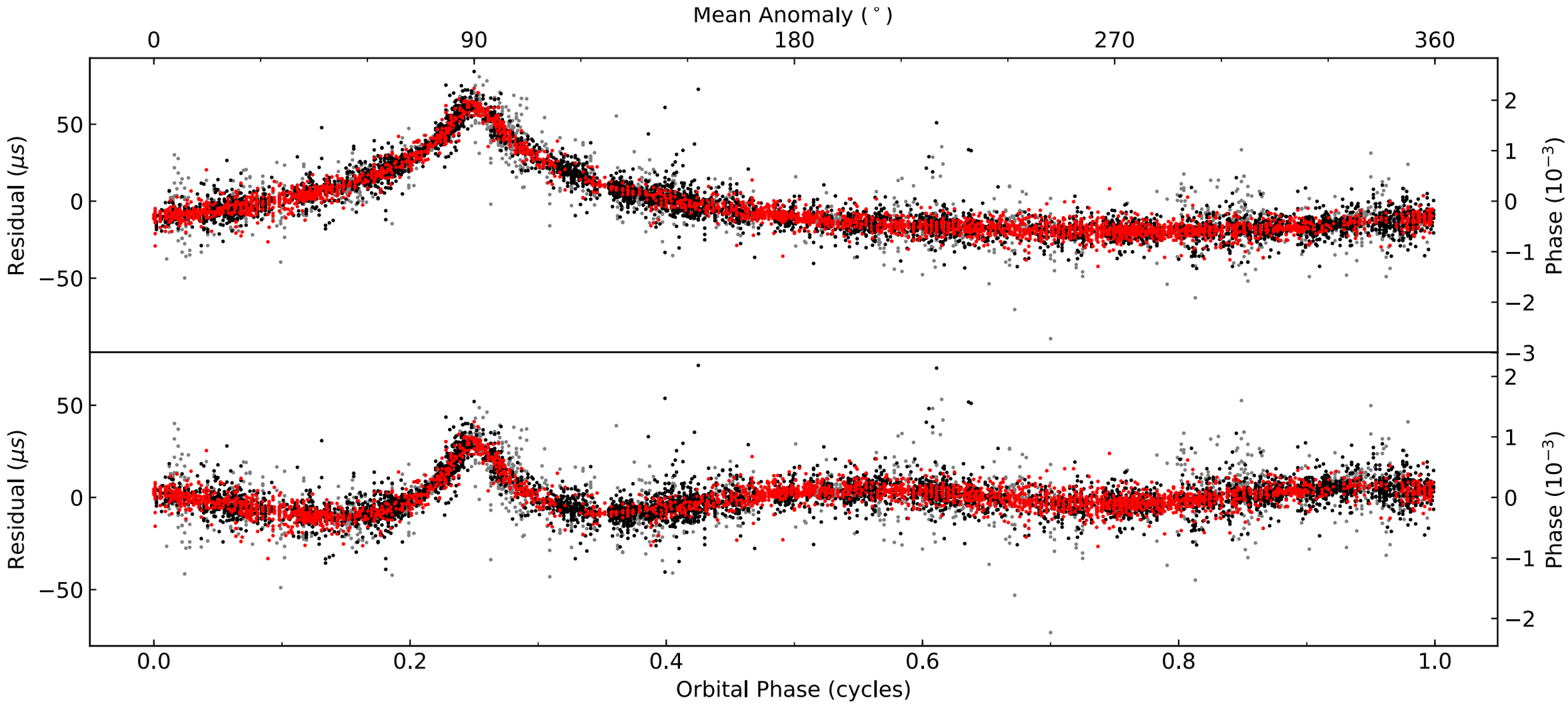

$$M_{\rm P} = 1.831(10)\,{\rm M}_\odot,\ M_{\rm c} = 1.319(4)\,{\rm M}_\odot$$

Mass of pulsar is between masses of PSR J1738+0333 and J0348+0432!

Periastron advance in PSR J2222-0137

Guo et al. (2021)

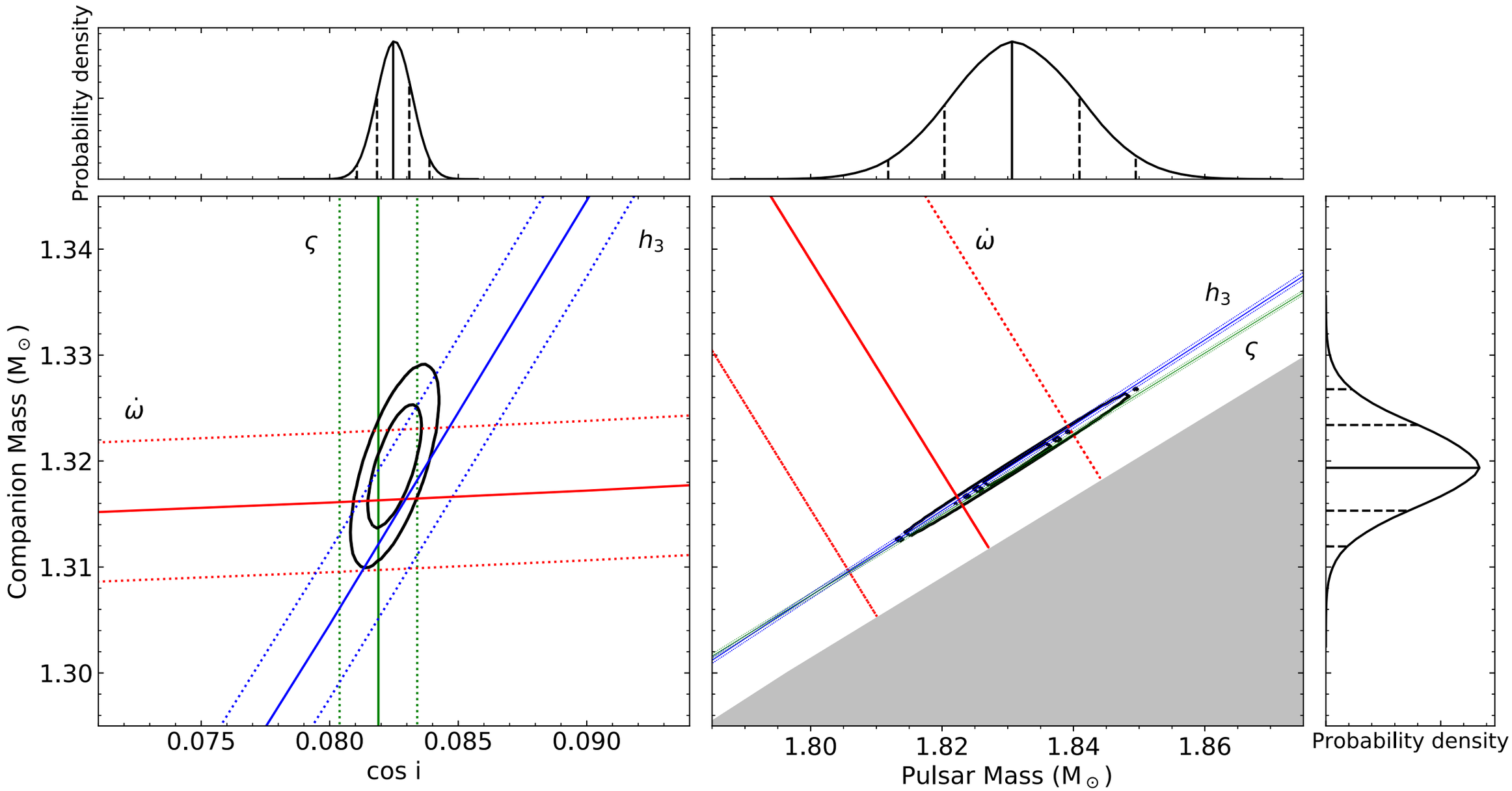

Precise measurement of variation of orbital period!

Guo et al. (2021)

$\dot{P}_{\rm b,obs}$	$\dot{P}_{\rm b,GR}$	$\dot{P}_{\rm b,Shk}$	Galactic model	$\dot{P}_{\rm b,Gal}$			$\dot{P}_{\rm b,xs}$
				Horizontal	Vertical	Total	
0.2509(76)	−0.00809(5)	0.2794(12)	Nice & Taylor (1995) [a]	−0.0014	−0.0128	−0.0142(13)	−0.0063(76)
			McMillan (2017)	−0.0016	−0.0145	−0.0161(15)	−0.0044(77)
			Piffl et al. (2014)	−0.0017	−0.0162	−0.0179(16)	−0.0026(77)
			Binney & Tremaine (2008)	−0.0014	−0.0123	−0.0137(12)	−0.0068(76)

Quadrupole term not even measured properly!
However, the excess is extremely small, constraining the emission of dipolar GWs for large NS masses!

Some important points about PSR J1913+1102:

Article

Asymmetric mass ratios for bright double neutron-star mergers

https://doi.org/10.1038/s41586-020-2439-x

Received: 19 December 2019

Accepted: 14 April 2020

Published online: 8 July 2020

Check for updates

R. D. Ferdman[1]✉, P. C. C. Freire[2], B. B. P. Perera[3], N. Pol[4,5], F. Camilo[6], S. Chatterjee[7,8], J. M. Cordes[7,8], F. Crawford[9], J. W. T. Hessels[10,11], V. M. Kaspi[12,13], M. A. McLaughlin[4,5], E. Parent[12,13], I. H. Stairs[14] & J. van Leeuwen[11]

The discovery of a radioactively powered kilonova associated with the binary neutron-star merger GW170817 remains the only confirmed electromagnetic counterpart to a gravitational-wave event[1,2]. Observations of the late-time electromagnetic emission, however, do not agree with the expectations from standard neutron-star merger models. Although the large measured ejecta mass[3,4] could be explained by a progenitor system that is asymmetric in terms of the stellar component masses (that is, with a mass ratio q of 0.7 to 0.8)[5], the known Galactic population of merging double neutron-star systems (that is, those that will coalesce within billions of years or less) has until now consisted only of nearly equal-mass ($q > 0.9$) binaries[6]. The pulsar PSR J1913+1102 is a double system in a five-hour, low-eccentricity (0.09) orbit, with an orbital separation of 1.8 solar radii[7], and the two neutron stars are predicted to coalesce in 470^{+12}_{-11} million years owing to gravitational-wave emission. Here we report that the masses of the pulsar and the companion neutron star, as measured by a dedicated pulsar timing campaign, are 1.62 ± 0.03 and 1.27 ± 0.03 solar masses, respectively. With a measured mass ratio of $q = 0.78 \pm 0.03$, this is the most asymmetric merging system reported so far. On the basis of this detection, our population synthesis analysis implies that such asymmetric binaries represent between 2 and 30 per cent (90 per cent confidence) of the total population of merging binaries. The coalescence of a member of this population offers a possible explanation for the anomalous properties of GW170817, including the observed kilonova emission from that event.

- P = 27.3 ms, P_b = 4.95 h, e = 0.089531
- Double neutron star system.
- Most massive double neutron star system in the Galaxy!
- Member of a new population of asymmetric, merging double neutron star systems!

Mass-mass diagram for PSR J1913+1102

Fig. 1 | Pulsar mass–companion mass diagram for the PSR J1913+1102 system. Shaded regions bounded by solid curves represent 1σ mass constraints from each measured post-Keplerian parameter, derived in the context of general relativity. These are: the orbital precession rate ($\dot{\omega}$), the time dilation/gravitational redshift (γ) and the rate of orbital decay ($\dot{P}_b$). The inset shows a zoom-in of the dotted square region in the main plot, with the 3σ confidence region for the mass measurements shaded in red. The two most precisely measured parameters allow us to determine the individual masses of this system. Each additional post-Keplerian parameter measurement provides an independent consistency test of the predictions of general relativity.

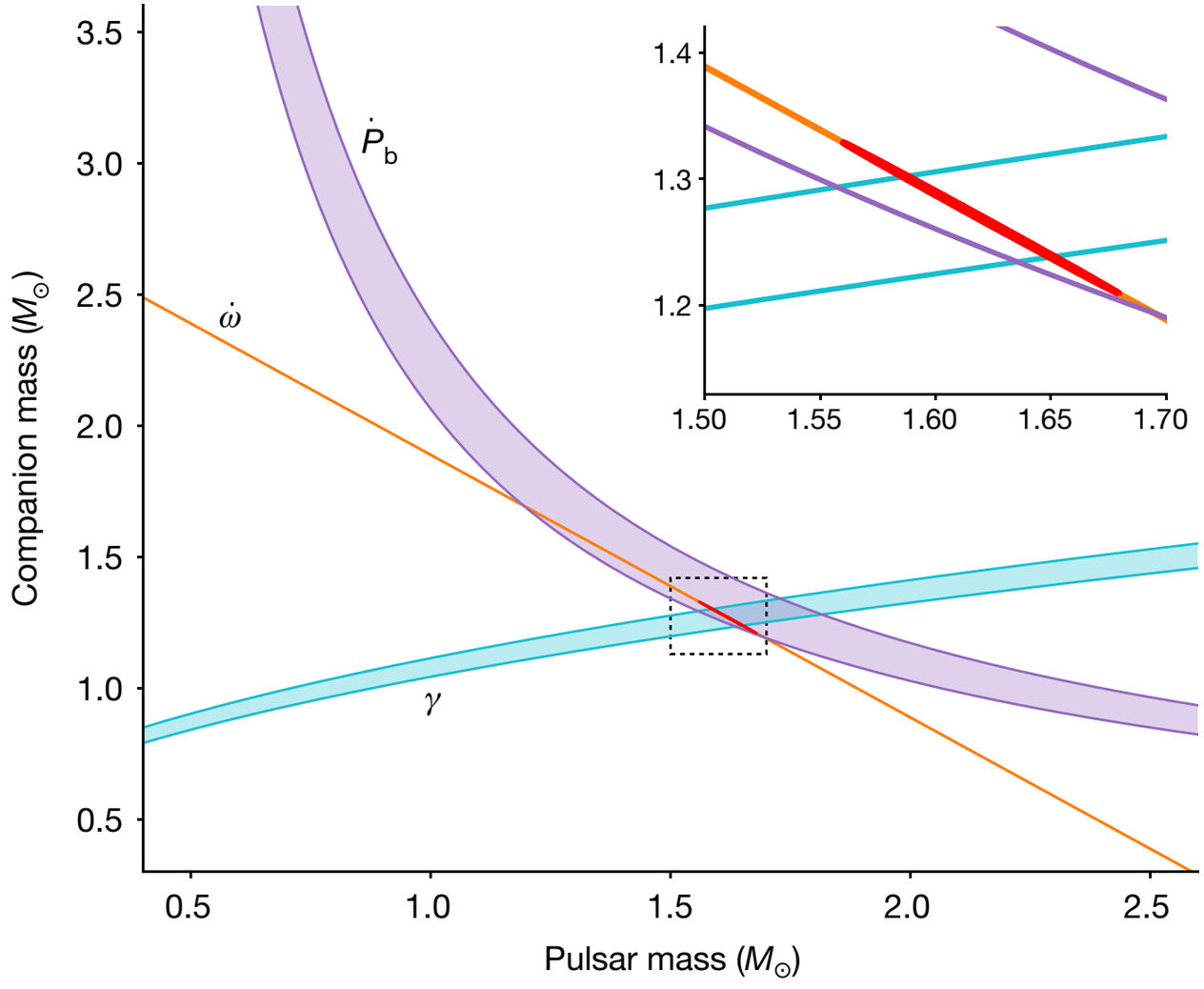

$$M = 2.8887(6)\,\mathrm{M}_\odot$$

$$M_\mathrm{P} = 1.62(3)\,\mathrm{M}_\odot, M_\mathrm{c} = 1.27(3)\,\mathrm{M}_\odot$$

Pulsar mass makes system interesting!

$$\dot{P}_\mathrm{B} = -0.48(3) \times 10^{-12}\,\mathrm{s\,s^{-1}}$$

Orbital decay agrees with GR!

Ferdman, Freire et al, (2020)

Prevalence of asymmetric systems

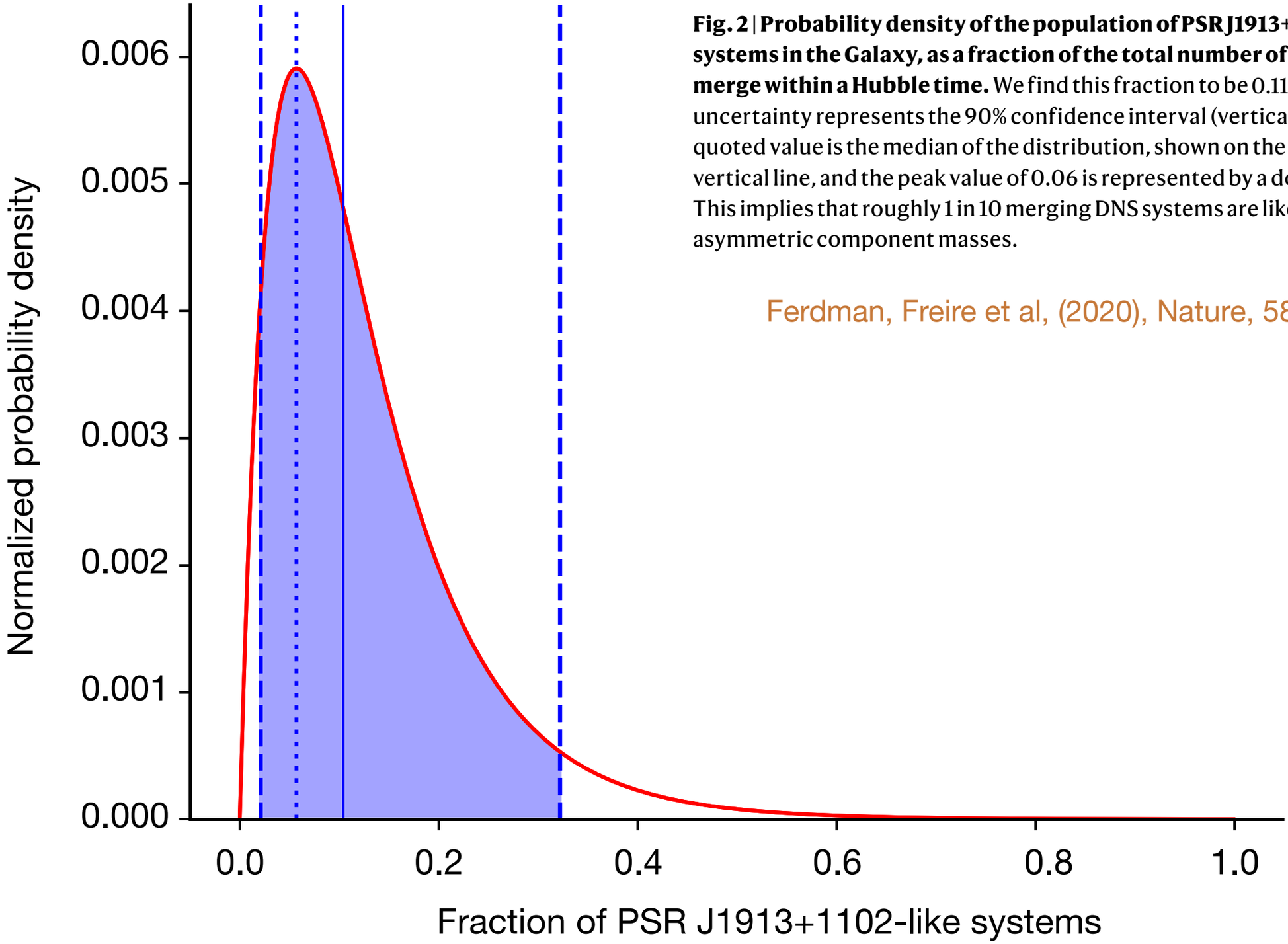

Fig. 2 | Probability density of the population of PSR J1913+1102 -like DNS systems in the Galaxy, as a fraction of the total number of DNSs that will merge within a Hubble time. We find this fraction to be $0.11^{+0.21}_{-0.09}$, where the uncertainty represents the 90% confidence interval (vertical dashed lines). The quoted value is the median of the distribution, shown on the plot as a solid vertical line, and the peak value of 0.06 is represented by a dotted vertical line. This implies that roughly 1 in 10 merging DNS systems are likely to have asymmetric component masses.

Ferdman, Freire et al, (2020), Nature, 583, 211

3.3 . The Nordtvedt effect

Lunar Laser Ranging

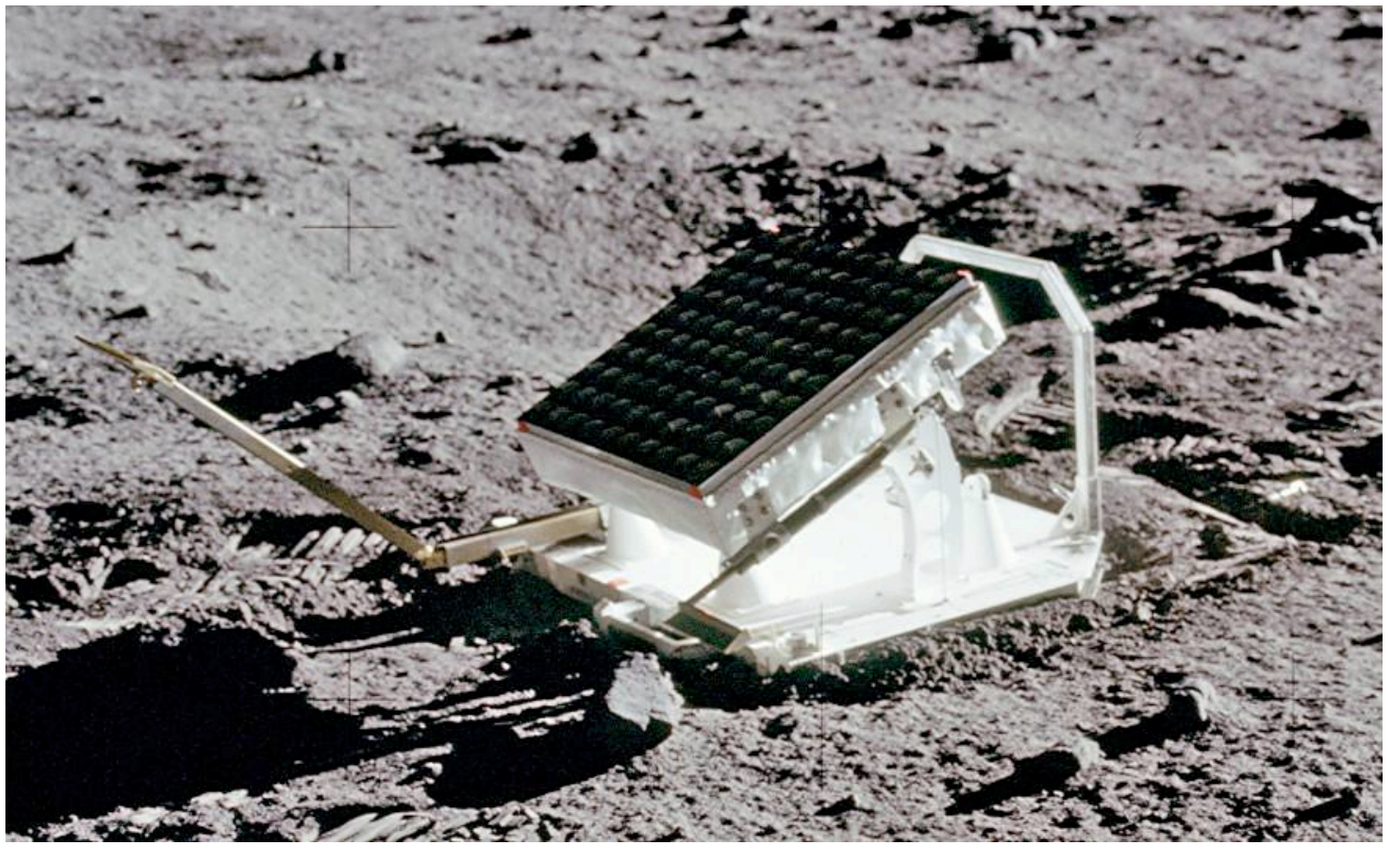

Apollo 15 LLR station. Credit: NASA

- Nortdvedt calculates that orbit of Earth and Moon should be polarized by Solar field in BD gravity (Nodtvedt effect)
- Detecting this effect is one of the main goals of LLR!

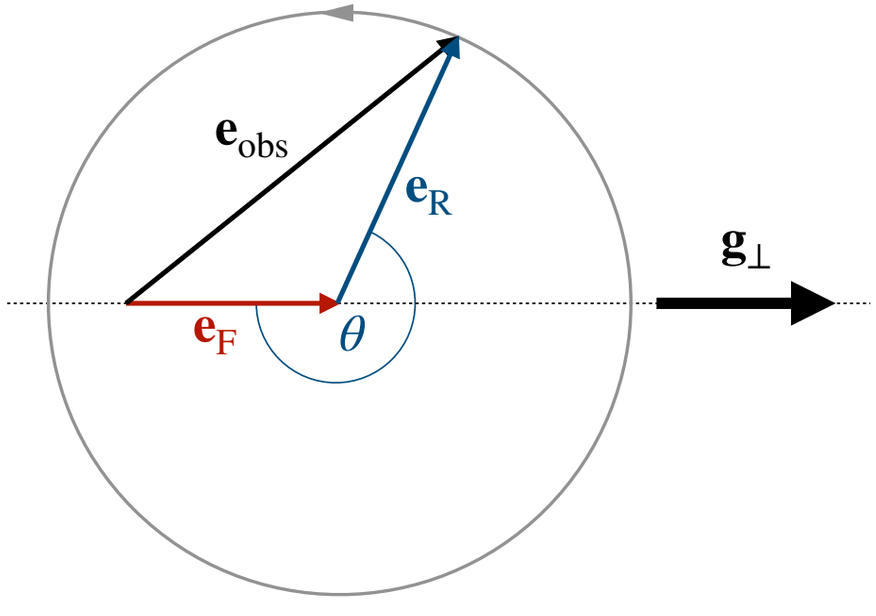

Tests of universality of free fall for self-gravitating objects

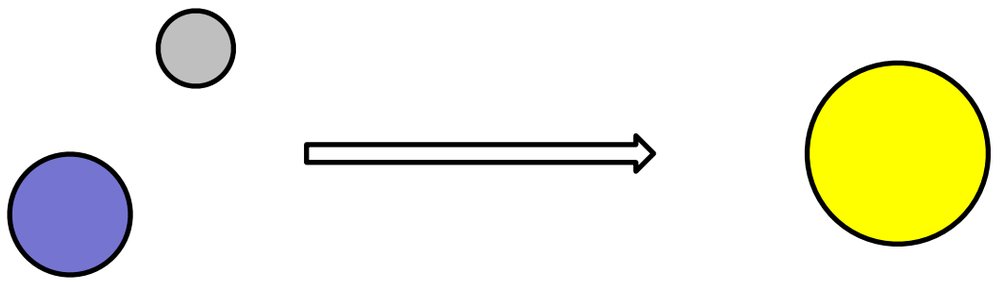

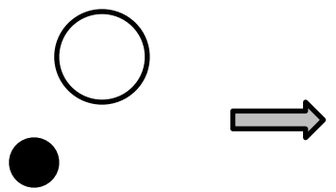

Damour-Schäfer test (1991), Phys. Rev. Lett. 66, 2549

Lunar Laser Ranging

Weakly self-gravitating objects

Gonzalez et al. (2011), ApJ, 743, 102

de/dt test (Freire, Kramer, Wex, 2012)

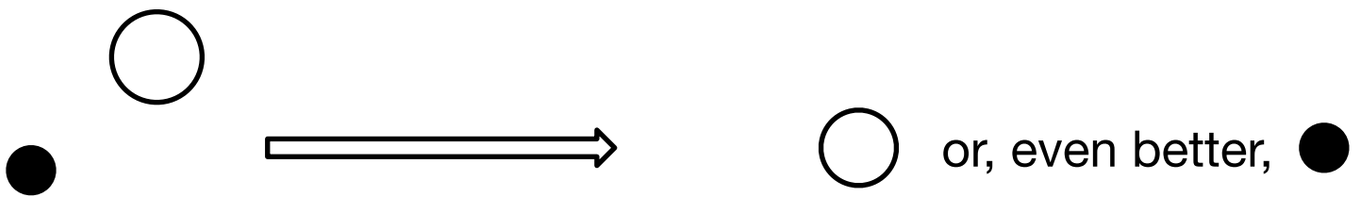

Pulsar in triple star system (Freire, Kramer, Wex, 2012)

The pulsar in a triple system and the strong-field Nordtvedt effect

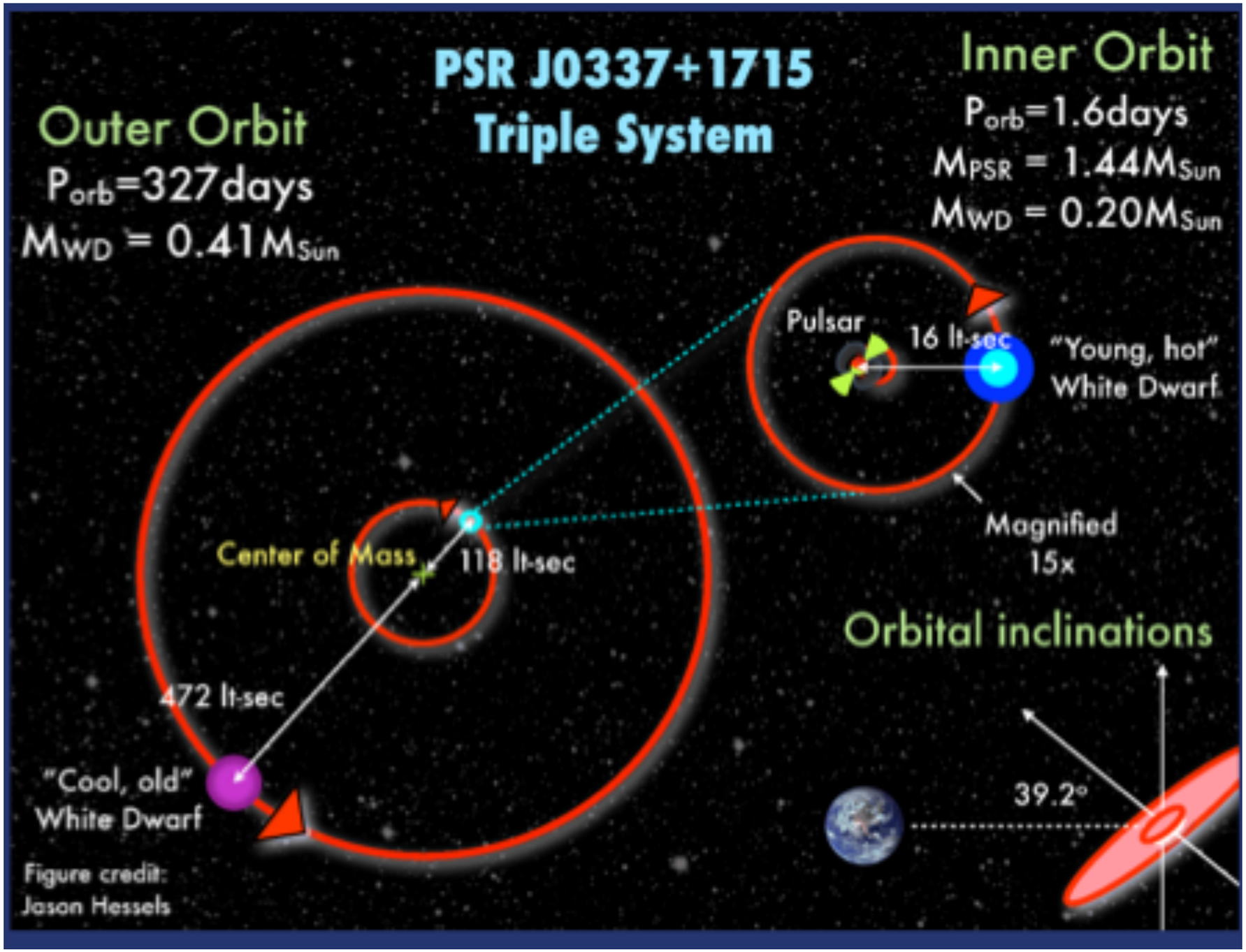

Ransom et al., (2014); Archibald et al. (2018)

$$|\Delta| < 2.6 \times 10^{-6}$$
$$\lesssim 2 \times 10^{-5} |\varepsilon|$$

Numerical integration of the equations of motion

- There are no analytical models to describe the motion.
- Therefore, phenomenological equations of motion for a n-body system in a wide class of alternative theories of gravity must be integrated with high precision and for the whole length of the timing study (~10 years).
- Initial parameters and theory parameters are then varied to minimize the residual rms.
- These can describe the timing perfectly!

$$\ddot{\boldsymbol{x}}_a = \sum_{b\neq a} \frac{G_{ab} m_b}{r_{ab}^2} \boldsymbol{n}_{ab} \left[1 - \frac{1}{c^2} \left(4\boldsymbol{v}_a \cdot \boldsymbol{v}_b - \boldsymbol{v}_a^2 - 2\boldsymbol{v}_b^2 + \frac{3}{2}(\boldsymbol{v}_b \cdot \boldsymbol{n}_{ab})^2 - \bar{\gamma}_{ab} (\boldsymbol{v}_a - \boldsymbol{v}_b)^2 \right) \right]$$
$$+ \sum_{b\neq a} \frac{G_{ab} m_b}{r_{ab}^2 c^2} (\boldsymbol{v}_b - \boldsymbol{v}_a) \left[\boldsymbol{n}_{ab} \cdot (4\boldsymbol{v}_a - 3\boldsymbol{v}_b - 2\bar{\gamma}_{ab}(\boldsymbol{v}_b - \boldsymbol{v}_a)) \right]$$
$$+ \sum_{b\neq a} \sum_{c\neq b} \frac{G_{ab} G_{bc} m_b m_c}{r_{ab} r_{bc} c^2} \left[\frac{1}{r_{bc}} \left(\frac{1}{2}(\boldsymbol{n}_{ab} \cdot \boldsymbol{n}_{bc}) \boldsymbol{n}_{ab} + \frac{7}{2} \boldsymbol{n}_{bc} \right) - \frac{\boldsymbol{n}_{ab}}{r_{ab}} + 2\bar{\gamma}_{ab} \frac{\boldsymbol{n}_{bc}}{r_{bc}} - 2\bar{\beta}^b_{ca} \frac{\boldsymbol{n}_{ab}}{r_{ab}} \right]$$
$$- \sum_{b\neq a} \sum_{c\neq a} \frac{G_{ab} G_{ac} m_b m_c}{r_{ab}^2 r_{ac} c^2} \boldsymbol{n}_{ab} \left[4 + 2\bar{\gamma}_{ac} + 2\bar{\beta}^a_{bc} \right]. \qquad \text{(A.2)}$$

Voisin et al. (2020), A&A, 638, A24

Best limits ever on any violations of the Universality of free fall for strongly gravitating objects!

- Delta parameter is smaller than 2×10^{-6} (95 % C. L., Voisin et al. 2020) !

- No more systematic effects, as in Archibald et al. (2018). Partly because kinematic effects induced by the finite size of the orbit must be taken into account.

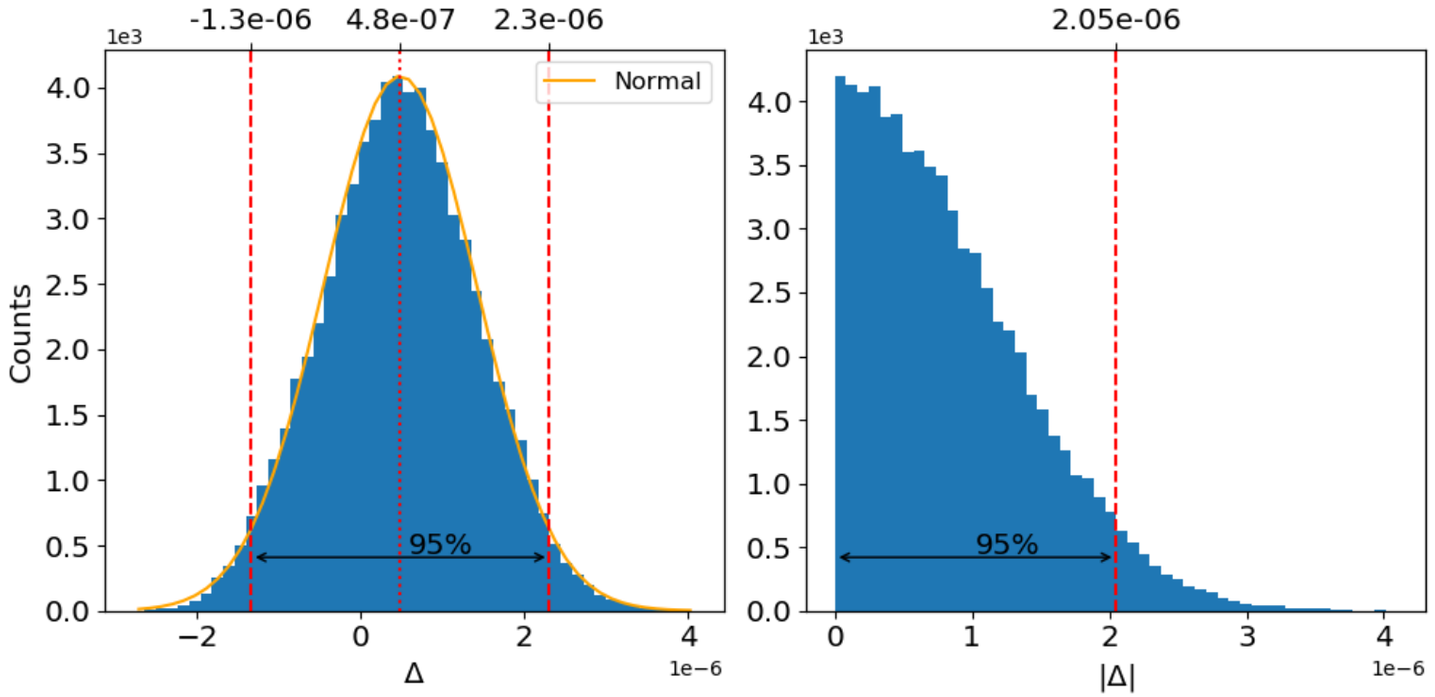

Fig. 7. *Left-hand side*: marginalised posterior probability distribution of the SEP violation parameter Δ sampled by MCMC and normal law with the same mean and standard deviation. The upper axis gives the mean value and the boundaries of the 95% confidence region. *Right-hand side*: distribution of distance to GR derived from the left-hand-side distribution.

Voisin et al. (2020)

5. Consequences for our understanding of gravity and alternative gravity theories

Precision relative to LIGO/Virgo

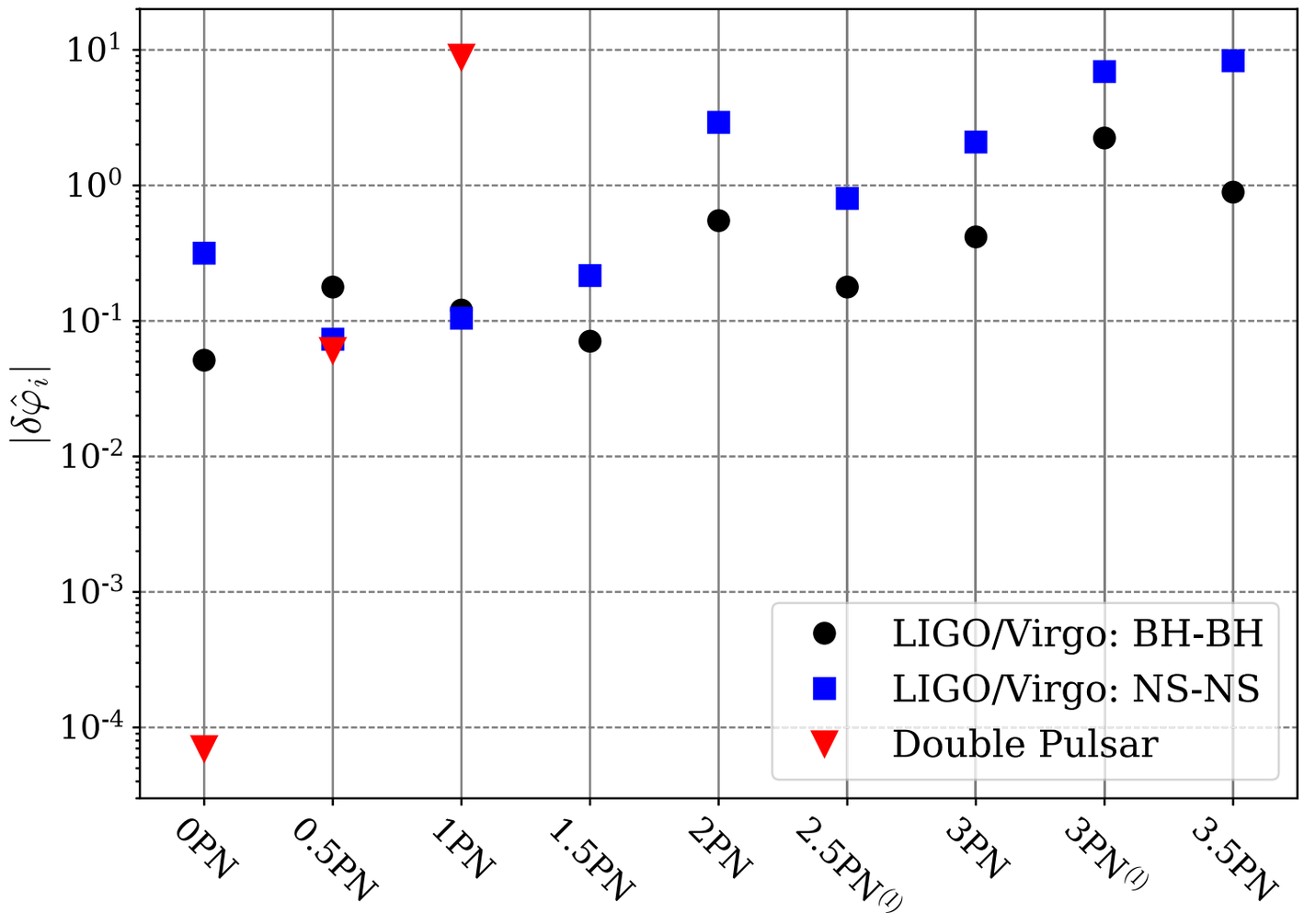

Kramer et al. (2021)

FIG. 7. Update of Fig. 6 in Ref. [178] (including data from Refs. [180,181]), which shows the 90% upper bounds on the absolute magnitude of the GR violation parameters $\delta\hat{\varphi}_i$, from 0PN through 3.5PN ("relative" order) in the inspiral phase (see, e.g., Ref. [182] for the definition of the PN phase coefficients and Ref. [178] for further details on the method). As discussed in Ref. [178], the 0.5PN parameter is zero in GR and, therefore, understood not as a relative but as an absolute shift. Black circles show the combined limits from the double BH mergers, blue squares are the limits from the double-NS merger GW170817, and red triangles give the limits derived from the double pulsar GW test in this paper. The PN order on the x axis is in the GR radiation reaction, where the leading contribution (0PN) corresponds to the dissipative 2.5PN term in the equations of motion. Note that such a comparison of tests with different compact objects (BHs vs NSs) as well as different gravity regimes (mildly relativistic vs highly relativistic strong field) does come with a caveat, which is explained in more detail in the text.

Constraints on DEF gravity

$$R^*_{\mu\nu} = \frac{8\pi G_*}{c^4}\left(T^*_{\mu\nu} - \frac{1}{2}T^* g^*_{\mu\nu}\right) + 2\partial_\mu\varphi\partial_\nu\varphi - 2\cancel{V(\varphi)}g^*_{\mu\nu}$$

$$\Box_{g_*}\varphi = -\frac{4\pi G_*}{c^4}(\alpha_0 + \beta_0\varphi)\,T_* - \cancel{V'(\varphi)}$$

$V''(\varphi) \ll 1/(\text{size of system})^2$

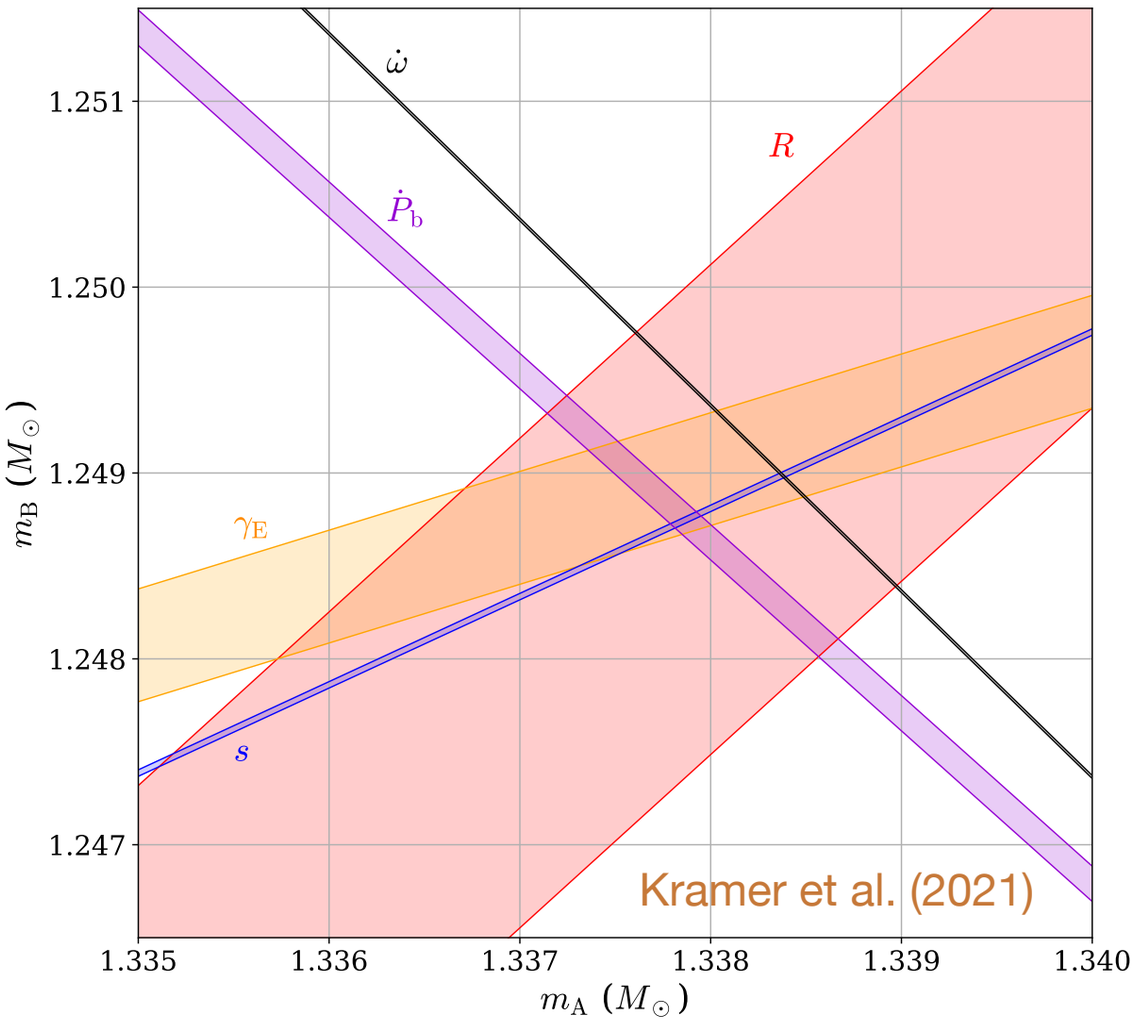

$\alpha_0 = 0.0005, \beta_0 = -4$, EOS MPA1

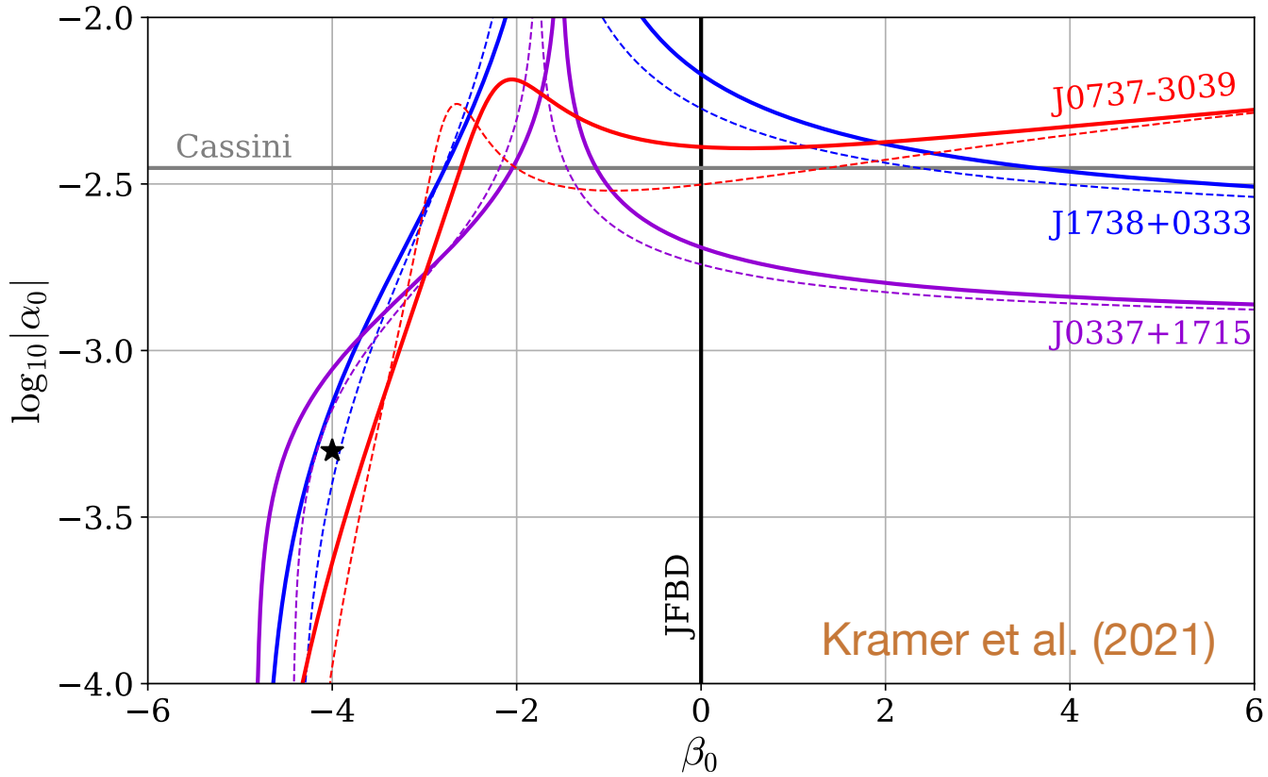

Solid lines: MPA1 EOS
Dashed lines: WFF1 EOS

Constraints on DEF gravity

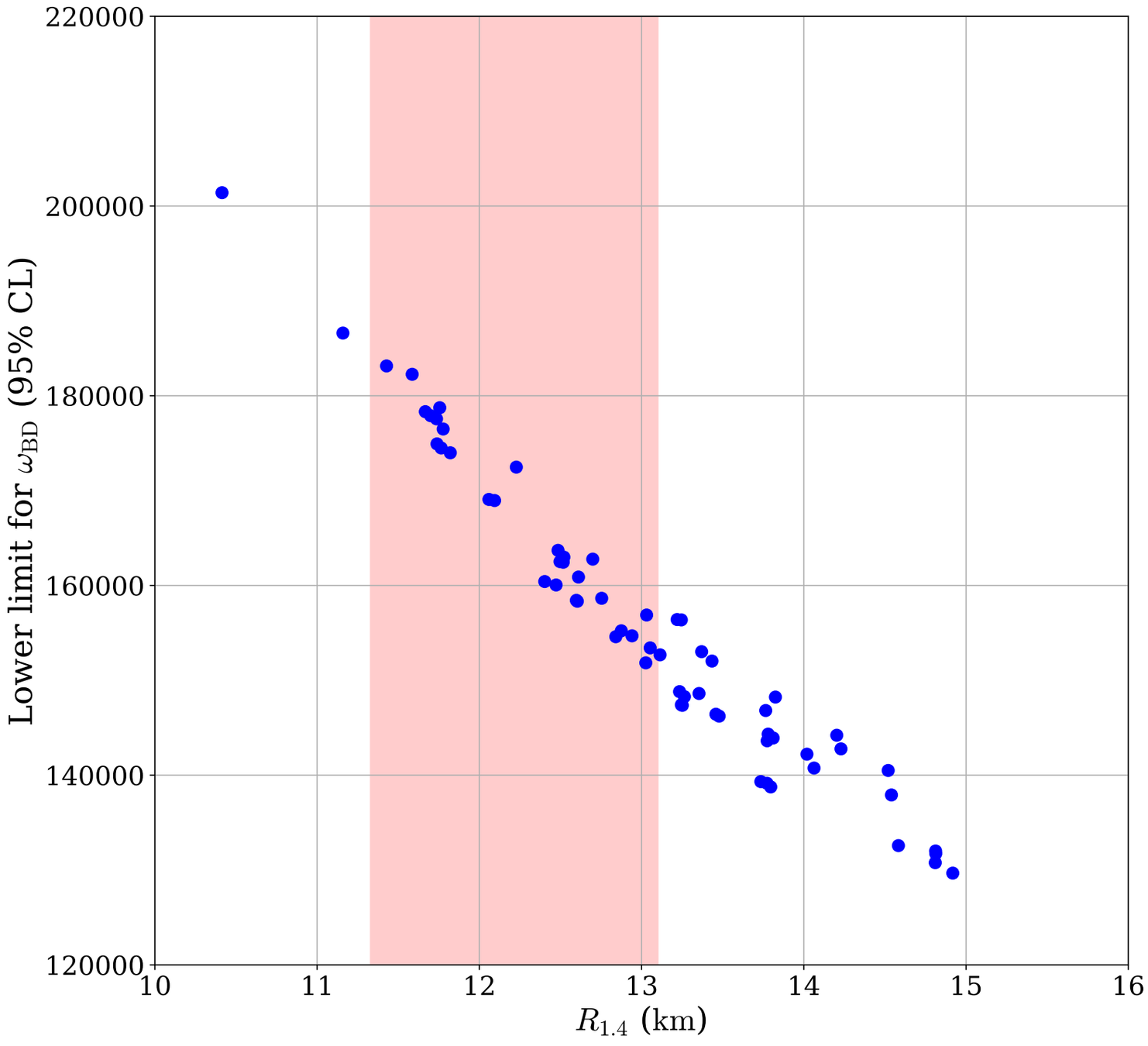

Best limit on Brans-Dicke parameter:

- Cassini: $\omega_{\rm BD} > 40{,}000$
- Triple system: $\omega_{\rm BD} > 150{,}000$

From: Freire & Wex, 2024, Living Reviews in Relativity,

The double pulsar and TeVeS

These results are already enough to exclude TeVeS - or at least a version that can yield MOND

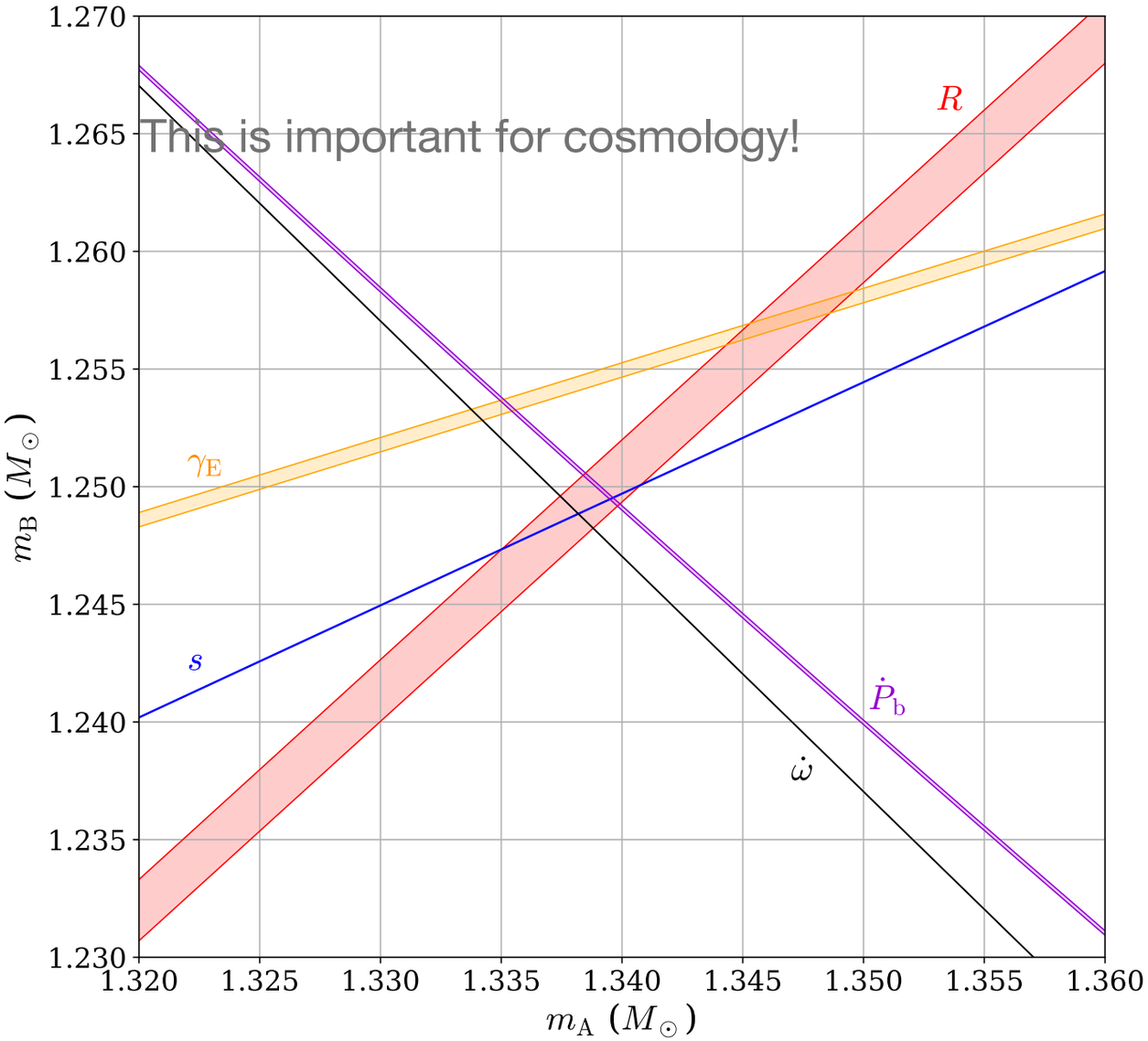

Kramer et al. (2021)

This is important for cosmology!

FIG. 14. Mass-mass diagram for Bekenstein's TeVeS with a "natural" transition from the Netownian to the MONDian regime ($\alpha_0 = 0.04$) [172]. Such a theory is obviously in contradiction with the Double Pulsar observations. The $\dot{P}_{\rm b}$ curve is based on Eq. (44). The 2PN and Lense-Thirring contributions to $\dot{\omega}$ have been calculated assuming GR, since any TeVeS related corrections for them are negligible in this test.

Letters

IOP Publishing

Classical and Quantum Gravity

Class. Quantum Grav. **39** (2022) 11LT01 (13pp)

https://doi.org/10.1088/1361-6382/ac69a3

Letter

Closing a spontaneous-scalarization window with binary pulsars

Junjie Zhao[1,2,*], Paulo C C Freire[3], Michael Kramer[3,4], Lijing Shao[3,5,6] and Norbert Wex[3]

[1] School of Physics and State Key Laboratory of Nuclear Physics and Technology, Peking University, Beijing 100871, People's Republic of China

[2] Department of Astronomy, Beijing Normal University, Beijing 100875, People's Republic of China

[3] Max-Planck-Institut für Radioastronomie, Auf dem Hügel 69, D-53121 Bonn, Germany

[4] Jodrell Bank Centre for Astrophysics, School of Physics and Astronomy, The University of Manchester, M13 9PL, United Kingdom

[5] Kavli Institute for Astronomy and Astrophysics, Peking University, Beijing 100871, People's Republic of China

[6] National Astronomical Observatories, Chinese Academy of Sciences, Beijing 100012, People's Republic of China

E-mail: junjiezhao@pku.edu.cn and lshao@pku.edu.cn

Received 10 January 2022, revised 11 April 2022
Accepted for publication 22 April 2022
Published 12 May 2022

Before

After

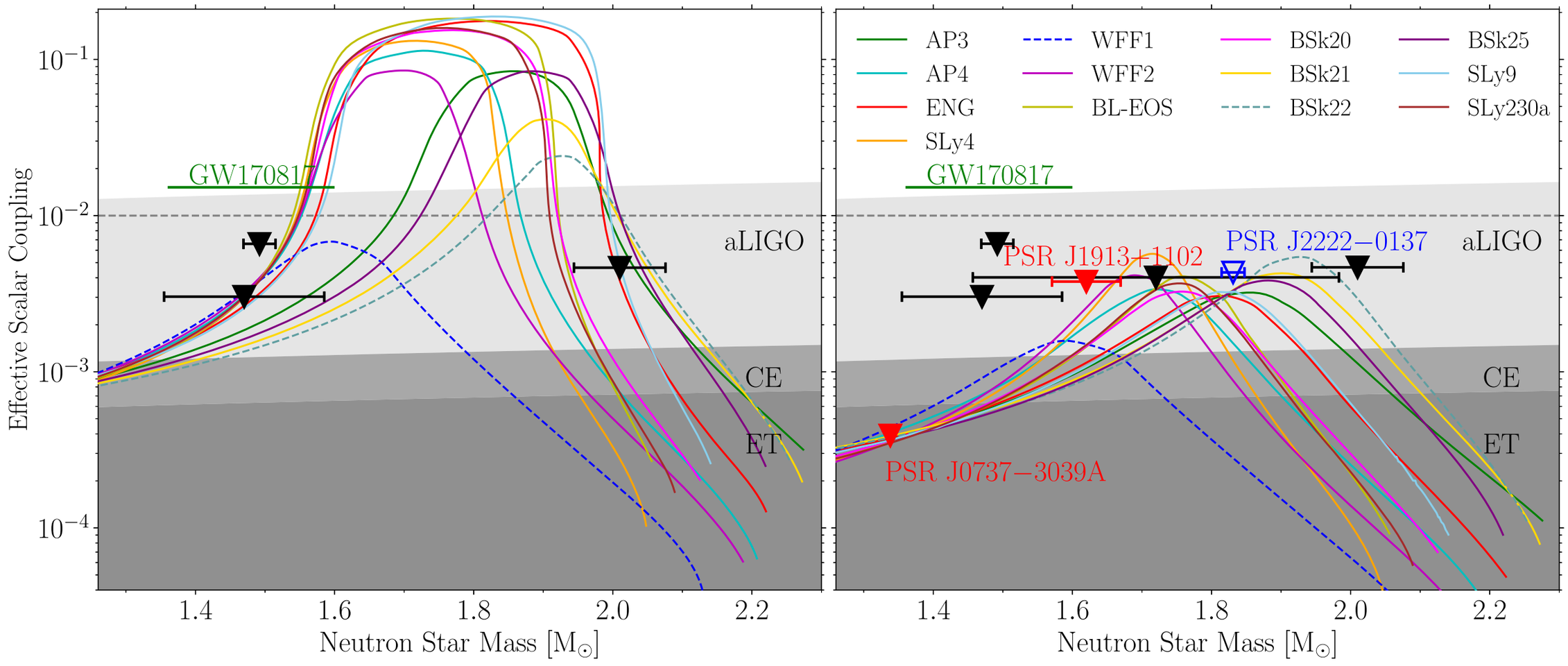

Zhao et al. (2022)

» Conclusions

- The measurement of the orbital decay in the Double Pulsar published in 2021 (Kramer et al. 2021) improved the precision of tests of the radiative properties of gravity—especially the leading order quadrupolar term predicted by GR—by a factor of 25 over the best previous test. The results agree with GR within the relative 1-σ uncertainty of 6.3×10^{-5}.
- The same system allowed several other independent, high-precision tests of GR as well, including the first pulsar tests of terms past the leading order.
- These include the most precise pulsar tests of the Shapiro delay, carried out in a spacetime with a curvature that is six orders of magnitude larger than the curvature probed with the Cassini-spacecraft test in the Solar system. More generally, it is the photon propagation test with the highest spacetime curvature, exceeding the images of the supermassive BHs M87* (Event Horizon Telescope Collaboration 2019a) and Sgr A* (Event Horizon Telescope Collaboration 2022) by more than nine and three orders of magnitude respectively.
- The MSP in a triple system, PSR J0337+1715, has allowed an improvement in our test of the UFF for NSs by three orders of magnitude (Archibald et al. 2018; Voisin et al. 2020). This test of the SEP provides some of the tightest constraints for many alternatives to GR, including JFBD gravity and a large part of the DEF-gravity parameter space.
- The latter parameter space was also constrained by tight constraints on the possibility of dipolar GW emission in a set of pulsar-WD systems with a wide range of pulsar masses;
- Regarding other gravity theories, pulsar tests have not only provided important limits on other types of scalar–tensor theories, scalar-Gauss-Bonnet gravity, Einstein-Aether (a tensor–vector theory which violates Lorentz invariance in the gravitational sector), etc., but also entirely ruled out others, like Bekenstein's TeVeS and some of its variations.

» Implications for our understanding of gravity and spacetime

Impressively, GR still passes all these precise and diverse tests. More generally, these experiments test some fundamental aspects and symmetries of gravitation and spacetime:

- The verification of the UFF for NSs via the non-detection of the Nordtvedt effect and of dipolar GW emission.
- The stringent limits on UFF violation and on preferred-location and preferred-frame effects for the gravitational interaction further support the SEP. This is of fundamental importance, particularly in view of the conjecture that GR is the sole valid gravity theory that fully embodies the SEP.
- Some of these radiative experiments are stringent probes into the nature of GWs, showing that they are, to leading order, quadrupolar as predicted by GR. These GW pulsar tests nicely complement GW tests obtained from merger observations with ground-based GW observatories.
- These radiative experiments have also excluded some strong-field highly nonlinear deviations from GR, like the phenomenon of spontaneous scalarisation predicted by DEF gravity.
- Finally, pulsars have also provided tight constraints for parameters of generic frameworks, like strong-field generalizations of PPN parameters and parameters of the gravitational sector in the SME. Some of them are directly related to the aforementioned limits on violations of symmetries associated with the SEP, like the UFF, local position and local Lorentz invariance.

Living Reviews in Relativity (2024)27:5
https://doi.org/10.1007/s41114-024-00051-y

REVIEW ARTICLE

Gravity experiments with radio pulsars

Paulo C. C. Freire[1] · Norbert Wex[1]

Received: 22 April 2024 / Accepted: 28 June 2024

Abstract

The discovery of the first pulsar in a binary star system, the Hulse–Taylor pulsar, 50 years ago opened up an entirely new field of experimental gravity. For the first time it was possible to investigate strong-field and radiative aspects of the gravitational interaction. Continued observations of the Hulse–Taylor pulsar eventually led, among other confirmations of the predictions of general relativity (GR), to the first evidence for the reality of gravitational waves. In the meantime, many more radio pulsars have been discovered that are suitable for testing GR and its alternatives. One particularly remarkable binary system is the Double Pulsar, which has far surpassed the Hulse–Taylor pulsar in several respects. In addition, binary pulsar-white dwarf systems have been shown to be particularly suitable for testing alternative gravitational theories, as they often predict strong dipolar gravitational radiation for such asymmetric systems. A rather unique pulsar laboratory is the pulsar in a hierarchical stellar triple, that led to by far the most precise confirmation of the strong-field version of the universality of free fall. Using radio pulsars, it could be shown that additional aspects of the Strong Equivalence Principle apply to the dynamics of strongly self-gravitating bodies, like the local position and local Lorentz invariance of the gravitational interaction. So far, GR has passed all pulsar tests with flying colours, while at the same time many alternative gravity theories have either been strongly constrained or even falsified. New telescopes, instrumentation, timing and search algorithms promise a significant improvement of the existing tests and the discovery of (qualitatively) new, more relativistic binary systems.

Keywords Pulsars · Binary star systems · Gravity · General relativity

Thank you!

For questions and suggestions, contact me at: pfreire@mpifr-bonn.mpg.de, or see my site at http://www3.mpifr-bonn.mpg.de/staff/pfreire/

To stay up to date on the latest precise NS mass measurements and GR tests, check: http://www3.mpifr-bonn.mpg.de/staff/pfreire/NS_masses.html